Towards Structure-Guided Design of Next-Generation Aminoglycoside Antibiotics

Angelia V. Bassenden

Department of Biochemistry
McGill University, Montréal
August 2020

A thesis submitted to McGill University in partial fulfillment
of the requirements of the degree of Doctor of Philosophy

Acknowledgements

I express my sincerest gratitude to my supervisor and mentor, Albert Berghuis, for recognizing my potential and giving me the opportunity to work alongside an incredible group of individuals. Your guidance and support always provided me with a unique perspective on challenges and gave me the motivation to overcome them.

I cannot begin to express my gratitude to my current and former lab members, Jonathan Blanchet, Ella Dekemp, Tolou Golkar, Jae Park, Pedro Romero, Dmitry Rodionov, Barry Sleno, Kun Shi, Brahm Yachnin, Amy Yan, and Michał Zieliński for their friendship, their helpful insight along the way, and of course for our unforgettable coffee time. I would be remiss not to specifically mention the brilliant contribution of Dmitry to the ANT(2″) project. I will forever be grateful for your guidance and our continued friendship beyond the lab. An exceptional thank you to Michał for our unforgettable shared experiences; your light-hearted spirit and sense of humour have made my time in the lab exceptionally memorable. Here's to many more laughs together!

I also had the privilege of working with one excellent project student, Linda Dumalo, over the last two years of my thesis. Your hard work and dedication brought a fascinating narrative to the AAC(2′)-Ia project.

I have also had the benefit of an immense support system outside the lab. I am thankful to the members of my RAC, Alba Guarné and Karine Auclair, for their guidance, thoughtful comments, and encouragement over the years. Additionally, I would like to thank the funding agencies that made this work possible: PROTEO, FRQS, and CIHR.

Many thanks to my friends for helping celebrate my achievements throughout my studies. To my parents, siblings, and many family members for their unconditional love and support throughout this journey. And finally, to my husband, Michael Penta, words cannot describe how lucky I am to have you by my side. I am beyond excited to continue our adventure together.

Abstract

Antibiotic resistance is currently the largest global threat to modern medicine. Drug-resistant infections are presently the cause of over 700,000 deaths worldwide and, if left unchecked, will lead to a 90% increase in antimicrobial resistance-related deaths, and a major financial impact on the world's GDP. The use and misuse of antibiotics have led to a universal resistance epidemic, where resistance is observed for every antibiotic currently used in the clinic.

Aminoglycosides are a major class of antibiotics used for the treatment of serious bacterial infections; however, their clinical use has waned as resistance has increased. The primary mechanism of aminoglycoside inactivation is through chemical modification by resistance enzymes such as ANT(2″). ANT(2″) is the most prevalent resistance factor in North America and is found in almost half of all clinical isolates worldwide. Additionally, ANT(2″) is capable of detoxifying two of the most widely used antibiotics in the clinic, tobramycin and gentamicin, rendering them ineffective in the treatment of severe bacterial infections, including those caused by *Pseudomonas aeruginosa* in cystic fibrosis patients.

In order to circumvent resistance from clinically widespread resistance enzymes such as ANT(2″), many efforts have been put into designing broad-spectrum next-generation aminoglycosides. The newest and most promising example of this is plazomicin, which is capable of evading the action of most aminoglycoside modifying enzymes. Still, resistance to plazomicin has been reported in bacterial populations expressing the enzyme AAC(2′)-Ia. AAC(2′)-Ia is chromosomally restricted to *Providencia stuartii* and far less widespread than ANT(2″), being present in only 1% of aminoglycoside resistant clinical isolates. However, the use of plazomicin in the clinic will likely lead to the spread and increased prevalence of the *aac2′-ia* resistance gene.

This thesis aims to generate an in-depth understanding of the underlying working mechanisms and substrate specificities of ANT(2″) and AAC(2′)-Ia through the elucidation of their three-dimensional structures. Four crystal structures of ANT(2″) outline the enzymes kinetic and

catalytic mechanisms and provide a framework for this enzyme's specificity for clinically used substrates. Additionally, four crystal structures of AAC(2′)-Ia have allowed us to provide an understanding of this enzyme's ability to modify a diverse set of aminoglycosides, including plazomicin. Ultimately, these structural insights will contribute to the design of novel drugs capable of evading these enzymes' activities, thus ensuring that viable treatment options remain available despite resistant organisms.

Abrégé

La résistance aux antibiotiques est actuellement la plus grande menace mondiale pour la médecine moderne. Les infections résistantes aux médicaments sont à l'origine de plus de 700,000 décès dans le monde et, si elles ne sont pas contrôlées, elles entraîneront une augmentation de 90% des décès liés à la résistance aux antimicrobiens et elles auront un impact financier majeur sur le PIB mondial. L'utilisation chronique des antibiotiques a engendré une épidémie de résistance universelle, où une résistance est observée pour chaque antibiotique actuellement utilisé en clinique.

Les aminoglycosides sont une catégorie importante d'antibiotiques utilisés pour le traitement des infections bactériennes graves. Cependant, leur utilisation clinique s'est affaiblie avec l'augmentation de la résistance. Le principal mécanisme d'inactivation des aminoglycosides est la modification chimique causée par des enzymes de résistance telles que l'ANT(2″). L'enzyme ANT(2″) est le facteur de résistance le plus répandu en Amérique du Nord et se retrouve dans près de la moitié des isolats cliniques dans le monde. De plus, ANT(2″) est capable de détoxifier deux des antibiotiques les plus utilisés en clinique, soit la tobramycine et la gentamicine, les rendant ainsi inefficaces dans le traitement des infections bactériennes sévères, y compris celles causées par *Pseudomonas aeruginosa* chez les patients atteints de fibrose kystique.

Pour contourner les effets d'enzymes de résistance cliniquement répandues telles que l'ANT(2″), de nombreux efforts ont été déployés dans la conception d'aminoglycosides de nouvelle génération. La plazomicine en est l'exemple le plus récent et le plus prometteur, étant capable d'échapper à l'action de la plupart des enzymes qui modifient les aminoglycosides. Néanmoins, la vulnérabilité de la plazomicine a été rapportée dans des populations bactériennes exprimant l'enzyme de résistance AAC(2′)-Ia. AAC(2′)-Ia est chromosomiquement limitée à *Providencia stuartii* et est beaucoup moins répandue que l'ANT(2″), étant présente dans seulement 1% des isolats cliniques résistants aux aminoglycosides. Cependant, l'utilisation clinique de la

plazomicine entraînera probablement la propagation et l'augmentation de la prévalence du gène de résistance *aac2′-ia*.

Cette thèse vise à générer une compréhension approfondie des mécanismes de travail sous-jacents et des spécificités de substrat de l'ANT(2″) et de l'AAC(2′)-Ia à travers l'élucidation de leurs structures tridimensionnelles. Quatre structures cristallines de l'ANT(2″) nous permettent de décrire ses mécanismes cinétique et catalytique et de fournir un cadre pour la spécificité de cette enzyme pour les substrats cliniquement utilisés. De plus, quatre structures cristallines d'AAC(2′)-Ia nous ont permis de comprendre la capacité de cette enzyme à modifier un ensemble diversifié d'aminoglycosides, dont la plazomicine. En définitive, ces connaissances structurelles contribueront à la conception de nouveaux médicaments capables d'éviter les activités de ces enzymes, garantissant ainsi que des options de traitement viables restent disponibles malgré les organismes résistants.

List of Tables

List of Figures

List of Abbreviations

AAC	Aminoglycoside acetyltransferase
ADP	Adenosine diphosphate
AME	Aminoglycoside modifying enzyme
AMP	Adenosine monophosphate
AMPCPP	α,β-Methyleneadenosine-5′-triphosphate
ANT	Aminoglycoside nucleotidyltransferase
APH	Aminoglycoside phosphotransferase
A-site	Aminoacyl site
ATP	Adenosine triphosphate
B-factor	Crystallographic temperature factor
BLAST	Basic local alignment search tool
CCD	Charged-coupled device
CoA	Coenzyme A
DEAE	Diethylaminoethyl
DNA	Deoxyribonuclease
EDTA	Ethylenediaminetetraacetic acid
F_c	Calculated structure factor
FF	Fast flow
F_o	Observed structure factor
GDP	Gross domestic product
GNAT	GCN5 related N-acetyltransferase
GTP	Guanosine triphosphate
HABA	4-amino-2-hydroxybutyrate
HEPES	4-(2-hydroxyethyl)-1-piperazineethanesulfonic acid
HF	High flux
IDA	Iminodiacetic acid
K_{cat}	Rate of catalysis
K_i	Inhibitory constant
K_M	Michaelis-Menten constant
MES	2-ethanesulfonic acid
MPD	2-Methyl-2,4-pentanediol

MRSA	methicillin-resistant *Staphylococcus aureus*
NMD1	New Delhi metallo-β-lactamase 1
Ni-IDA	Nickle-Iminodiacetic acid
PSI-BLAST	Position-specific iterative-basic local alignment search tool
P-site	Peptidyl site
PCR	Polymerase chain reaction
PDB	Protein Data Bank
PEG	Polyethylene glycol
pET	Peptide expression system
polβ	Polymerase-β
RMSD	Root-mean-square deviation
RPM	Revolutions per minute
R_{work}	Reliability factor
R_{free}	Free reliability factor
RNA	Ribonucleic acid
rRNA	Ribosomal ribonucleic acid
SDS-PAGE	Sodium dodecyl sulfate-polyacrylamide gel electrophoresis
TB	Tuberculosis
TCEP	Tris (2-carboxyethyl) phosphine
tRNA	Transfer ribonucleic acid
TRIS	2-Amino-2-(hydroxymethyl)1,3-propanediol
Tris-HCl	2-Amino-2-(hydroxymethyl)1,3-propanediol hydrochloride

Table of Contents

Chapter 1 – Introduction

1.1 Preface

Sections 1.2 and 1.3 were partially adapted from Bacot-Davis, V.R., Bassenden, A.V., and Berghuis, A.M. "Drug-target networks in aminoglycoside resistance: hierarchy of priority in structural drug design". Med. Chem. Commun. **7**: 103-113. With permission from The Royal Society of Chemistry.

Individual author contributions for Chapter 1 are as follows, with percent of overall contribution in parentheses:

Bassenden, A.V. (65%): Preparation of written text and figures.

Bacot-Davis, V.R (20%). Preparation of written text.

Berghuis, A.M. (15%): Editing of written text and figures.

1.2 Antibiotics and Resistance

1.2.1 The Rise and Golden Age of Antibiotics

Devastating diseases caused by primary and opportunistic microbial infections have plagued modern humans since their evolution 200,000 years ago (Stock 2008, Riley, Sieber et al. 2013). Prehistoric human fossils and ancient written records detail the ravages of leprosy, pneumonia, meningitis, rabies, and many other microbial plagues, some of which persist as problems today (Hulse 1972, Baer 1994, Olshansky, Carnes et al. 1997, Schultz 2001). Infections caused by bacterial transmission remain a leading cause of human mortality despite centuries of medical progression (Lumen 2015). Foremost among these advancements was the clinical introduction of antimicrobial compounds, known as antibiotics, which allowed successful treatment of potentially fatal bacterial infections (Bonafede and Rice 1997, Spellberg, Guidos et al. 2008). From 1950 to 1960, the so-called "Golden Age" of prolific antibiotic discovery brought about over half of the antibiotic classes currently in use (Davies 2006) (Figure 1 – 1). In conjunction with their effectiveness against bacterial pathogens, antibiotics also generated substantial breakthroughs in modern medical procedures, including cancer treatment, organ transplants, and open-heart surgery (Hutchings, Truman et al. 2019). Moreover, the introduction of antibiotics in animal feed in 1953 revolutionized the industry with a surge in animal growth and feed efficiency (Assembly of Life Sciences (U.S.). Committee to Study the Human Health Effects of Subtherapeutic Antibiotic Use in Animal Feeds. 1980).

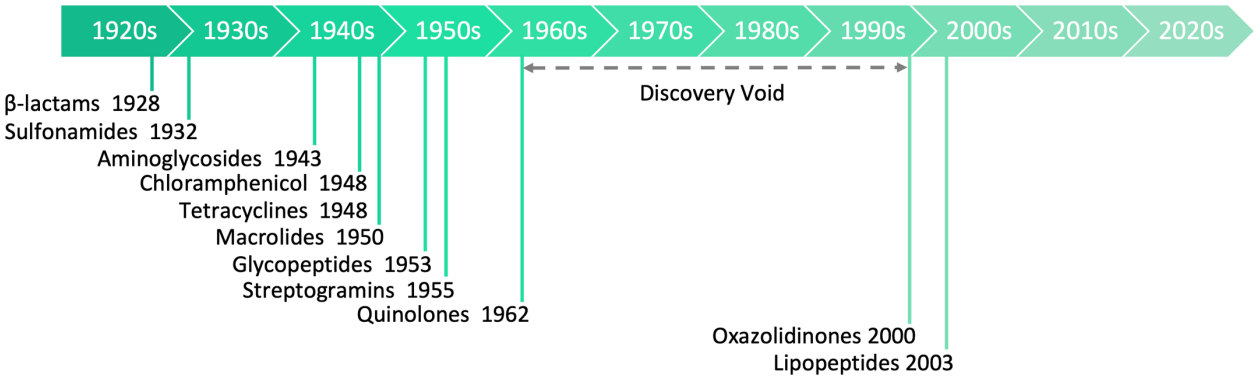

Figure 1 – 1. Discovery timeline of major antibiotic classes.

1.2.2 The Rise of Resistance and the Fall of Antibiotics

The swell of new antibiotics discovered came to an abrupt halt in the 1970s, where the "Golden Age" quickly turned into the "Discovery Void", with no new antibiotic classes being introduced into the clinical repertoire for over 30 years (Figure 1 – 1) (Fischbach and Walsh 2009). The decline of antibiotic discovery can be attributed to several factors, including the downturn in the number of antibiotics uncovered in ecological soil samples, and the withdrawal of pharmaceutical companies from research into new antibacterials (Aminov 2010, Silver 2011). Decades after the unparalleled success of early antibiotic regimens, selective pressures have led to an increasing prevalence of microbial populations capable of surviving exposure to formerly toxic concentrations of antibiotics (Spellberg, Guidos et al. 2008). Human behaviour, including the persistent use and misuse of antibiotics in the clinic and husbandry, has facilitated the emergence of resistance (Gonzalez-Bello 2017). Currently, resistance exists for every class of antibiotics in use (Pass, Kalil et al. 2007). As the effectiveness of antibiotics continues to wane and therapeutic options become limited, we risk entering a post-antibiotic era (Appelbaum 2012). Now, it is estimated that by 2050, emerging antibiotic resistance will cost $100 trillion in lost GDP revenue and 10 million global deaths every year (Boucher, Talbot et al. 2013, World Health Organization 2014, Demirjian, Sanchez et al. 2015).

1.2.3 Counteracting Antibiotic Resistance

The rise and spread of antibiotic resistance have brought about a considerable need for action. From 2000 to 2010, human antibiotic usage spiked 36%; still, 20% of global deaths today can be attributed to infectious diseases (Laxminarayan, Matsoso et al. 2016, Martens and Demain 2017, Ribeiro da Cunha, Fonseca et al. 2019). Overcoming this growing problem has been impeded by substantial challenges, including our inability to bypass complex resistance mechanisms, the uninterrupted chronic use of antibiotics in agriculture, and the continued widespread, and predominantly unregulated access to antibiotics (Levy and Marshall 2004, Laxminarayan, Duse et al. 2013). Efforts to counteract these hurdles have led to the implementation of strategic approaches and commitments, including supporting rational antibiotic use in hospitals and communities, controlling the non-therapeutic use of antibiotics, administering targeted treatments for bacterial infections, and continuing the surveillance of resistance (Laxminarayan, Duse et al. 2013). However, these strategies alone are not enough to curb the current state of antibiotic resistance; there is still a desperate need for new antibiotics. Following the "Discovery Void", research efforts into uncovering new antimicrobials were rejuvenated, with the discovery of two new antibiotic classes, oxazolidinones and lipopeptides, in 2000 and 2003, respectively (Figure 1 – 1) (Coates, Halls et al. 2011). Since then, the amount of antibiotic drug candidates has been steadily increasing, with an impressive number of antibiotic candidates in the early stages of drug approval (Phases I-III). However, the number of antibiotics close to approval (New Drug Submissions and Phase IV), remains alarmingly low (Ribeiro da Cunha, Fonseca et al. 2019). In conjunction with the systematic approaches being utilized, several new antibiotic development strategies are being pursued to help outpace the spread of resistance. Some of the strategies being used to expand the current library of effective antibiotics are discussed below.

Although the "Golden Age" of discovering soil-dwelling antimicrobials is far behind us, researchers have employed novel screening techniques to help push the discovery of new antibiotics. One approach focuses on culturing "unculturable" soil bacteria to find strains that make new antibiotics (von Bubnoff 2006, Kealey, Creaven et al. 2017). Other scientists are focusing their discovery efforts in more unusual places by isolating bacterial DNA from lichens, seaweed, and deep-sea mud (von Bubnoff 2006). Meanwhile, some researchers are employing metagenomic techniques by expressing DNA extracted from soil isolates and screening for antibiotic production (von Bubnoff 2006, Kealey, Creaven et al. 2017). To date, several promising compounds have been identified through these methods; however, enormous challenges lie ahead, especially given the fact that any isolated candidates would need to display activity against multi-drug resistant bacteria (von Bubnoff 2006, O'Connell, Hodgkinson et al. 2013).

Another approach employs the use of non-antibiotic compounds, or adjuvants, in combination with existing antibiotics, to potentiate the activity and efficacy of the drug (Kalan and Wright 2011). Adjuvants often come in the form of compounds that directly target mechanisms of resistance by acting as inhibitors, extending the spectrum of antibiotics and rescuing antibiotic activity (Laxminarayan, Matsoso et al. 2016). This strategy has proven particularly effective in recapturing the activity of β-lactam antibiotics, which, when used in combination with compounds such as clavulanic acid, sulbactam, or avibactam, recover their bactericidal properties (Kalan and Wright 2011).

Finally, antibiotic semi-synthesis is a technique that has been applied to most antibiotic classes to rejuvenate members that are no longer effective due to their susceptibility to resistance mechanisms. Exploiting information about an antibiotic's cellular targets and binding modes allows for the rational design of modified chemical analogues (Fair and Tor 2014). This method

has proven fruitful in the past with the development of several promising antibiotics including, meropenem, amikacin, azithromycin, tigecycline, rifampicin, and telavancin. More recently, it has brought about two next-generation antibiotics, eravacycline, a semisynthetic tetracycline, and plazomicin, a semisynthetic aminoglycoside (Newman and Cragg 2007, Aggen, Armstrong et al. 2010, Bassetti and Righi 2014).

1.3 Aminoglycosides

1.3.1 History

Currently, there are eighteen main classes of antibiotics, of which many have predominant roles in human therapy, e.g. β-lactams, macrolides, quinolones, sulfonamides, tetracyclines, and aminoglycosides (Coates, Halls et al. 2011). The first aminoglycoside, streptomycin, was isolated from *Streptomyces griseus* in 1943 and brought about the long-sought out cure for tuberculosis (Arya 2007, Gould 2016). Streptomycin remained widely popular until the 1950s and is still a chemotherapeutic pillar for the treatment of this disease (Forge and Schacht 2000). Early success with the isolation of streptomycin brought about the methodical screening of actinomycetes, where a new group of aminoglycosides derived from 2-deoxstreptamine were discovered (Arya 2007). Although the chemical library of naturally isolated and synthetically-derived aminoglycosides steadily grew through to the 1970s, their ototoxic and nephrotoxic effects combined with rapidly growing resistance, led to a decline in their clinical use (Forge and Schacht 2000). By the 1980s, aminoglycosides had fallen out of favor, being replaced by less toxic alternatives such as broad-spectrum β-lactams (Drusano and Louie 2011). Recently, the global spread of multidrug-resistant pathogens has brought about a resurgence in aminoglycoside interest (Serio, Keepers et al. 2018). Increased research into the expansion of this class of antibiotics has thus far yielded one new aminoglycoside, plazomicin, approved for the treatment of complicated urinary tract infections, including pyelonephritis in 2018 (Achaogen 2018).

1.3.2 Chemical Composition

Chemically, the majority of aminoglycosides are characterized by a deoxystreptamine ring that is substituted at two positions (Mingeot-Leclercq, Glupczynski et al. 1999, Pilch, Kaul et al. 2003, Chittapragada, Roberts et al. 2009). Specifically, the deoxystreptamine core can be 4,5-

disubstituted, or 4-6-disubstituted. 4,5-disubstituted aminoglycosides include neomycin, lividomycin, ribostamycin, paromomycin, and butirosin, while 4,6-disubstituted aminoglycosides encompass kanamycin, amikacin, isepamicin, tobramycin, gentamicin, dibekacin, netilmicin, and sisomicin (Figure 1 – 2). In addition to these two main classes of aminoglycoside antibiotics there is a third small but diverse group of non-deoxystreptamine aminoglycosides, which possess a slightly different pseudo-oligosaccharide core (Figure 1 – 2). This group contains the founding member of the aminoglycoside class of antibiotics, streptomycin, and two additional drugs: hygromycin, and spectinomycin. Note that unlike all other aminoglycosides, the non-deoxystreptamine compounds hygromycin and spectinomycin do not have the same mode of action, nor is spectinomycin considered a bactericidal antibiotic.

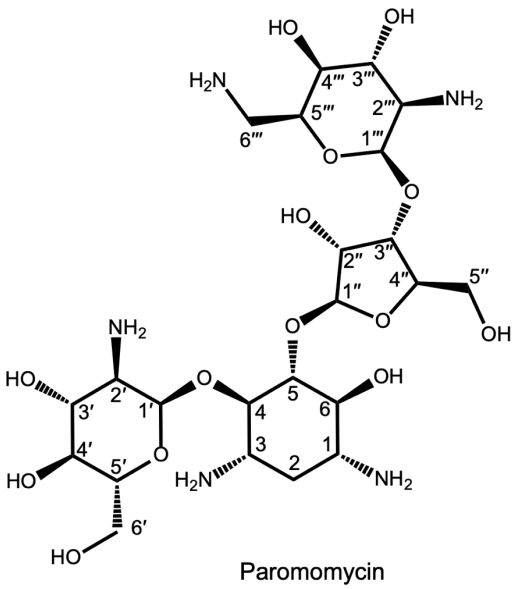

Paromomycin

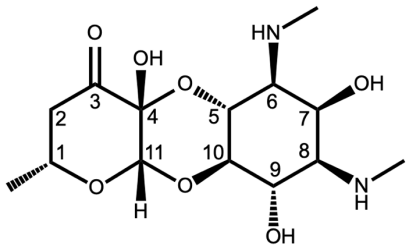

Spectinomycin

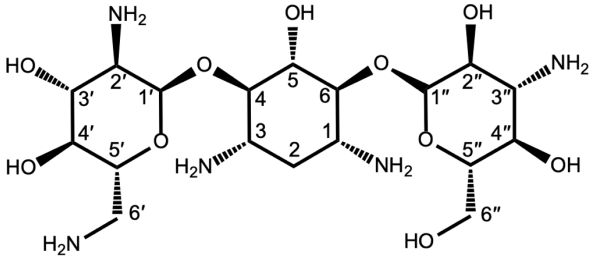

Kanamycin

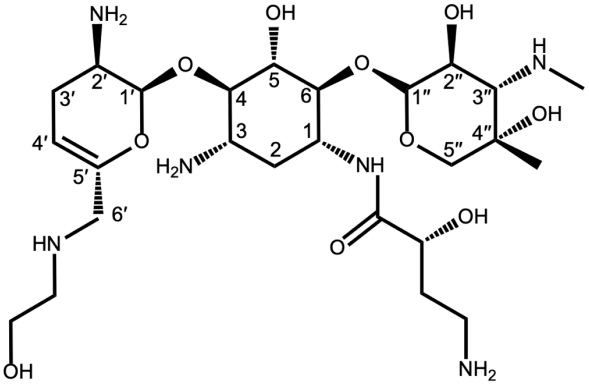

Plazomicin

Figure 1 – 2. Chemical structures of representative aminoglycoside antibiotic classes. a) 4,5-disubstituted aminoglycoside paromomycin. b) Non-deoxystreptamine aminoglycoside spectinomycin. c) 4,6-disubstituted aminoglycoside kanamycin. d) Next-generation 4,6-disubstituted aminoglycoside plazomicin.

1.3.3 Clinical Use of Aminoglycosides

4,5-disubstituted aminoglycosides remain very influential drugs to human health. Neomycin has common antiseptic topical uses and is the active ingredient in commercially available Neosporin. In addition, lividomycin is utilized as a second-line antibiotic to treat *Mycobacterium tuberculosis*, *Pseudomonas aeruginosa*, and urinary tract infections (Kobayashi,

Yamaguchi et al. 1972, Tsukamura 1972, Leroy, Humbert et al. 1976). Likewise, ribostamycin was declared a critical antibiotic in human health by the World Health Organization, and is commonly employed against pelvic inflammatory diseases that can go on to cause life-long infertility (Kurumbang, Liou et al. 2011), while paromomycin is effective against gastrointestinal and liver infections (Bode, Schafer et al. 1997)

4,6-disubstituted aminoglycosides also play pivotal roles in treating human disease. Tobramycin, amikacin, and gentamicin are all used in inhalable forms to clear chronic infections associated with cystic fibrosis (Prayle and Smyth 2010, Shi, Caldwell et al. 2013). Furthermore, isepamicin and dibekacin, in combination with penicillin derivatives, treat potentially deadly, methicillin-resistant *Staphylococcus aureus* (MRSA) and *P. aeruginosa* skin, lung, and soft-tissue infections (Aonuma, Ariji et al. 1987, Deguchi, Koguchi et al. 1996). Netilmicin is only used for gentamicin resistant infections because it must be injected (Agence française de sécurité sanitaire des produits de 2012), while sisomicin is largely employed to clear systemic urinary tract infections (Rodriquez Torres 1979). Equally important, non-deoxystreptamine aminoglycosides, like streptomycin, are used in combination to clear serious *M. tuberculosis* infections, especially tuberculosis un-responsive to other antibiotics (drug-resistant TB) (Zumla, Nahid et al. 2013). Also, spectinomycin is given to patients with *Neisseria gonorrhoeae* (Gonorrhea), and particular those with penicillin allergies.

1.3.3 Mechanism of Action

Aminoglycoside antibiotics are particularly attractive for the treatment of serious bacterial infections due to their bactericidal properties. They act by interfering with bacterial protein synthesis by binding the 30S ribosomal subunit to obstruct tRNA translocation from the A-site and P-site (Finberg, Moellering et al. 2004). This interaction thereby counteracts bacterial translation

and propagation ultimately producing a bactericidal effect (Davies, Gorini et al. 1965, Borovinskaya, Pai et al. 2007).

X-ray crystal structures have revealed the structural basis for aminoglycoside binding to the ribosomal A-site (Fourmy, Yoshizawa et al. 1998). Primarily, binding of both 4,5- and 4,6-disubstituted aminoglycosides takes place in the major groove of the 16S rRNA decoding site where they induce conformational changes of nucleotides A1492 and A1193, which are universally conserved in the prokaryote-specific binding pocket (Recht, Douthwaite et al. 1999, Bottger, Springer et al. 2001). Ultimately, the effectiveness of aminoglycoside-induced miscoding stems from their ability to mimic the conformation of the codon-anticodon recognition site (Tsai, Uemura et al. 2013).

1.3.4 Aminoglycoside Resistance

There are five major mechanisms microbes utilize to impart aminoglycoside resistance: (a) revision of the 30S ribosomal subunit target by mutation, (b) methylation of aminoglycoside binding targets, (c) decrease in intracellular aminoglycoside concentrations by active efflux pumps, (d) reduction of effective aminoglycoside concentration by decreased inner membrane transport or changes of outer membrane permeability, and (e) substrate deactivation by aminoglycoside modifying enzymes (AMEs) (Jana and Deb 2006, Shakil, Khan et al. 2008, Ramirez and Tolmasky 2010, Zgurskaya, Weeks et al. 2015). 30S ribosomal mutations can occur in the A-site, which alters physiochemical base-stacking interactions to affect shape, dynamics, and electrostatic properties. The resulting changes disrupt aminoglycoside-RNA binding interactions necessary for tRNA recognition (Romanowska, McCammon et al. 2011). *M. tuberculosis* is a significant human health example of 30S ribosome mutational accumulations that evade aminoglycoside utility. *M. tuberculosis* directly mutates its 16S rRNA, as well as the

ribosomal S12 protein, to achieve resistance. Interestingly, some variants can then go on to become aminoglycoside dependent, with the antibiotic actually lowering rates of translation error instead of the intended, opposite effect (Mayers 2009).

Ribosomal RNA modification by methyltransferases to circumvent aminoglycoside recognition also presents a dire dilemma (Liou, Yoshizawa et al. 2006, Dunkle, Vinal et al. 2014). Most notably, New Delhi metallo-β-lactamase 1 (NDM1) drug-resistant microorganisms are a cause for alarm, as these bacteria are often resistant to several different classes of antibiotics (Hidalgo, Hopkins et al. 2013, Fair and Tor 2014, Lee, Vasoo et al. 2014). With respect to aminoglycoside susceptibility, the *NDM1* gene has been observed to be associated with the gene that encodes RmtF 16S rRNA methyltransferase (Lee, Vasoo et al. 2014). This implies that bacteria possessing such a resistance plasmid, as has been observed in *Klebsiella pneumoniae*, are completely unresponsive to many clinically used β-lactam and all 4,6-disubstituted aminoglycoside antibiotics (Galimand, Courvalin et al. 2012, Hidalgo, Hopkins et al. 2013).

Furthermore, efflux pumps play a significant role in aminoglycoside resistance amongst *Salmonella, Escherichia coli,* and *Pseudomonas aeruginosa* clinical isolates (Rosenberg, Ma et al. 2000, Poole 2005, Samadi, Pakzad et al. 2015). *E. coli* such as pathogenic *E. coli* O157:H7, and opportunistic pathogen *Acinetobacter baumannii,* are just two examples of gram-negative bacteria with a high rate of aminoglycoside resistance due to encoding aminoglycoside efflux pumps (Rosenberg, Ma et al. 2000, Magnet, Courvalin et al. 2001). In *E. coli*, AcrD is one such transporter, whose presence decreases bacterial aminoglycoside concentration to ineffective levels by an impressive factor of two to eight (Rosenberg, Ma et al. 2000).

Additionally, anaerobic bacteria alter outer membrane permeability as well as inner membrane transport in response to environmental cues and are inherently more difficult to target

with aminoglycoside antibiotics. *E. coli* and *Clostridium perfringens* are both major causes of food poisoning (Emsley, Lohkamp et al. 2010). When grown anaerobically, *E. coli* and *C. perfringens* become resistant to gentamicin and other aminoglycoside antibiotics due to decreased membrane potential. A quinone oxidation-reduction cycle is required for aminoglycoside trafficking, rendering the aminoglycoside class ineffectual for the majority of anaerobes as well as facultative anaerobes under such low oxygen conditions (Bryan and Kwan 1981). However, the principal aminoglycoside resistance mechanism remains direct enzyme catalysis as carried out by aminoglycoside modifying enzymes (Ramirez and Tolmasky 2010, Vaziri, Peerayeh et al. 2011). For this reason, these enzymes are of great medical and pharmacological interest, and will be discussed in further detail below.

1.3.5 Aminoglycoside Modifying Enzymes

Enzymatic aminoglycoside inactivation is carried out by acetylation, phosphorylation, or nucleotidylation. A class of enzymes expressed by pathogenic bacteria has the ability to carry out each mechanism: N-acetyltransferases (AACs), O-phosphotransferases (APHs), and O-nucleotidyltransferases (ANTs) (Shaw, Rather et al. 1993). Aminoglycoside N-acetyltransferases (AACs) are a major source of resistance in gram-negative bacteria such as Enterobacteriacae, but are also found in gram-positive organisms, such as Staphylococci, Enterococci, and Streptococci (Ferretti, Gilmore et al. 1986, Miller, Sabatelli et al. 1997, Wolf, Vassilev et al. 1998). AACs utilize acetyl-CoA as a donor to facilitate N-acetylation of aminoglycoside antibiotics. Aminoglycosides have many amine functional groups, and AACs have been found that modify the deoxystreptamine ring and 6-aminohexose ring through amino group acetylation (Benveniste and Davies 1973, Foster 1983, Lovering, White et al. 1987).

Aminoglycoside O-phosphotransferases (APHs) are primarily found in gram-positive bacteria such as S. aureus, complications of which can cause serious skin infection and toxic shock syndrome (Gray and Fitch 1983, Fong and Berghuis 2002, Thompson, Boehr et al. 2002). Interestingly, APH presence is known to confer a high level of aminoglycoside resistance (Shi and Berghuis 2012, Shi, Caldwell et al. 2013). APHs bind ATP or GTP as the phosphate donor. The APHs then transfer the γ-phosphate from the nucleotide triphosphate to a hydroxyl group of the aminoglycoside, succeeded by release of modified substrate and ADP or GDP (Shi and Berghuis 2012, Shi, Caldwell et al. 2013)

Aminoglycoside O-nucleotidyltransferases (ANTs) are a major source of aminoglycoside resistance found amongst gram-negative clinical organisms, such as Enterobacteriaceae and Pseudomonas, which are prevalent pathogens in food poisoning and cystic fibrosis (Miller, Sabatelli et al. 1997, Davies 2002). The ANT class catalyzes a nucleotidyltransfer reaction, where ATP binds to the enzyme followed by the aminoglycoside substrate. ANTs nucleotidylate the aminoglycoside by direct nucleophilic attack of the aminoglycoside hydroxyl on the ATP molecule α-phosphate (Van Pelt, Iyengar et al. 1986). This reaction covalently links AMP to the now modified aminoglycoside, releasing pyrophosphate, and the modified aminoglycoside no longer efficiently impedes bacterial translation. Acetylation, phosphorylation, or nucleotidylation all decrease modified-aminoglycoside recognition of the 30S ribosome by 10-15-fold, such that bacterial translational error never approaches toxic levels (McKay, Thompson et al. 1994, Thompson, Hughes et al. 1996, Disney 2012, Salian, Matt et al. 2012).

1.3.6 Aminoglycoside Drug-Target Network

The number of enzymes identified that are able to confer resistance to aminoglycoside antibiotics through acetylation, phosphorylation, or nucleotidylation have been steadily growing.

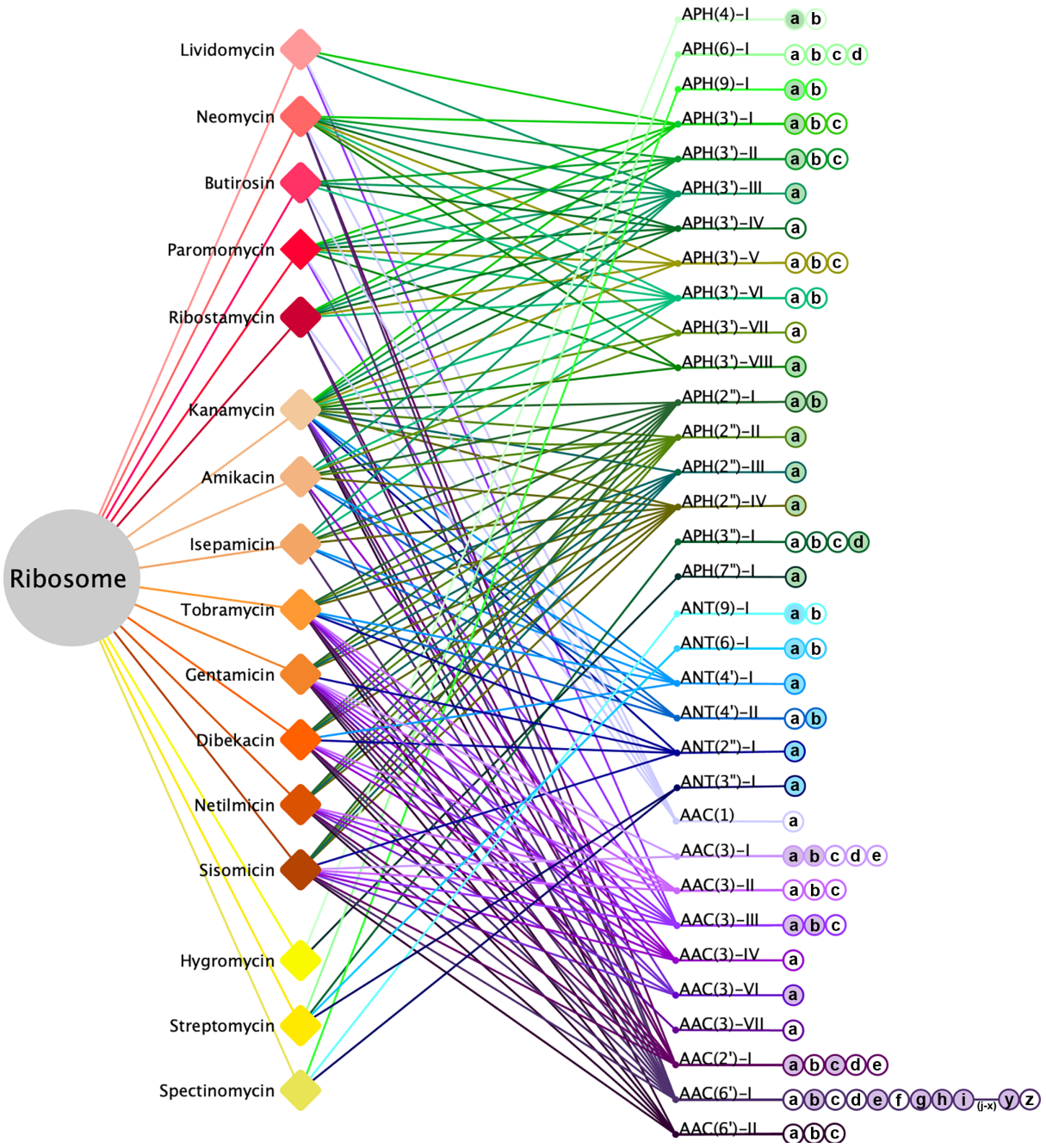

Figure 1 – 3. Aminoglycoside drug-target network. Drug-target network of known aminoglycosides with modifying enzymes. The bacterial ribosome is the primary node (grey). Aminoglycosides are represented as diamonds and are separated into their three classes: 4,5-disubstituted aminoglycosides (red), 4,6-disubstituted aminoglycosides (orange) and non-deoxystreptamine aminoglycosides (yellow). Aminoglycoside interactions with the ribosome are depicted as lines colored according to their corresponding diamond. AME nodes are colored by enzyme class: APH's (green), ANT's (blue), and AAC's (purple). Lines colored according to their corresponding modifying enzyme represent interactions of AMEs with their respective aminoglycosides. Enzymes are listed in numerical order and according to their gene nomenclature (ex: a, b, c) as hollow nodes. Solid colored nodes represent enzymes with a currently known structure (Bacot-Davis, Bassenden et al. 2016).

Currently, nearly a hundred different bacterial enzymes have been described, most identified in clinical isolates. Anticipating the deluge, Shaw in 1993, systematized the nomenclature of these enzymes, in which the enzyme name reflects its modification activity, the site of modification on the antibiotic, and the antibiotic substrate spectrum (Shaw, Rather et al. 1993). If multiple enzymes were found with the identical activity, subscripts were additionally used as unique identifier. Nonetheless, the plethora of enzymes and the diversity of aminoglycosides they provide resistance to have become sufficiently complex to present and describe aminoglycoside resistance in the format of a drug-target network (Figure 1 – 3).

Describing enzyme mediated aminoglycoside resistance as a drug-target network highlights the complexity facing those that pursue avenues to combat antibiotic resistance. As shown in Figure 1 – 3, aminoglycoside antibiotics are able to interact with the ribosome, thereby precipitating a cascade of events that ultimately results in a bactericidal outcome, or alternatively can interact with a large number of different resistance enzymes that will detoxify the drug. Simplistically, this illustration emphasizes that overcoming resistance implies blocking or avoiding interactions with a large number of AMEs.

While the aminoglycoside drug-target network emphasizes and highlights the complexity of AME mediated resistance, it also can enable the prioritization of avenues for addressing this phenomenon. The addition of currently known structural data can suggest a hierarchy of which enzymes are lacking detailed information on their drug-target interactions. Prior to the commencement of this thesis, an abundance of structural data was available for aminoglycoside interactions with AAC and APH enzymes; however, similar information for ANT enzymes was limited to one structure, ANT(4')-IIb. Although there are significantly fewer aminoglycosides that can be detoxified by ANTs compared to AACs and APHs, this enzyme class still houses a number

of clinically relevant AMEs, including ANT(2") (Table 1). Including additional structural data to build a comprehensive drug-target network is a significant step in pursuing new therapeutic avenues.

Table 1 – 1. Susceptibility of Aminoglycosides to AMEs. For each aminoglycoside antibiotic information is provided on the site(s) of modification, which AME class performs the modification(s), and how many different enzymes are capable of rendering the aminoglycoside ineffective (Bacot-Davis, Bassenden et al. 2016).

	Position of Modification by:			**No. AACs**	**No. APHs**	**No. ANTs**	**Total AMEs**
Antibiotic	**AACs**	**APHs**	**ANTs**				
Lividomycin	1, 3	3'	-	4	4	0	8
Neomycin	1, 2', 6'	3'	-	32	15	0	47
Butirosin	1, 6'	3'	-	27	15	0	42
Paromomycin	1, 3	3'	-	15	15	0	30
Ribostamycin	1, 2', 6'	3'	-	32	13	0	45
Kanamycin	3, 2', 6'	3', 2"	4', 2"	40	20	4	64
Amikacin	3, 6'	3', 2"	4'	27	8	3	38
Isepamicin	6'	3', 2"	4'	26	7	3	36
Tobramycin	3, 2', 6'	2"	4', 2"	48	5	4	57
Gentamicin	3, 2', 6'	2"	2"	48	5	1	54
Dibekacin	3, 2', 6'	3', 2"	4', 2"	41	5	2	48
Netilmicin	3, 2', 6'	2"	-	42	5	0	47
Sisomicin	3, 2', 6'	2"	2"	48	5	1	54
Hygromycin	-	4, 7"	-	0	3	0	3
Streptomycin	-	6, 3"	6, 3"	0	7	3	10
Spectinomycin	-	9	9, 3"	0	2	3	5

1.4 Aminoglycoside O-Nucleotidyltransferase (2″)

1.4.1 Prevalence

ANT(2″), encoded by the plasmid borne *aadB* gene, was first identified in 1971 in a gentamicin-resistant strain of *Klebsiella pneumonia* (Benveniste and Davies 1971, Schmidt 1984) The *aadB* gene is located on Tn-21-related transposons and is widely distributed as a gene cassette in class 1 and 2 integrons (Schmidt 1984, Vakulenko and Mobashery 2003, Ramirez, Quiroga et al. 2005) Due to its gene's presence on mobile genetic elements, ANT(2″) causes widespread aminoglycoside resistance amongst Gram-negative bacterial pathogens (Shaw, Rather et al. 1993, Poole 2005). Moreover, ANT(2″) serves as the most frequent mechanism of aminoglycoside resistance amongst clinical isolates in North America and is the largest determinant of aminoglycoside resistance in *Pseudomonas aeruginosa* (Miller, Sabatelli et al. 1997, Denisuik, Karlowsky et al. 2015).

1.4.2 Catalytic and Kinetic Mechanism

Due to its clinical importance, many attempts have been made to elucidate the kinetic mechanism of ANT(2″) (Van Pelt, Iyengar et al. 1986, Gates and Northrop 1988a, Gates and Northrop 1988b, Gates and Northrop 1988c, Wright and Serpersu 2005, Bassenden, Park et al. 2020). ANT(2″) catalyzes the adenylation of the 2″-hydroxyl group of its aminoglycoside substrates. In 1988, Gates and Northrop speculated, based on velocity patterns and dead-end inhibition studies, that the kinetic patterns were consistent with ANT(2″) utilizing a Theorell-Chance kinetic mechanism (Figure 1 – 4) (Gates and Northrop 1988b). The order of substrate binding and product release was proposed, where Mg-ATP binds followed by an aminoglycoside, and pyrophosphate is released prior to modified aminoglycoside (Figure 1 – 4) (Gates and Northrop 1988b). Still, detailed studies of this enzyme's catalytic mechanism have been hindered

by the low stability and solubility of overexpressed ANT(2″) (Van Pelt and Northrop 1984, Wright and Serpersu 2004).

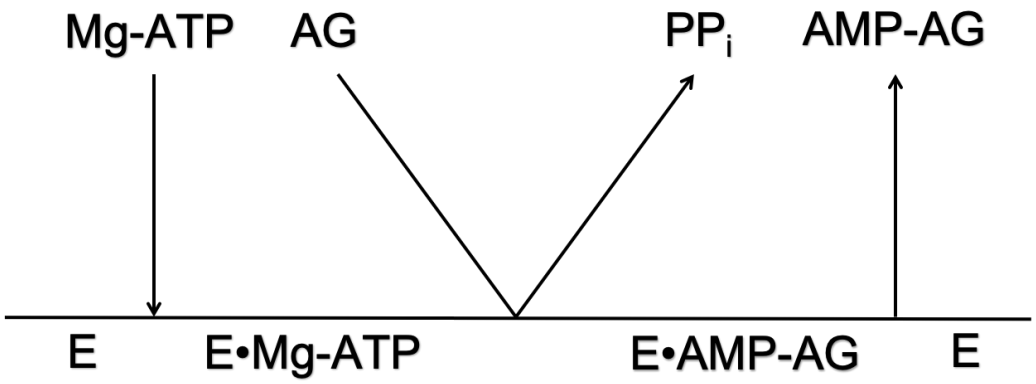

Figure 1 – 4. Putative Reaction Scheme of ANT(2″). Cleland diagram of proposed Theorell-Chance kinetic mechanism, where the apo enzyme (E) binds to Mg-ATP, followed by aminoglycoside (AG), the nucleotidyltransfer reaction occurs and pyrophosphate (PP_i) is released first, followed by the adenylated aminoglycoside (AMP-AG), thereby reconstituting the apo enzyme. Figure adapted from Gates and Northrop 1988a.

1.4.3 Substrate Specificity

ANT(2″) can chemically detoxify a broad range of naturally-occurring 4,6-disubstituted aminoglycosides, including kanamycin, tobramycin, gentamicin, dibekacin, and sisomicin (Cameron, Groot Obbink et al. 1986). To extend their clinical value, a number of these aminoglycosides have been the subject of next-generation analogue development. Derivative antibiotics, including amikacin, arbekacin, netilmicin and plazomicin, have been constructed using the aminoglycoside core (Coates, Halls et al. 2011). These antibiotics can evade the action of several AMEs, including ANT(2″) (Price, DeFuria et al. 1976). Although these semisynthetic derivatives all incorporate a hydroxyl-group at their 2″ position, a chemical substitution at their N1 position interferes with ANT(2″)'s ability to detoxify them.

1.5 Next-generation Aminoglycosides Resistance

1.5.1 Plazomicin

The latest aminoglycoside approved for clinical use in 2018, plazomicin, was identified as a potential agent to combat emerging clinical drug-resistant bacteria from over 400 sisomicin analogues in a focused medicinal chemistry campaign (Aggen, Armstrong et al. 2010). This next-generation semi-synthetic derivative of sisomicin incorporates a modification at the N1 position, identical to amikacin, and a second modification on the N6′ position (Figure 1 – 2). Plazomicin also lacks 3′- and 4′-hydroxyl groups, protecting it from modification by enzymes capable of inactivating amikacin, enhancing the scope of its activity against AME-possessing pathogens (Armstrong and Miller 2010, Zhanel, Lawson et al. 2012, Shaeer, Zmarlicka et al. 2019). This new antibiotic has already proven effective, displaying broad-spectrum activity against methicillin-resistant *S. aureus* and other multi-drug resistant pathogens in Gram-negative bacteria (Zhanel, Lawson et al. 2012, Bassetti and Righi 2015, Olsen and Carlson 2015). Although the chemical additions at Plazomicin's N-1 and N-6′ position substantially increase its protection against most AMEs, plazomicin is still susceptible to this prevalent mechanism of aminoglycoside resistance (Shaeer, Zmarlicka et al. 2019).

1.5.2 Action of AAC(2′)-Ia Against Plazomicin

It is predicted that AME-mediated resistance for plazomicin is limited to select enzymes capable of modifying amino moieties at the 2′ position (Armstrong and Miller 2010). Aminoglycoside 2′-N-acetyltransferase-Ia [AAC(2′)-Ia] is chromosomally found in *Providencia stuartii* (Rather, Orosz et al. 1993). Currently, there are few observations of this AME in clinical strains, and there is no evidence that this resistance factor has transferred to other Enterobacteriaceae (Shaw, Rather et al. 1993, Armstrong and Miller 2010). In addition to its ability

to inactivate plazomicin, AAC(2′)-Ia can also utilize Acetyl-CoA as a co-substrate to modify other 4,6-disubstituted aminoglycosides, including gentamicin, tobramycin, dibekacin, kanamycin, and netilmicin (Ramirez and Tolmasky 2010). Although this enzyme's substrate specificity is remarkably similar to that of ANT(2″)-I, AAC(2′)-Ia's ability to modify N-1 substituted semi-synthetic aminoglycosides will undoubtedly increase its clinical relevance as plazomicin usage becomes more frequent (Bassenden, Rodionov et al. 2016).

1.6 Thesis Objectives

This thesis aims to generate an in-depth understanding of the underlying working mechanism of ANT(2″) through the elucidation of their three-dimensional structures. Ultimately, these structural insights will contribute to the knowledge behind their ability to bind and modify their aminoglycoside substrates, which can, in turn, aid in the design of novel drugs capable of evading the activity of this widespread resistance enzyme. Additionally, we aim to understand AAC(2′)'s unique ability to bind and modify the only available next-generation aminoglycoside, plazomicin. Understanding the structure and function of these two resistance enzymes is critical to ensure that viable treatment options remain available against antibiotic-resistant organisms.

In Chapter 2, we focus on the nucleotide binding site of ANT(2″) and address the following questions:

- How does the ANT(2″) nucleotide binding pocket change between the substrate-bound, intermediate-like, and product-bound states of the enzyme?
- How can structural and kinetic data inform the underlying kinetic mechanism of ANT(2″)?
- What are the critical residues involved in the catalytic cycle of ANT(2″)?

In Chapter 3, we focus on the aminoglycoside binding site of ANT(2″) and undertake the following points:

- How does ANT(2″) interact with two of its clinically relevant aminoglycoside substrates, tobramycin and gentamicin?
- How do other enzymes within the tobramycin and gentamicin clinical resistome interact with these antibiotics, and how does this compare with their binding to their intended target, the ribosomal A-site?

- What inferences can be made about next-generation aminoglycoside drug design based on these binding patterns?

Finally, in Chapter 4, we focus on four structures of AAC(2′)-Ia that describe the enzyme's aminoglycoside binding pocket and examine the following topics:

- How is AAC(2′)-Ia able to detoxify a wide range of chemically unique 4,6-disubstituted aminoglycosides?
- How can these structures help infer the substrate specificity of other AAC(2′) homologues?
- Based on this homologue analysis, what speculations can be made concerning the future of plazomicin resistance?

Chapter 2 – Revisiting the Catalytic Cycle and Kinetic Mechanism of ANT(2″): A Structural and Kinetic Study

2.1 Preface

The primary mechanism of aminoglycoside inactivation is through chemical modification by resistance enzymes. ANT(2″) is decidedly the most prevalent nucleotidyltransferase resistance factor and is widespread amongst clinical pathogens worldwide. Dissecting the underlying kinetic and catalytic mechanism of ANT(2″) at a near-atomic level is a critical step in advancing our fundamental knowledge of this enzyme. Moreover, this information is key for the development of novel therapies such as adjuvant inhibitors and next-generation aminoglycosides, where the latter will be discussed in chapter 3.

In this chapter, we describe three crystal structures of ANT(2″), one in a substrate-bound state in complex with tobramycin and AMPCPP, one in an inactive intermediate state in complex with tobramycin and AMP, and one in a product-bound state complex with adenylyl-2″-tobramycin and pyrophosphate. These structures capture clinical states along ANT(2″)'s reaction coordinate. Additionally, isothermal titration calorimetry (ITC)-based studies are presented that assess the order of substrate binding and product release. Combined, these results outline the kinetic and catalytic mechanism for a clinically important resistance enzyme.

Adapted with permission from Bassenden, A.V., Park, J., Rodionov, D., and Berghuis, A.M. (2020). " Revisiting the Catalytic Cycle and Kinetic Mechanism of Aminoglycoside O-Nucleotidyltransferase (2″): A Structural and Kinetic Study" ACS Chemical Biology **15**(3): 686-694.

Individual Author Contributions are as follows, with percent of overall contribution in parentheses:

Bassenden, A.V. (60%): Experimental design; protein expression, purification and crystallization; data collection and analysis; preparation of manuscript.

Park, J. (20%). Experimental design; kinetic experiments; preparation of manuscript.

Rodionov, D. (5%): Aid in data collection and analysis.

Berghuis, A.M. (15%): Supervisory guidance of experimental design; editing of manuscript.

2.2 Introduction

Antibiotics were once considered the "wonder drug" of the 20th century, leading to substantial medical breakthroughs in the treatment of infectious diseases. However, careless widespread use and misuse of antibiotics in the clinic and in animal husbandry has led to a universal resistance epidemic. If left unchecked, this global health issue is predicted to contribute to a 90% increase in antimicrobial resistance-related deaths by the year 2050 (World Health Organization 2014).

One broad-spectrum sub-class of antibiotics, aminoglycosides, are used in the treatment of serious infections caused by Gram-positive and -negative bacteria (Becker and Cooper 2013). At present time, resistance is observed for every aminoglycoside in use (Becker and Cooper 2013, Bacot-Davis, Bassenden et al. 2016). Though microbes employ many mechanisms to confer aminoglycoside resistance, the most prevalent mechanism by far is through enzyme-catalyzed covalent inactivation via *N*-acetylation, *O*-phosphorylation, and *O*-nucleotidylation (Shaw, Rather et al. 1993, Ramirez and Tolmasky 2010). Upon modification, altered antibiotics are consequently no longer able to bind to the ribosomal A-site, where they would otherwise induce a bactericidal effect (Moazed and Noller 1987, Carter, Clemons et al. 2000).

Aminoglycoside *O*-nucleotidyltransferases (ANT's) are a class of AMEs that confer resistance through the metal-dependent transfer of AMP from ATP to the hydroxyl groups of aminoglycosides (Gates and Northrop 1988a, Wright and Serpersu 2005). ANT(2″) is the most widespread enzyme in this class, being found in over 42% of clinical isolates around the world and is the most prevalent aminoglycoside nucleotidyltransferase resistance factor in North America (Shimizu, Kumada et al. 1985, Shaw, Rather et al. 1993, Denisuik, Karlowsky et al. 2015). This inactivating enzyme is capable of nucleotidylating the 2″-hydroxyl groups of the majority of 4,6-

disubstituted aminoglycosides, including tobramycin and gentamicin, two of the most widely used aminoglycosides in the clinic (Bassenden, Rodionov et al. 2016).

Due to ANT(2″)'s clinical importance, many efforts have focused on determining its mechanism of action. Extensive kinetic studies have previously indicated that this enzyme should follow an ordered Theorell-Chance binding mechanism in which ATP binds prior to aminoglycoside, and pyrophosphate release precedes the rate-limiting release of nucleotidylated aminoglycoside (Gates and Northrop 1988b). Moreover, studies have shown that substrate modification should occur via a direct attack from the 2″ hydroxyl resulting in a stereochemical inversion at the phosphoryl center (Van Pelt, Iyengar et al. 1986). Finally, initial structural studies have proposed Asp-86 as a catalytic residue, however, due to the absence of a nucleotide in these structures, the catalytic details are incomplete (Cox, Stogios et al. 2015).

Nucleotidylation reactions are fundamental in numerous biological processes and are intrinsic to enzymes belonging to the DNA polymerase-β (polβ) superfamily (Aravind and Koonin 1999). It has been shown that members of this family, including the repair enzyme DNA polymerase β, have structural similarities with aminoglycoside nucleotidyltransferases, including exceptionally high conservation in the active site, suggesting an evolutionary link (Holm and Sander 1995, Aravind and Koonin 1999, Cox, Stogios et al. 2015). Given the structural and functional similarities between enzymes of the polβ superfamily and ANT(2″), it is surprising that the proposed details of the reaction mechanism outlined for this aminoglycoside nucleotidyltransferase are inconsistent with the current metal-dependent two-proton transfer reactions scheme proposed for polβ family members (Castro, Smidansky et al. 2007, Cox, Stogios et al. 2015).

We report here crystal structures for three ternary complexes of ANT(2″): a tobramycin- and AMPCPP- and Mn^{2+}-bound structure, a tobramycin- and AMP-bound structure, and an adenylyl-2″-tobramycin (AMP-tobramycin), pyrophosphate- and Mn^{2+}-bound structure. These crystal structures enable the reconstruction of critical steps in the ANT(2″) catalytic cycle. Moreover, we describe kinetic data obtained from product-inhibition studies that independently corroborate key aspects of the presented structural analysis. Our results expand on the previously reported catalytic mechanism and corrects the kinetic mechanism for ANT(2″).

2.3 Experimental procedures

2.3.1 Cloning

The ANT(2″) gene was generously provided by E. H. Serpersu (Ekman, DiGiammarino et al. 2001). ANT(2″)'s open reading frame was amplified by PCR using oligonucleotides 5′-AAACATATGGACACAACGCAGGTCACA-3′ and 5′-AAAGCGGCCGCGGCCGCATATCG-3′. The PCR product was sub-cloned into the pET-22b(+) expression vector between the *NdeI* and *NotI* restriction sites and verified by DNA sequencing; the resulting vector was used to transform *E. coli* BL21(DE3) cells.

2.3.2 Expression and purification

Protein expression was carried out according to the Studier method for auto-induction as described in (Studier 2005). Briefly, a 1mL non-inducing starter culture grown in ZYP-0.8G was used to inoculate 1L of ZYP-5052 auto-inducing media containing 100 mg mL^{-1} ampicillin. The culture was incubated at 37˚C at 200 RPM for 3 hours, followed by an overnight growth at 20˚C. Cells were harvested by centrifugation at 6000g for 15 minutes at 4˚C and resuspended in 40 mL of lysis buffer containing 50 mM TRIS-HCl, pH 8.0, 200 mM NaCl, 10 mM β-mercaptoethanol, 10% (v/v) glycerol and one EDTA-free protease inhibitor tablet (Roche). Cells were then lysed by sonication and cell debris was subsequently removed by centrifugation at 50000g for 30 minutes at 4˚C. The supernatant was further clarified by filtration through a 0.22 μm syringe-driven filter. The resulting clarified material was applied on a 26mm i.d.x50mm Ni-IDA-Sepharose® column equilibrated in 50 mM TRIS-HCl, pH 8.0, 200 mM NaCl, 10 mM β-mercaptoethanol, 10% (v/v) glycerol and eluted step-wise with starting buffer supplemented with 150 mM imidazole. ANT(2″) containing fractions were identified by SDS-PAGE and pooled. The pool was desalted on HiPrep™ 26/10 Desalting column (GE) equilibrated in 25 mM piperazine, pH 5.5, 10 mM β-

mercaptoethanol and 10% (v/v) glycerol. The desalted material was applied on DEAE Sepharose® FF 26mm i.d. x 140mm column equilibrated in identical buffer and eluted with 0–400 mM NaCl gradient over 16 column volumes. ANT(2″) was determined to be non-aggregated and monodisperse in its final storage buffer consisting of 10 mM Bis-TRIS propane, pH 7.0 and 1 mM TRIS (2-carboxyethyl) phosphine hydrochloride (TCEP) using dynamic light scattering. Peak fractions from the previous DEAE column were pooled and buffer exchange was performed on the aforementioned desalting column equilibrated in the final storage buffer. ANT(2″) was then concentrated to 10 mg mL^{-1} and stored at 4˚C.

2.3.3 Crystallization

Crystals of ANT(2″) in complex with, AMPCPP, Mn^{2+} and tobramycin were grown at 22˚C using the hanging-drop vapor diffusion method. Drops contained a 1:1 ratio of 10 mg mL^{-1} ANT(2″) in storage buffer supplemented with 10 mM AMPCPP, 1 mM manganese(II) chloride and 10 mM tobramycin. Reservoir solution consisted of 100 mM MES, pH 6.0, 5% (w/v) PEG 3000 and 28% (v/v) PEG 200. ANT(2″) in complex with tobramycin and adenosine monophosphate (AMP) was crystallized at 22˚C by the sitting-drop vapor diffusion method. The best quality crystals were obtained from wells containing a 1:1 ratio of 10 mg/ml ANT(2″) in storage buffer supplemented with 10 mM AMP and 10 mM tobramycin and reservoir solution consisting of 0.04 M potassium di-hydrogen phosphate, 16% (w/v) PEG 8000 and 20% (v/v) glycerol. ANT(2″) in complex with adenylyl-2″-tobramycin, pyrophosphate and Mn^{2+} was crystallized at 22˚C using the hanging-drop vapor diffusion method. Crystals were obtained from drops containing a 1:1 ratio of 10 mg/mL ANT(2″) in storage buffer supplemented with 10 mM ATP, 10 mM tobramycin and 1 mM manganese(II) chloride and reservoir solution consisting of 100 mM sodium acetate, pH 4.5 and 22% (v/v) 1,4-butanediol. It is important to note that we

supplemented the drops for the substrate- and product-bound complexes with $MnCl_2$ instead of $MgCl_2$ to take advantage of the stronger anomalous signal from Mn^{2+} upon interaction with x-rays.

2.3.4 Data collection

The diffraction data was collected on the Rigaku home source consisting of a MicroMax-007HF generator (copper anode) fitted with a VariMax-HF optic coupled with a Saturn-944+ CCD detector mounted on an AFC-11 partial-Chi goniometer. The data collection strategy for 15-fold redundant dataset was calculated for ANT(2″) in complex with AMP and tobramycin and ANT(2″) using the *d*TREK suite* (Pflugrath 1999). Analogously, a 20-fold redundant dataset was collected for the two other ANT(2″) complexes.

2.3.5 Structure solution and refinement

The data for the three structures was processed using the *xia2* pipeline (Winter 2010) [*CCP4* (Collaborative Computational Project 1994), *POINTLESS* (Evans 2006), *XDS* (Kabsch 2010)]. The structure of ANT(2″) in complex with AMP and tobramycin was solved by S-SAD using the *Crank2* pipeline (Skubak and Pannu 2013) [*SHELXC* (Sheldrick 2008), *SHELXD* (Sheldrick 2008), *REFMAC5* (Murshudov, Skubak et al. 2011), *Solomon* (Abrahams and Leslie 1996), *Multicomb* (Skubak, Waterreus et al. 2010), *Parrot* (Cowtan 2000), *Buccaneer* (Cowtan 2006)]. The structures of ANT(2″) in complex with tobramycin, AMPCPP and Mn^{2+}, and in complex with adenylyl-2″-tobramycin, pyrophosphate and Mn^{2+} were solved by molecular replacement with the AMP-tobramycin complex as the search model using *Phaser* (McCoy, Grosse-Kunstleve et al. 2007). All three structures were refined by iterative cycles of reciprocal-space refinement with *phenix.refine* (Adams, Afonine et al. 2010) and real-space refinement and model building in *Coot* (Emsley, Lohkamp et al. 2010). The presence of manganese ions in the tobramycin and AMPCPP complex and in the adenylyl-2″-tobramycin and pyrophosphate

complex were validated using *ANODE* (Thorn and Sheldrick 2011). The dictionaries for AMP, AMPCPP, tobramycin, pyrophosphate and adenylyl-2″-tobramycin were generated with the *GRADE* server v.1.2.7 (http://grade.globalphasing.org/)**.** Final refinement statistics are listed in table 2.1.

2.3.6 Kinetic Assay

The assay was carried out by reaction calorimetry at 30 °C with a MicroCal iTC200 system (Malvern). The purified enzyme was dialyzed overnight against reaction buffer (10 mM Bis-TRIS propane, pH 7.0), and the substrate, product inhibitor, and $MgCl_2$ solutions were prepared in the used dialysate. We used $MgCl_2$ because (although we used $MnCl_2$ for the crystallization experiments) Mg^{2+} is the preferred divalent cation required for ANT(2″) activity (Wright and Serpersu 2005). First, to determine the molar enthalpy of reaction (ΔH), 10 μL of 5 mM kanamycin solution was injected into the calorimetric cell containing 5 mM $MgCl_2$, 500 μM ATP, and 2 μM ANT(2″). The volume of the reaction chamber was 200 μL. In the alternate experiment that demonstrated substrate inhibition, 10 μL of 5 mM ATP was used as the injectant, and the cell solution contained 500 μM kanamycin instead of ATP. Heats of dilution were measured in an analogous titration without the enzyme and subtracted from the actual reaction data. The data were processed with the Origin software package provided with the ITC instrument. Briefly, ΔH was determined based on the following relationship:

$$\boldsymbol{Q = n\Delta H = [S_0]V\Delta H}, \text{ (i)}$$

in which Q is the total heat associated with producing n moles of the product, $[S_0]$ is the starting concentration of the limiting substrate, and V is the volume of the calorimetric cell. Q was calculated by integrating the thermal power (dQ/dt) measured over the complete course of the reaction, whereas $[S_0]$ and V were known. Once ΔH was determined (-7.735 kcal/mol; Figure 2 –

4), the substrate concentration ([*S*]) could be determined as a function of time as described in the following equation:

$$[\boldsymbol{S}] = [\boldsymbol{S_0}] - \frac{\int_0^t \frac{\boldsymbol{dQ}}{\boldsymbol{dt}}\boldsymbol{dt}}{\boldsymbol{V\Delta H}}, \text{ (ii)}$$

and the rate of reaction calculated from dQ/dt for any given time point:

$$\boldsymbol{v} = \frac{\boldsymbol{d[P]}}{\boldsymbol{dt}} = -\frac{\boldsymbol{d[S]}}{\boldsymbol{dt}} = \frac{\boldsymbol{1}}{\boldsymbol{V\Delta H}}\frac{\boldsymbol{dQ}}{\boldsymbol{dt}}. \text{ (iii)}$$

For the subsequent kinetic studies, only the initial maximal rates were used for analysis. The starting concentration of the limiting substrate was varied from 20 to 150 μM, while those of the other substrate, $MgCl_2$, and the enzyme were kept constant at 2 mM, 5 mM, and 1 μM, respectively. To determine the kinetic parameters K_m and k_{cat}, the data were fitted to the general Michaelis-Menten equation. The data set produced with kanamycin as the limiting substrate was also fitted to the following equation accounting for substrate inhibition:

$$\boldsymbol{v} = \frac{\boldsymbol{V_{max}[S]}}{\boldsymbol{K_m + [S] + [S]^2/K_i}}. \text{ (iv)}$$

For product inhibition studies, the concentrations of added inorganic pyrophosphate (PP_i) were 125 and 250 μM when kanamycin was the limiting substrate, and 50 and 100 μM when ATP was the limiting substrate. All reactions were carried out in duplicate, and the rate data were analyzed with *GraFit 5* (Erithacus Software).

Table 2 – 1. Data Collection and Refinement Statistics of Substrate State, Intermediate State, and Product State of ANT(2″) complexes

	ANT(2″)• Tobramycin• AMP	**ANT(2″)• Tobramycin• AMPCPP•Mn^{2+}**	**ANT(2″)•Adenylyl-2″-tobramycin• PP_i•Mn^{2+}**
Data Collection Statistics			
Resolution range (Å)	47.99 - 1.88 (1.947 - 1.88)	37.1 - 1.7 (1.761 - 1.7)	30.83 - 1.82 (1.885 - 1.82)
Space group	P $4_3 2_1 2$	P $2_1 2_1 2_1$	P 2_1
Unit cell (Å, ˚)	42.0 42.0 192.0	40.7, 46.0, 90.0	46.1 41.9 47.1, 90 105.1 90
Total reflections	469834 (21389)	489594 (16066)	311065 (16977)
Unique reflections	14841 (1394)	19150 (1872)	15725 (1535)
Multiplicity	31.7 (15.3)	25.6 (8.6)	19.8 (11.1)
Completeness (%)	99.3 (96.6)	100 (100)	99.7 (97.1)
Mean I/sigma(I)	53.5 (5.1)	39.4 (3.1)	41.8 (4.3)
Wilson B-factor	22.4	17.8	18.3
R-merge	0.057 (0.56)	0.058 (0.61)	0.072 (0.62)
R-meas	0.058	0.059	0.074
$CC_{1/2}$	1.00 (0.89)	1.00 (0.83)	1.00 (0.88)
CC*	1.00 (0.97)	1.00 (0.95)	1.00 (0.97)
Refinement Statistics			
R_{work}	0.167 (0.271)	0.169 (0.218)	0.145 (0.205)
R_{free}[b]	0.188 (0.243)	0.190 (0.254)	0.174 (0.253)
Number of non-hydrogen atoms	1624	1706	1699
macromolecules	1424	1437	1388
ligands	38	92	98
water	162	177	213
Protein residues	175	176	174
RMS(bonds, Å)	0.003	0.004	0.006
RMS(angles, ˚)	0.88	0.89	1.16
Ramachandran favored (%)	99	99	98
Ramachandran outliers (%)	0	0.55	0
Clashscore	1.05	2.01	2.10
Average B-factor (Å^2)	25.7	24.2	24.5
macromolecules	25.1	22.5	23.0
ligands	18.0	28.1	25.5
solvent	32.9	35.6	34.0

[a]Statistics for the highest-resolution shell are shown in parentheses.

[b]R_{free} was calculated by randomly omitting 10% of observed reflections from refinement

2.4 Results

2.4.1 Structure Characteristics.

Three crystal structures of ANT(2″) were determined, the first in complex with AMPCPP and tobramycin refined to 1.70 Å (substrate-bound state), the second in complex with adenosine monophosphate (AMP) and tobramycin refined to 1.88 Å (inactive intermediate), and finally in complex with adenylyl-2″-tobramycin (modified aminoglycoside), pyrophosphate (PP_i) and Mn^{2+} refined to 1.82 Å (product-bound state). The discovery maps for each of the ANT(2″) crystal structures allowed us to unambiguously place its substrates and products within the enzyme's active site. (Figure 2 – 1A,B,C). Data collection and final refinement statistics for each of these crystal structures are listed in table 2 – 1. Each of the Mn^{2+}-bound complexes contain two manganese in the active site: Mn_A and Mn_B (Figure 2 – 1A,C).

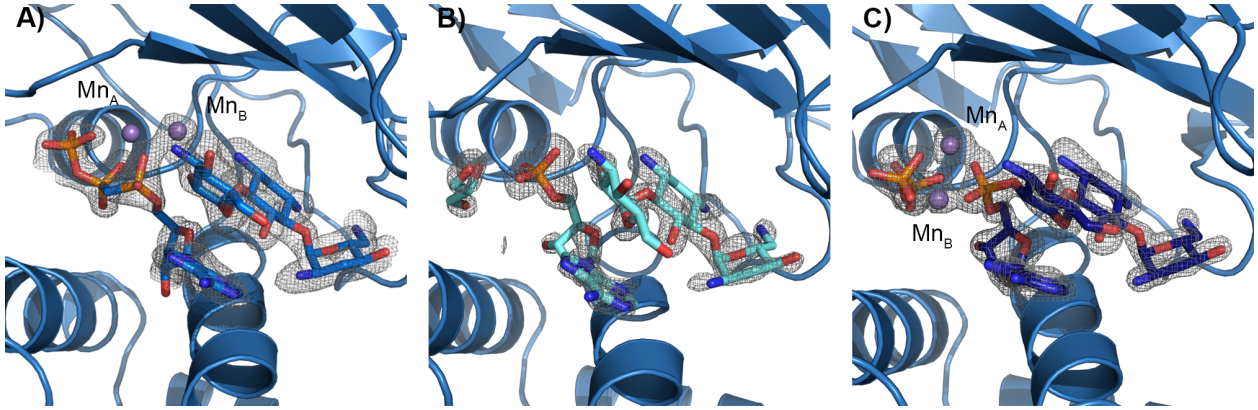

Figure 2 – 1. View of ANT(2″) active site in its substrate-bound, intermediate-like and product-bound state. In panel A, the enzyme is shown in complex with tobramycin and AMPCPP (Bassenden, Rodionov et al. 2016). The ligands are shown in stick representation and colored in blue. In panel B, the enzyme is shown in complex with tobramycin and AMP. The ligands are shown in stick representation colored in light blue. In panel C, the enzyme is shown in complex with its products, adenylyl-2″-tobramycin and pyrophosphate shown in stick representation and colored in dark blue. Also depicted in panels A and C are manganese atoms drawn as purple spheres. All three panels show the F_o-F_c discovery map for the ligands at contour level 3σ.

2.4.2 Nucleotide Binding.

Note, this Chapter focuses on the nucleotide binding site and details about the kinetic and catalytic mechanism of the enzyme; whereas Chapter 3 focuses exclusively on the aminoglycoside binding pocket and next-generation drug design. The substrate-bound form of ANT(2″) reveals that AMPCPP sits adjacent to the double prime ring of the aminoglycoside and resides in the active site cleft with the adenosine rings fairly exposed, whereas the triphosphate group is buried in the active site pocket (Figure 2 – 2A). The adenine plane is sandwiched between the aminoglycoside and the active site wall. The adenine moiety forms few interactions with the enzyme, except for parallel-displaced pi-stacking with the aromatic side chain of Tyr-135 (Figure 2 – 2A). The ribose moiety, on the other hand, is void of interactions with the enzyme and solely interacts with the 2″-OH of tobramycin, the site of aminoglycoside modification, via the internal oxygen of the ribose ring. Contrarily, the triphosphate moiety interacts with a large number of basic residues to accommodate its overall negative charge. The substrate-bound complex positions the γ-phosphate deep in the binding pocket through interactions with Arg-40, His-42, and Lys-147 (Figure 2 – 2A). Cox and colleagues previously proposed that these residues may be involved in triphosphate moiety binding, but lacked structural evidence (Cox, Stogios et al. 2015). We can now confirm that these positively charged residues play a major role in ATP binding, however, they are only involved in stabilizing the γ-phosphate. The α- and β- phosphates, on the other hand, do not participate in hydrogen bonding; however, they play an important role in coordinating both Mn^{2+} ions. The Mn^{2+} coordination site is lined by acidic residues Asp-44, -46 and -86 (Figure 2 – 3A). Mn_A is coordinated by all three phosphate groups as well as Asp-44, -46 and a water molecule in an octahedral fashion and sits high up in the AMPCPP binding pocket. Mn_B sits further outside of the active site and is coordinated by Asp-44, -46 and 86 and tobramycin, in an octahedral fashion

as well (Figure 2 – 3A). Asp-46 also interacts with the α-phosphate of AMPCPP (Figure 2 – 2A). Finally, as previously reported, Asp-86 interacts with 2″-OH modification-site of tobramycin (Figure 2 – 2A) (Cox, Stogios et al. 2015).

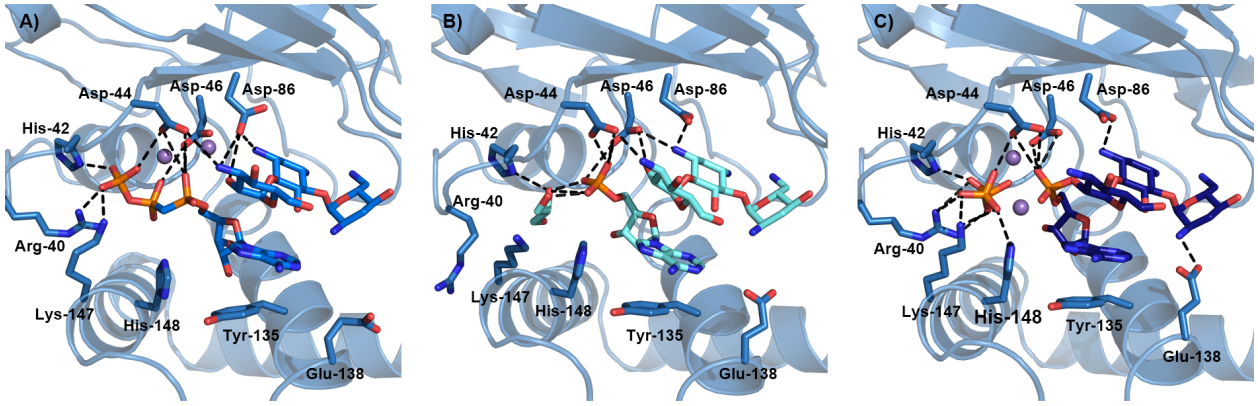

Figure 2 – 2 . Binding of ligands to ANT(2″) (A) substrate-bound state (blue) (Bassenden, Rodionov et al. 2016), (B) inactive intermediate state (light blue), and (C) product-bound state (dark blue). Black dashed lines represent hydrogen-bond interactions.

2.4.3 Product binding

Consistent with the substrate-bound form of ANT(2″), the adenosine moiety of the modified tobramycin does not form hydrogen bonds with the enzyme and the adenine ring is still capable of forming pi-stacking interactions with Tyr-135 (Figure 2 – 2C). The by-product, pyrophosphate, now sits directly perpendicular to its β- and γ-phosphate precursor and its binding pocket is still characterized by the same basic residues that house the negatively charged phosphate groups. Arg-40 and His-42 now interact with the former β-phosphate while Arg-40, Lys-147, and His-148 interact with the former γ-phosphate (Figure 2 – 2C). The most notable change in the product-bound form is the shift of Mn_B, which has now migrated to accompany the pyrophosphate leaving group, sitting between its α- and β-phosphates (Figure 2 – 2C). Moreover, the Asp-86, previously responsible for coordinating Mn_B in the substrate-bound complex has its carboxylate group rotated 90˚ from its previously occupied site (Figure 2 – 2C). On the other hand, Mn_A remains essentially stationary, still coordinated by Asp-44 and -46 and a water molecule, however,

is now also coordinated by pyrophosphate and the adenylyl phosphate group of the modified product, still in an octahedral geometry (Figure 2 – 3B). Due to the large shift in the location of Mn_B it now is coordinated by 2 water molecules, the adenylyl phosphate group of the modified product, the β-phosphate of the pyrophosphate leaving-group and the α- and β-phosphates of a second pyrophosphate, also in an octahedral geometry (Figure 2 – 3B). The most noticeable structural change between the substrate and product bound site is an additional hydrogen bond formed in the product bound state. Glu-138 flips in towards the active site, hydrogen bonding with the 2′-amine of the modified product, closing this portion of the active site (Figure 2 – 2C).

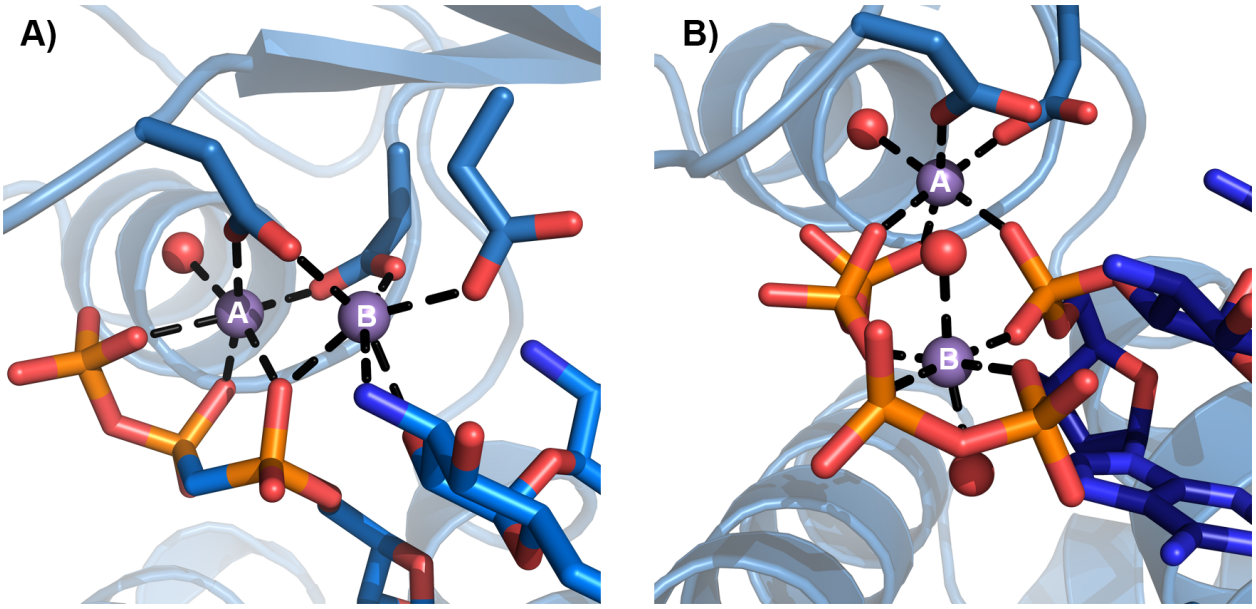

Figure 2 – 3. Mn^{2+}ion (purple) coordination in (A) substrate-bound ANT(2″) and (B) product-bound ANT(2″). Coordination demonstrated using black-dashed lines.

2.4.4 An Inactive Intermediate State.

ANT(2″) was crystallized in the absence of manganese to demonstrate an inactive form of the enzyme in complex with tobramycin and AMP, the moiety of ATP poised to be transferred to the aminoglycoside substrate. This structure also contains a glycerol molecule in the active site pocket, where the by-product pyrophosphate would sit (Figure 2 – 2B). This structure shows a possible intermediate transition state before product formation. Compared to the substrate-bound

form, AMP still sits in the same pocket as its AMPCPP precursor and forms the same interactions. The α-phosphate of AMP also sits in-between those of the substrate- and product-bound form of the enzyme. This structure reaffirms the rigidity of the enzyme, with no major structural rearrangements between this structure and the substrate- and product-bound forms of the enzyme. The absence of the β- and γ-phosphates within this structure does introduce some slight structural changes including Arg-40 and Lys-147, which would normally hydrogen bond to these phosphates in AMPCPP in the substrate-bound form and pyrophosphate in the product-bound form, now flip outward, opening up the active site at this region (Figure 2 – 2B). Slight conformational changes of Glu-138 and His-148 suggest an enclosure on the active site on the C-terminal end of the enzyme as these residues move closer into the active site pocket when progressing from the substrate-, intermediate-, and product-bound form of the enzyme (Figure 2 – 2B). Finally, the acidic group of Asp-86 is shifted 90˚ from the active site, just as in the product-bound state due to the absence of an Mn^{2+} ion at this site in both structures (Figure 2 – 2B).

2.4.5 Kinetic Analysis.

To confirm the order of substrate binding and product release revealed by the structural data, we carried out a product inhibition kinetic analysis, using PP_i as a probe. It is noteworthy that many previous kinetic studies of ANT(2″) employed the use of pyrophosphatase-coupled assays (Gates and Northrop 1988b, Ekman, DiGiammarino et al. 2001, Wright and Serpersu 2004, Wright and Serpersu 2005). With such assay systems it is impossible to challenge the reaction with PP_i. We instead used reaction calorimetry, which does not require any reporter molecules or labels. In this method, one follows the progress of a chemical reaction by monitoring the heat absorbed or released during that reaction. The heat flow is measured in terms of thermal power (μcal s^{-1}) as a function of time (s) and is directly proportional to the rate of reaction at the given time point. If

the molar enthalpy of reaction (ΔH; the amount of heat exchanged per mole of product formed) is known, the rate of reaction can be calculated from the measured heat flow (see Experimental Procedures for derivation).

To first determine the molar enthalpy of ANT(2″) reaction, we measured the total heat produced in modifying 0.05 μmoles of kanamycin (red thermogram, Figure 2 – 4). The downward deflection in the thermogram reflects the exothermic nature of this reaction. After reaching its maximum output at ~20 s, the heat flow returned to baseline at ~160 s, indicating complete consumption of the limiting substrate kanamycin. ΔH was calculated as defined by eq. (i) (Experimental Procedures) and consistent between the duplicate runs at −7.8 and −7.6 *k*cal mol^{-1}. Once ΔH was determined, the thermal data could be converted into rate data and plotted as a function of product formation (red curve, Figure 2 – 4 inset). An analogous experiment with a slight modification produced an interesting result (blue curves, Figure 2 – 4). This reaction reached its peak also at ~20 s, but its maximal rate was significantly lower than that of the previous reaction (~2-fold). In addition, the heat flow decreased back to baseline at a much slower pace as the reaction continued until past 800 s. For both reactions, the catalytic endpoint was identical (i.e., 250 μM final product concentration). The only difference was the substrate added in excess; ATP

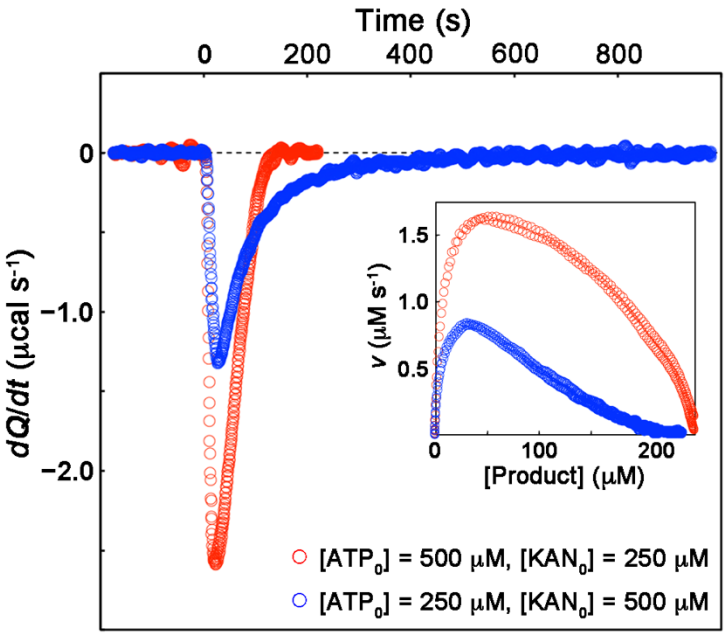

Figure 2 – 4. ANT(2″) reaction progress monitored by calorimetry. Reactions were carried out in the excess of kanamycin (thermogram in red) or ATP (blue) in duplicate (both sets are plotted). The initial molar concentrations of the substrates are indicated. Shown in the inset are the rate data calculated from the primary thermal data.

for the former (i.e., red) and kanamycin for the latter (blue). These observations suggest that ANT(2″) activity is inhibited in the presence of excess kanamycin. Previous studies have also reported substrate inhibition by kanamycin and nearly all other aminoglycosides (Gates and Northrop 1988a, Wright and Serpersu 2005).

We next carried out initial rate studies to investigate the effects of PP_i on ANT(2″) kinetics (left panel, Figure 2 – 5). The Michaelis-Menten parameters determined in the absence of PP_i were comparable to the previously reported literature values (Wright and Serpersu 2005, Cox, Stogios et al. 2015). In the presence of added PP_i, initial rates decreased in a concentration- and substrate-dependent manner. Clear inhibition was observed with 50 and 100 μM PP_i when kanamycin was the saturating substrate (middle panel, Figure 2 – 5A; K_i = 26.7 μM). With ATP as the saturating substrate, higher concentrations of PP_i were required to produce appreciable levels of inhibition (middle panel, Figure 2 – 5B; K_i = 369.8 μM). Regardless of the presence of added PP_i, substrate inhibition by kanamycin was present (at 140 μM; middle panel, Figure 2 – 5B). While these results hint at the mode of inhibition by PP_i, the double-reciprocal plots clarify it unequivocally; PP_i is a competitive inhibitor with respect to ATP (right panel, Figure 2 – 5A) and a noncompetitive inhibitor with respect to kanamycin (right panel, Figure 2 – 5B). The directly competitive relationship between ATP and PP_i agrees well with the kinetic mechanism alluded by our crystal structures; ATP is the first substrate to bind, and PP_i is the last product to be released.

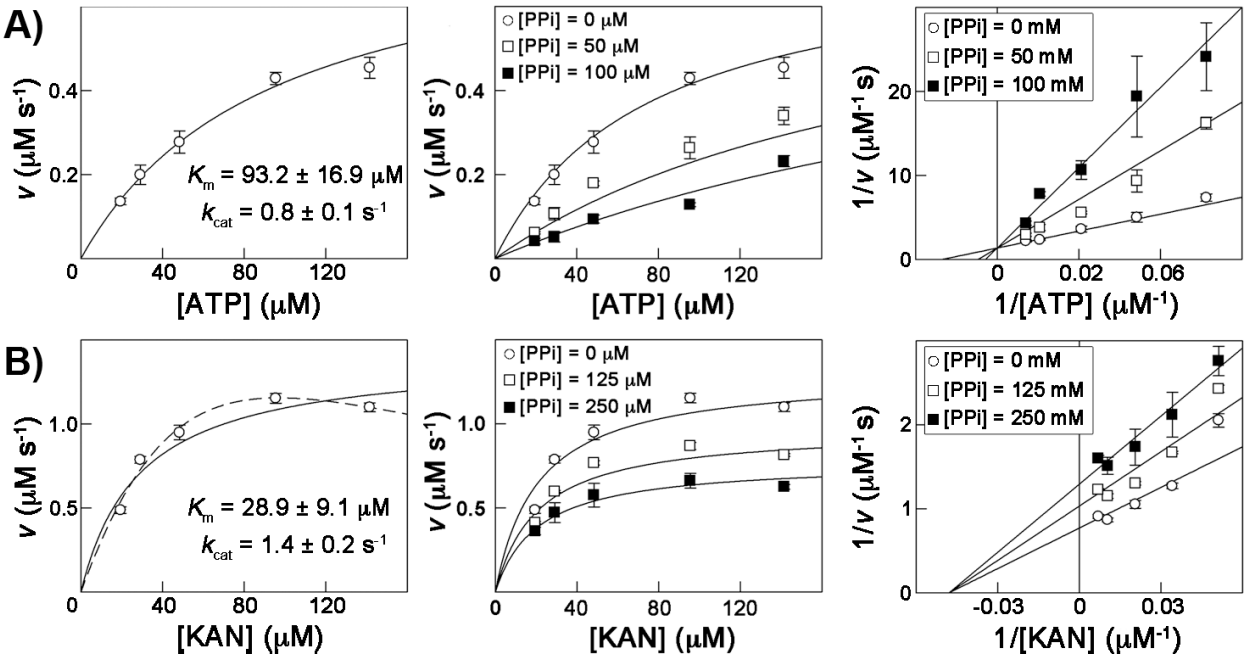

Figure 2 – 5. Analysis of ANT(2″)'s kinetic activity. In the left and middle pannels, initial rates were determined at a fixed concentration of kanamycin (A) and ATP (B). Left panels show Michaelis-Menten plots and the kinetic parameters determined. The dotted line represents a curve fit to Eq. (4) (see Experimental Procedures). In the middle panels, the curves represent non-linear regression fit of the data to the Michaelis-Menten equation for competitive inhibition (A) and noncompetitive inhibition (B). The initial molar concentration of PPi is indicated. Ki values were determined to be 26.7 μM in (A) and 369.8 μM in (B). In the right panels are Lineweaver-Burk plots showing product inhibition by PP_i. The plot in (B) shows a profile characteristic of substrate inhibition; high concentration data points start trending up along the y-axis.

2.5 Discussion

2.5.1 Structures of ANT(2″).

The nucleotide-binding site is important when considering therapeutics such as inhibitor design. Notably, analogous to what is pursued for enzymes that confer resistance to aminoglycosides through phosphorylation, inhibitors that block the nucleotide-binding site of ANT(2″) can find use as potential adjuvants to be used in conjunction with aminoglycosides (Burk and Berghuis 2002, Fong, Burk et al. 2005, Shi, Caldwell et al. 2013). Our crystal structures are allowing us to analyze ANT(2″)'s nucleotide-binding pocket in three states: the substrate-bound state characterized by the AMPCPP-tobramycin-Mn^{2+} complex, the product-bound state characterized by the adenylyl-2″-tobramycin-PP_i-Mn^{2+} complex and the intermediate state characterized by the AMP-tobramycin complex. These various views of the nucleotide-binding site will aid in the development of specific inhibitors to this widespread and prevalent antibiotic resistance mechanism.

2.5.2 The order of substrate binding and product release

In a three-part kinetic study of ANT(2″), Gates and colleagues supported a previously established order of substrate binding, in which metal-complexed nucleotide binds before the aminoglycoside substrate (Lombardini and Cheng-Chu 1980, Gates and Northrop 1988a, Gates and Northrop 1988b, Gates and Northrop 1988c). These studies were performed in the absence of any structural data. Cox and colleagues also suggested that this order was correct, but based their assertion only on a binary kanamycin-bound structure (Cox, Stogios et al. 2015). Our crystal structure of the ternary substrate-bound form is consistent with the suggested order of binding. In absence of any structural rearrangements, ATP binds first as the aminoglycoside blocks the active site pocket where ATP's triphosphate moiety is poised to bind. The study by Gates and co-workers

also attempted to establish the order of product release. They report that the enzyme acts via a Theorell-Chance binding mechanism where pyrophosphate is released before the modified aminoglycoside (Gates and Northrop 1988b). Structural analysis of the product-bound state of ANT(2″) reveals that pyrophosphate is buried within the active site behind the modified aminoglycoside and void of any major structural rearrangements, this action would be impossible. Our structures, on the other hand, show the opposite to be true, i.e. the modified product should leave the enzyme first, followed by pyrophosphate. Thus, an ordered sequential mechanism is proposed where: Mn-ATP binds prior to aminoglycoside and modified aminoglycoside leaves prior to PP_i.

This order of the reaction is also supported by our kinetic data. Two experiments were done when determining the enthalpy of ANT(2″) reaction, one in excess of ATP and the other in excess of kanamycin. Since this reaction proceeds in a one-to-one substrate stoichiometry, any excess of one substrate over the other is preserved throughout the entire course of reaction. Our reaction progress analysis showed that, in the presence of excess kanamycin, catalysis proceeds much more slowly (Figure 2 – 4). The initial maximal rate of the excess-kanamycin reaction was 2-fold lower than that of the excess-ATP reaction (inset, Figure 2 – 4). Furthermore, the difference in the reaction rate continued to increase as the limiting substrate was depleted (inset, Figure 2 – 4). Based on our crystal structures, substrate inhibition by kanamycin is likely a result of its binding to the enzyme first, thereby blocking the unoccupied ATP site and forming a dead-end complex. The pattern of product inhibition in this two-substrate enzyme reaction is also a clear diagnostic of the mechanism of catalysis. For an ordered Bi-Bi mechanism, the final product acts as a competitive inhibitor with respect to the first substrate and a noncompetitive inhibitor with respect to the second substrate. Our product inhibition experiments clearly demonstrated that PP_i is a

competitive inhibitor of ANT(2″) with respect to ATP (right panel, Figure 2 – 5A) and a noncompetitive inhibitor with respect to kanamycin (right panel, Figure 2 – 5B). In random kinetic mechanisms, each product can be a competitive inhibitor for each substrate.

2.5.3 The catalytic cycle of ANT(2″)

A previously resolved crystal structure of kanamycin-bound ANT(2″) had elucidated Asp-86 as the catalytic residue, but in the absence of a nucleotide, the study could not outline the entire catalytic mechanism (Cox, Stogios et al. 2015). It is well established that ANT(2″) is structurally related to the catalytic domain of DNA polymerase-β and based on the three structures presented here, it is evident that the catalytic progression is similar to that of other members of the poly-β superfamily (Holm and Sander 1995, Cox, Stogios et al. 2015). The family's namesake, DNA polymerase-β, follows a two-proton two-metal-ion-dependent reaction scheme, where the binding of the second metal ion activates the 3′ hydroxyl group of the nucleotide for the nucleophilic attack, the enzyme then accepts the proton from the hydroxyl group and finally, a second residue donates a proton to the PP_i leaving group (Castro, Smidansky et al. 2007). Although the previous study by Cox and colleagues established the proton acceptor in this reaction scheme, the rest of the catalytic cycle has not been outlined. The three crystal structures being presented here: substrate-bound, inactive intermediate and product-bound, show evidence of a similar catalytic progression for ANT(2″).

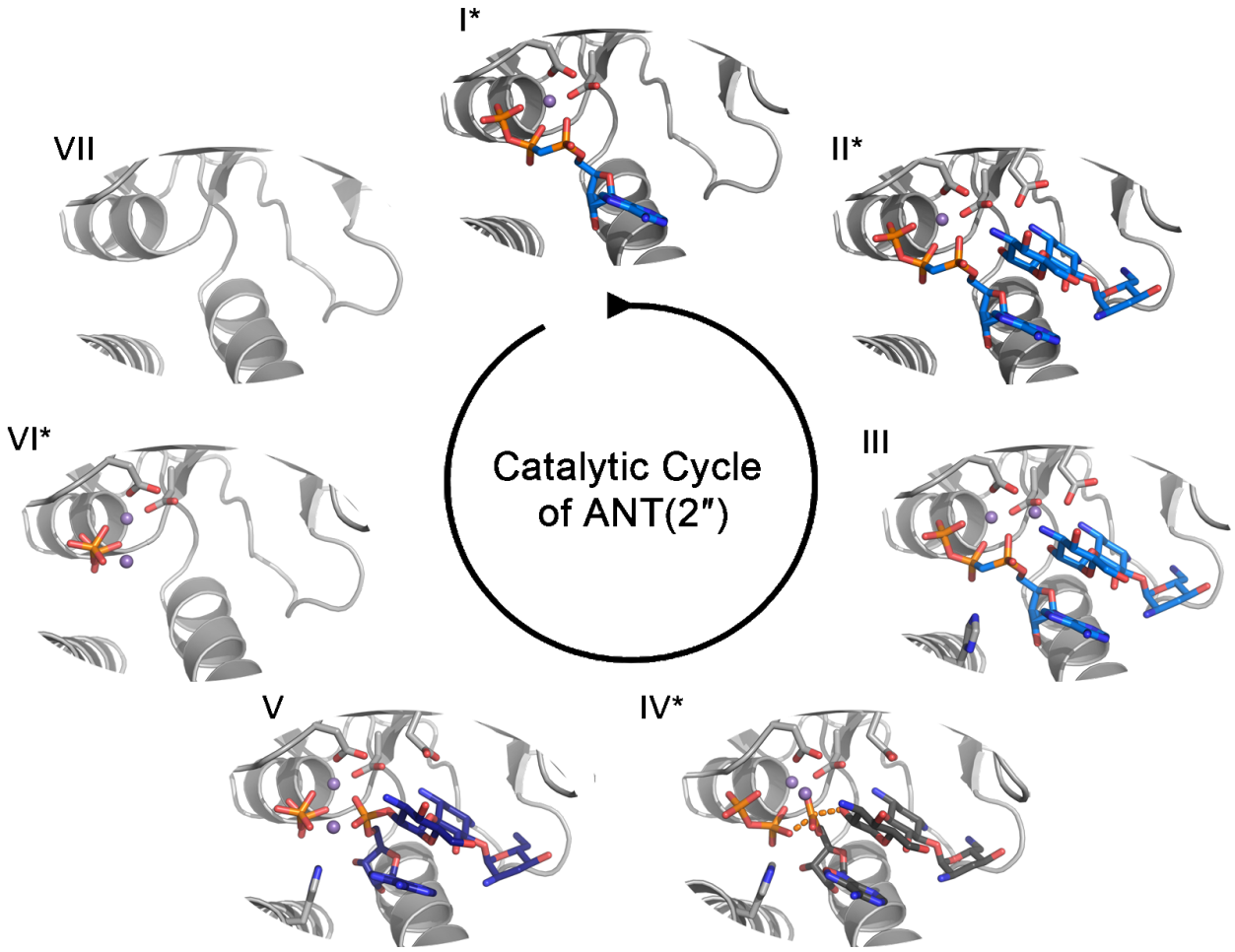

Figure 2 – 6. Complete catalytic cycle of ANT(2″). Asterisk (*) indicates a model based on its most similar structure. I) E•Mn^{2+}•ATP, II) E•Mn^{2+}•ATP•AG, III) E•2Mn^{2+}•ATP•AG (ES), IV) ES‡, V) E•2Mn^{2+}•PP_i•AMP-AG (EP), VI) E•2Mn^{2+}•PPi, VII) E

First, the substrate-bound state shows the ligand-binding progression. In step I, Mn-ATP binds first, with Mn_A coordinated by Asp-44, -46 and the ATP triphosphate group (Figure 2 – 6). Next in step II, aminoglycoside binds with the 2″-hydroxyl group interacting with Asp-86 (Figure 2 – 6). Step III involves Mn_B binding, where it is coordinated by Asp-44,-46 and -86 residues, the α-phosphate of AMPCPP and the 2″-OH. This Mn_B atom acts to lower the pKa of the 2″-OH, facilitating the proton transfer from the hydroxyl group to Asp-86, while His-148 donates a proton to the PP_i leaving group (Figure 2 – 6). It has been shown for related nucleotidyltransferases, including DNA polymerase-β, that the second metal ion in this type of reaction binds only after

the nucleotide and hydroxyl group are in place, and there is no reason to believe ANT(2″) is different (Johnson, Taylor et al. 2003, Castro, Smidansky et al. 2007). Once this metal ion binds, catalysis is then initiated (Castro, Smidansky et al. 2007). In step IV, an intermediate state was modeled using all three structures, showing the continuing progression of the reaction. This model depicts the likely "transition state" as bond-breaking and bond-formation occurs concurrently as the reaction proceeds (see above; Figure 2 – 6). In step V, the product-bound form shows that the modified tobramycin is solvent-exposed and is readily accessible to leave the enzyme, while pyrophosphate remains in the positively charged cleft (Figure 2 – 7). The Mn_B ion shifts 5Å during catalysis to coordinate the PP_i leaving group and the acidic group of Asp-86 turns 90˚ away from the active site once the reaction is complete, showing its importance in Mn_B coordination (Figure 2 – 6). Finally, steps VI and VII (Cox, Stogios et al. 2015) show the order of product release with modified aminoglycoside leaving first followed by magnesium pyrophosphate (Figure 2 – 6).

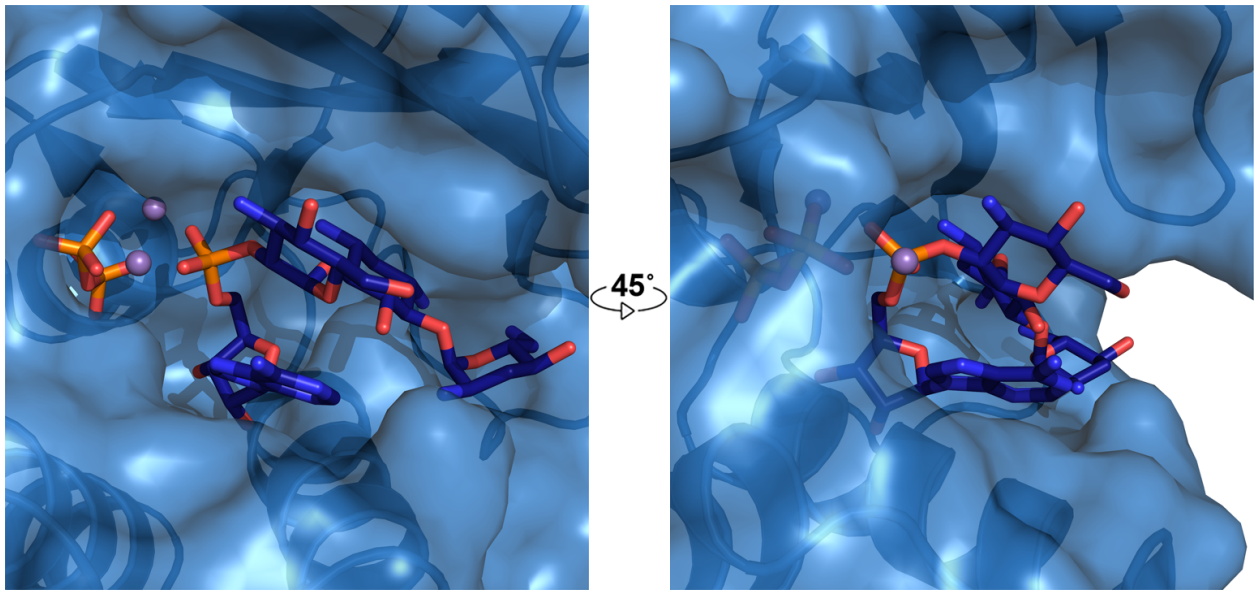

Figure 2 – 7. Active site pocket of product-bound ANT(2″).

Additionally, examination of the active site overlay between the substrate and product-bound state, the crystal structures demonstrate that the α-phosphate of AMPCPP undergoes stereochemical inversion upon product formation, a phenomenon that was predicted by Van Pelt

and colleagues in 1986 (Figure 2 – 8) (Van Pelt, Iyengar et al. 1986). This is indicative of a single displacement reaction that follows the classical S_N2 pathway. The reaction coordinate distance between the phosphorus and the entering oxygen further supports an associative substitution mechanism, with a distance of 3.8 Å before modification, allowing no room for a non-bonded metaphosphate intermediate that would be seen in a dissociative mechanism (Lombardini 1980, Mildvan 1997).

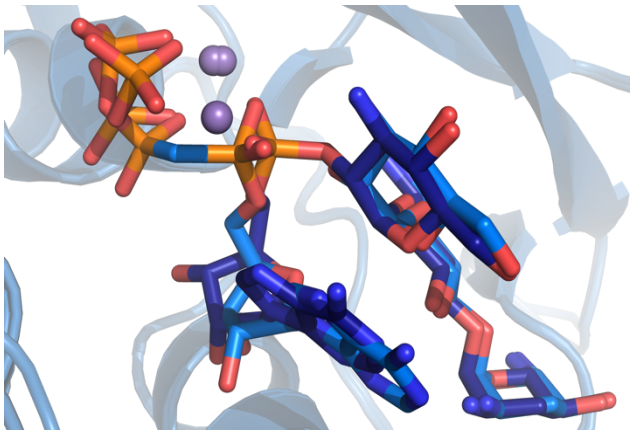

Figure 2 – 8. Structural overlay of substrate-bound (blue) and product-bound (dark blue) state of ANT(2″).

Chapter 3 – Structural analysis of the tobramycin and gentamicin clinical resistome

3.1 Preface

In the previous chapter, we described the nucleotide binding pocket of ANT(2″) in several states along its reaction progress, and the potential for adjuvant development to combat resistance. Analogously, our structures can be used to assess the binding modes of aminoglycosides to targets in their clinical resistome. This information can be used to inform the design of a novel and broad-spectrum antibiotic capable of evading action by several notable detoxifying enzymes.

We describe here a fourth ternary structure of ANT(2″) in complex with AMPCPP and a second medically important aminoglycoside, gentamicin. Together with the analogous tobramycin complex from chapter 2, these structures outline ANT(2″)'s specificity for clinically used substrates. Importantly, these structures, in conjunction with previously solved structures of APH(2″) and AAC(6′), complete our structural knowledge for the set of enzymes that most frequently confer clinically observed resistance to tobramycin and gentamicin. Comparison of tobramycin and gentamicin binding to enzymes in this resistome, as well as to the intended target, the bacterial ribosome, reveals surprising diversity in observed drug–target interactions. Analysis of the diverse binding modes informs that there are limited opportunities for developing aminoglycoside analogs capable of evading resistance.

Adapted with permission from Bassenden, A.V., Rodionov, D., Shi, K., and Berghuis, A.M. (2016). "Structural Analysis of the Tobramycin and Gentamicin Clinical Resistome Reveals Limitations for Next-generation Aminoglycoside Design." ACS Chemical Biology **11**(5): 1339-1346.

Individual Author Contributions are as follows, with percent of overall contribution in parentheses:

Bassenden, A.V. (50%): Experimental design; protein expression, purification and crystallization; data collection and analysis; preparation of manuscript.

Rodionov, D. (30%): Aid in experimental design; protein purification and crystallization; data collection and analysis; editing of manuscript.

Shi, K. (5%): Cloning of initial construct.

Berghuis, A.M. (15%): Supervisory guidance of experimental design; editing of manuscript.

3.2 Introduction

The discovery of antibiotics in the 20th century led to substantial medical breakthroughs in the treatment of infectious diseases. However, our hyper-dependence on antibiotics has now led to a progressive increase in bacterial resistance. Aminoglycosides are a major class of antibiotics that induce their bactericidal effect by binding to the 16S ribosomal RNA (rRNA) A-site, causing errors in translation (Ramirez and Tolmasky 2010). The largest group of aminoglycosides are chemically characterized as 4,6-disubstituted 2-deoxystreptamine compounds (Becker and Cooper 2013). Two examples of these are tobramycin and gentamicin, which are widely used as second-line defense therapeutics for serious Gram-negative infections, including those caused by *Pseudomonas aeruginosa* in cystic fibrosis patients (Prayle and Smyth 2010, Lopez-Novoa, Quiros et al. 2011, Matt, Ng et al. 2012). Still, these aminoglycosides are susceptible to the effects of resistant bacteria, primarily through covalent modification of their amino- or hydroxyl- groups via three classes of enzymes: aminoglycoside *O*-phosphotransferases (APH's), aminoglycoside *N*-acetyltransferases (AAC's), and aminoglycoside *O*-nucleotidyltransferases (ANT's) (Ramirez and Tolmasky 2010). Consequently, these altered antibiotics have reduced affinity for their A-site target, abolishing their toxic effects (Becker and Cooper 2013).

Despite large differences in their three-dimensional fold, many aminoglycoside modifying enzymes (AMEs) have strikingly similar substrate specificity. Within each of the enzyme classes, ANT(2″), APH(2″) and AAC(6′) are the largest mediators of 4,6-disubstituted aminoglycoside resistance (Shaw, Rather et al. 1993). Moreover, they are capable of rendering two of the most clinically relevant aminoglycosides, tobramycin and gentamicin, ineffective through different catalytic mechanisms (Becker and Cooper 2013). Currently, crystal structures of APH(2″) and AAC(6′) exist in complex with tobramycin and/or gentamicin, which revealed the structural details

of their drug-target interactions (Young, Walanj et al. 2009, Shi, Houston et al. 2011, Stogios, Kuhn et al. 2017). However, it has yet to be understood how ANT(2″) performs this analogous task.

ANT(2″) is the primary cause of broad-spectrum aminoglycoside resistance in North America and is capable of detoxifying virtually all 4,6-disubstituted aminoglycosides (Shimizu, Kumada et al. 1985, Shaw, Rather et al. 1993). ANT(2″) confers resistance to this group of antibiotics by catalyzing the ATP-dependent adenylation of their 2″ hydroxyl group (Gates and Northrop 1988a). Although ANT(2″) is a large determinant of aminoglycoside resistance, information for the structural basis of its antibiotic selectivity has been limited. Prior to our investigation, structural data for the apo state and kanamycin bound form has been reported, but data on interactions with clinically used antibiotics had been absent (Cox, Stogios et al. 2015).

We report here the crystal structure of ANT(2″) in ternary complex with AMPCPP (α- β non-hydrolyzable analogue of ATP) and gentamicin. Together with our previously solved ternary complex of ANT(2″) with tobramycin and AMPCPP, these structures complete the characterization of clinically significant AMEs in the tobramycin and gentamicin resistome. Furthermore, we outline the structural basis of the resistome's ability to detoxify a number of medically relevant aminoglycosides in conjunction with how they interfere with the ribosome, inferring viable strategies for successful next-generation aminoglycoside design.

3.3 Experimental Procedures

3.3.1 Crystallization

ANT(2″) was expressed and purified using the protocol described in Chapter 2 and desalted on a HiPrep 26/10 Desalting column (GE) into a final storage buffer containing 10 mM Bis-TRIS propane, pH 7.0, and 1 mM TCEP. Crystals of ANT(2″) in complex with, AMPCPP, Mn^{2+} and gentamicin were grown at 22˚C using the sitting-drop vapour diffusion method. Drops contained a 1:1 ratio of 10 mg mL^{-1} ANT(2″) in storage buffer supplemented with 10 mM AMPCPP, 1 mM manganese(II) chloride and 10 mM gentamicin. Reservoir solution consisted of 100 mM MES, pH 6.3, 5% (w/v) PEG 3000 and 30% (v/v) PEG 200.

3.3.2 Data collection

Diffraction data was collected on a Rigaku MicroMax-007HF generator (copper anode) fitted with a VariMax-HF optic coupled with a Saturn-944+ CCD detector mounted on an AFC-11 partial-Chi goniometer. A 20-fold redundant data collection strategy was calculated for ANT(2″)-gentamicin-AMPCPP-Mn^{2+} complex using the *d*TREK suite* (Pflugrath 1999).

3.3.3 Structure solution and refinement

The dataset was processed using *xia2* pipeline (Winter 2010), [*CCP4* (Collaborative Computational Project 1994), *POINTLESS* (Evans 2006), *XDS* (Kabsch 2010)]. The structure of ANT(2″) in complex with gentamicin, AMPCPP and Mn^{2+} was determined by Fourier synthesis performed by *phenix.refine* (Adams, Afonine et al. 2010) using the structure of ANT(2″)-tobramycin-AMPCPP-Mn^{2+} complex stripped of all non-protein atoms. The structure was refined by iterative cycles of reciprocal-space refinement with *phenix.refine* and real-space refinement and model building in *Coot* (Emsley, Lohkamp et al. 2010). Inspecting the anomalous Fourier maps generated with ANODE (Thorn and Sheldrick 2011) validated the presence and location of

Mn^{2+}ions. The dictionaries for AMPCPP and gentamicin were generated with the *GRADE* server v.1.2.7. The data collection and final refinement statistics for this structure are listed in Table 3 – 1.

Table 3 – 1. Data Collection and Refinement Statistics of Gentamicn-AMPCPP-Mn^{2+} bound ANT(2″) complex

	ANT(2″)•Gentamicin•AMPCPP•Mn^{2+}
Data Collection Statistics	
Resolution range (Å)	31.99 - 1.5 (1.543 - 1.49)
Space group	P $2_12_12_1$
Unit cell (Å)	40.6, 46.0, 89.0
Total reflections	481172 (19451)
Unique reflections	27909 (2691)
Multiplicity	17.2 (7.2)
Completeness (%)	99.7 (97.5)
Mean I/sigma(I)	31.2 (3.3)
Wilson B-factor	12.9
R-merge	0.060 (0.54)
R-meas	0.062
$CC_{1/2}$	1.00 (0.72)
CC*	1.00 (0.92)
Refinement Statistics	
R_{work}	0.149 (0.234)
R_{free}[a]	0.174 (0.197)
Number of non-hydrogen atoms	1818
macromolecules	1502
ligands	86
water	230
Protein residues	175
RMS(bonds, Å)	0.013
RMS(angles, °)	1.52
Ramachandran favored (%)	98
Ramachandran outliers (%)	0.53
Clashscore	5.22
Average B-factor (Å²)	18.9
macromolecules	16.9
ligands	19.5
solvent	31.2

Statistics for the highest-resolution shell are shown in parentheses.

[a] R_{free} was calculated by randomly omitting 10% of observed reflections from refinement.

3.4 Results and Discussion

3.4.1 Structure characteristics

The high-resolution crystal structure of ANT(2″) in ternary complex with AMPCPP and gentamicin was determined at 1.5 Å. The discovery map unequivocally indicated the presence of gentamicin and AMPCPP in the active site of the crystal structure (Figure 3 – 1A)**.** Comparison of the gentamicin-bound structure with the tobramycin and AMPCPP structure from chapter 2 shows the two manganese ions within their active sites, one coordinated by the β- and γ-phosphates of AMPCPP and the other one coordinated by the α-phosphate of AMPCPP and the 2″ hydroxyl group of the aminoglycoside (Figure 3 – 1B). Structural observations indicate that the aminoglycoside-bound forms of the enzyme have no major structural differences, with an RMSD of 0.26 Å (Figure 3 – 1B)**.** Data collection details and final refinement statistics for the gentamicin-bound crystal structure is given in Table 3 – 1.

3.4.2 Interactions of tobramycin and gentamicin with ANT(2″)

The active sites of the AMEs have been extensively studied, particularly the antibiotic binding pocket in prospect of designing novel broad-spectrum aminoglycosides. It is understood that the binding pocket of ANT(2″) is highly negatively charged in order to accommodate a variety of aminoglycosides such as tobramycin, gentamicin, kanamycin, dibekacin and sisomicin, which are universally positively charged (Becker and Cooper 2013, Cox, Stogios et al. 2015). This negatively charged binding pocket is also observed in other structurally characterized aminoglycoside nucleotidyltransferases capable of detoxifying 4,6-disubstituted antibiotics, i.e. ANT(4′) (Pedersen, Benning et al. 1995).

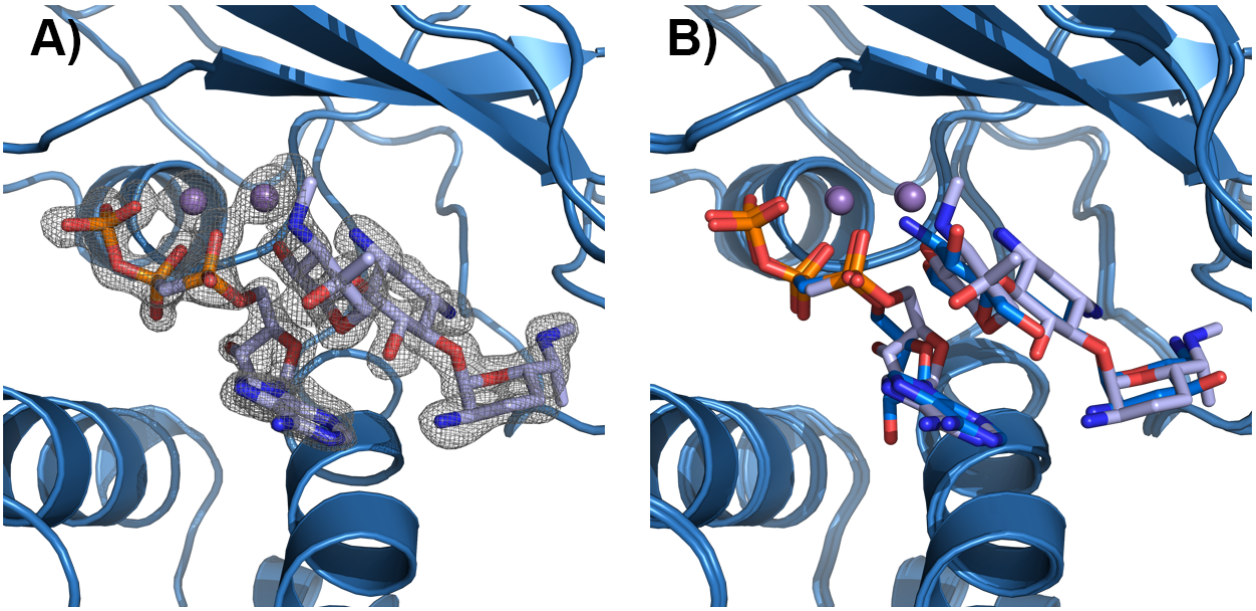

Figure 3 – 1. Tobramycin versus gentamicin binding to ANT(2″). View of the ANT(2″) active site. In panel (A) the enzyme is shown in complex with gentamicin and AMPCPP. The aminoglycoside and nucleotide are colored in light blue, and manganese atoms are drawn as purple spheres. Also depicted is the F_o–F_c discovery map for the ligands at a contour level of 3σ. (B) Superposition of tobramycin- and gentamicin-bound structures of ANT(2″) showing little deviation between the two forms of the enzyme. The tobramycin-bound structure ligands are colored in blue.

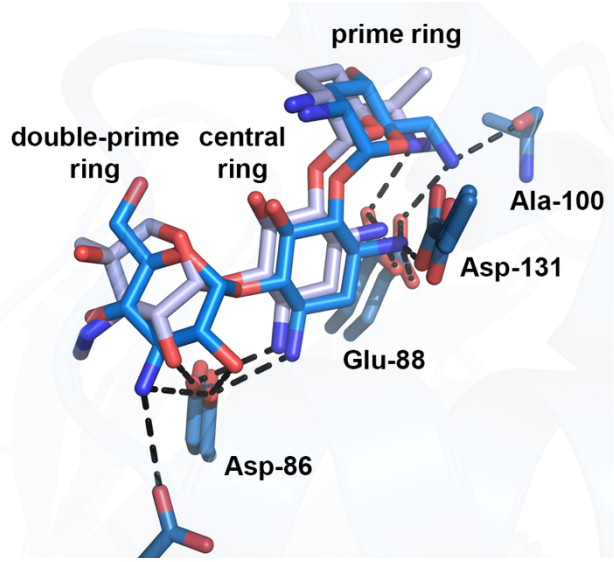

Figure 3 – 2. Binding of tobramycin and gentamicin to ANT(2″). Superposition of tobramycin (blue) and gentamicin (light-blue) bound to ANT(2″). Prime ring, central ring and double-prime ring are depicted. Black dashed lines represent hydrogen-bond interactions.

Superposition of the two aminoglycoside-bound ternary complexes of ANT(2″) show that although their functional groups vary, the conformation of the aminoglycosides remain virtually identical, with the molecules adopting a crescent-like shape with a concave and convex side (Figure 3 – 2). The enzyme's binding pocket for the 4,6-disubstituted antibiotic substrates can conceptually be separated into three sub-sites for analysis: the central 2-deoxystreptamine ring site, the prime ring (4-substituted ring) site and

the double-prime ring (6-substituted ring) site (Figure 3 – 2). The pattern of hydrogen bonds between ANT(2″) and its clinically relevant aminoglycoside substrates reveals that the majority of these interactions occur in the central ring site. The central ring of tobramycin and gentamicin are anchored at position-1 by Asp86 and position-3 by residues Glu88 and Asp131. The double prime ring of the two antibiotics interact with Asp86 at the 2″-position. Additionally, tobramycin exclusively interacts with Asp44 at the 3″-positions due to the presence of a methylamine group at this position in gentamicin, making it unable to form this interaction. The prime ring also has limited hydrogen bonding with the enzyme, with only the amine group at the 6′-position interacting with Glu88 for both aminoglycosides and the carboxyl group of Ala100 in tobramycin. Again, the hydrogen bond discrepancy for gentamicin at the 6′-position is due to the methylation of the amine group (Figure 3 – 2). To conclude, the majority of the interactions take place with functional groups that are conserved between both antibiotics, while the majority of the variable moieties do not interact with the enzyme. Furthermore, it is expected that all antibiotic substrates of ANT(2″) should form these same hydrogen bond interactions as these same functional groups are conserved across all 4,6-disubstituted aminoglycosides. This is further confirmed by a previously determined structure of ANT(2″) in complex with kanamycin, which reveals the same interactions as tobramycin in ternary complex with ANT(2″) (Cox, Stogios et al. 2015).

The ternary complexes of ANT(2″) additionally reveal critical interactions that occur between its aminoglycoside and nucleotide substrates (Figure 3 – 3). The nucleotide interactions with tobramycin and gentamicin are identical, with their 5′-hydroxyl group interacting with N3 of the adenine ring and the 2″-hydroxyl group interacting with the α-phosphate of AMPCPP. The interaction between the 2″-hydroxyl and α-phosphate is expected as the aminoglycoside is to be adenylated at this position. Tobramycin makes additional contact with the α-phosphate of

AMPCPP at its 3″-amine group, while gentamicin does not make this contact, due to steric clashes between its methylamine group and the α-phosphate of AMPCPP.

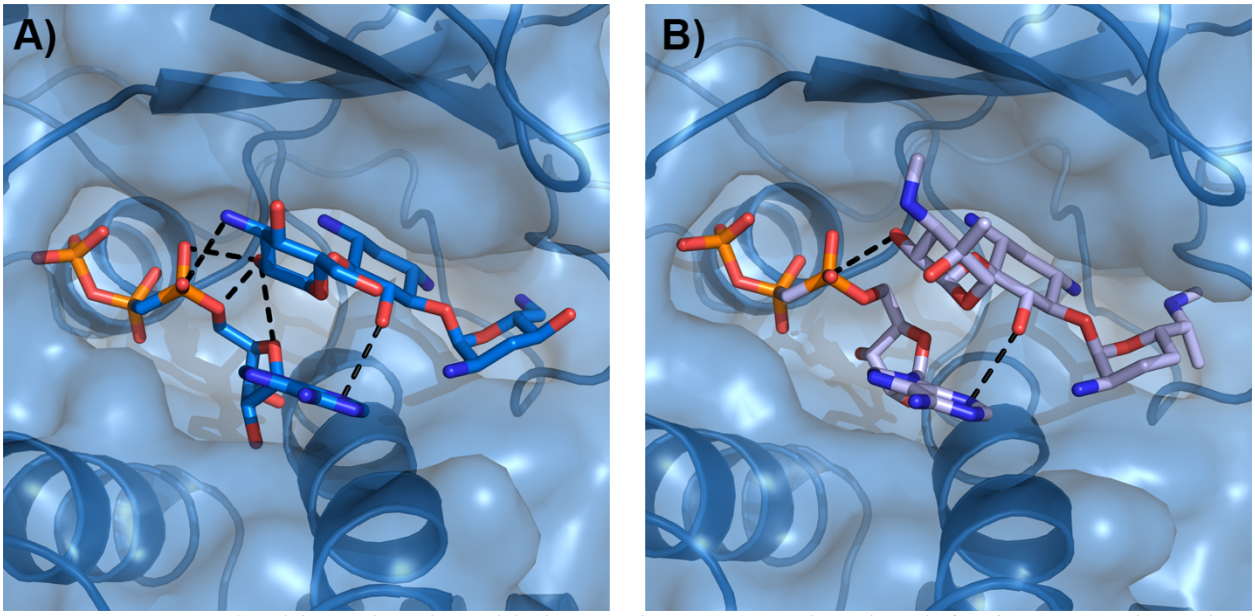

Figure 3 – 3. Nucleotide-aminoglycoside interactions. (A) Active site cleft of ANT(2″) bound to tobramycin and AMPCPP, with dashed lines representing key hydrogen bond interactions between the two substrates. (B) Analogous view for the enzyme bound to gentamicin and AMPCPP. The color scheme used is identical to that for Figures 3 – 1 and 3 – 2.

3.4.3 Resistome of tobramycin and gentamicin

Although ANT(2″) is a primary factor in tobramycin and gentamicin resistance, other AMEs have similar substrate specificity and are partially responsible for the widespread resistance to these 4,6-disubstituted aminoglycosides. There are five enzymes that comprise the complete resistome of tobramycin and gentamicin: ANT(2″), APH(2″), AAC(2′), AAC(3) and AAC(6′) (Bacot-Davis, Bassenden et al. 2016). Among Gram-negative clinical isolates, ANT(2″) is found in on average 42% of them, second only to AAC(6′) being found in on average 80% of isolates around the world (Shimizu, Kumada et al. 1985, Costello, Deshpande et al. 2019). It is important to note that this study focuses solely on the type I variant of AAC(6′), which is capable of modifying two of the three gentamicin components with the highest antibacterial activity: gentamicin C_{1a} and C_2 (Shaw, Rather et al. 1993). Though there is a rare variant of AAC(6′) capable

of modifying all three gentamicin components, it is far less clinically prevalent (Shaw, Rather et al. 1993, Becker and Cooper 2013). Of the aforementioned acetyltransferases, AAC(2′) and AAC(3) are far less prevalent, being found in up to 8 and 16% of these isolates respectively (Shimizu, Kumada et al. 1985). Among Gram-positive clinical isolates, APH(2″) is found in approximately 80% of high-level gentamicin resistant strains around the world (Chow 2000, Zarrilli, Tripodi et al. 2005, Abbassi, Achour et al. 2007). Thus, we performed structural analysis on the most clinically prevalent enzymes for each type of transferase: ANT(2″), APH(2″) and AAC(6′). Currently, five crystal structures of these three enzymes exist in their aminoglycoside-bound form: ANT(2″) in complex with tobramycin and gentamicin C_1 reported here, APH(2″) in complex with tobramycin and gentamicin C_{1a} and finally AAC(6′) in complex with tobramycin (Young, Walanj et al. 2009, Shi, Houston et al. 2011, Stogios, Kuhn et al. 2017). For comparison, gentamicin C_{1a} binding to AAC(6′) was predicted using the tobramycin-bound structure. As previously reported, these enzymes are capable of binding their aminoglycoside substrates via their negatively charged active sites (Young, Walanj et al. 2009, Shi, Houston et al. 2011, Cox, Stogios et al. 2015).

The comparison of tobramycin and gentamicin-bound structures of ANT(2″), APH(2″) and AAC(6′), shows that despite the large conformational space accessible to aminoglycosides, they bind remarkably similar to the enzymes that catalyze completely different reactions, with pairwise RMSD values for aminoglycosides ranging between 0.5–1.6 Å. The aminoglycoside conformations are especially conserved at the central and double-prime rings. Recognition and binding of tobramycin and gentamicin by ANT(2″), APH(2″) and AAC(6′) also showed remarkable similarities. Not only are the residues that interact with the aminoglycosides all acidic in nature, but also seemed to favor the functional groups that are conserved in both tobramycin

and gentamicin across all enzymes in their resistome (Figure 3 – 4A). All three enzymes evolved to interact at the same five sites of tobramycin and gentamicin: their 3″-, 1-, 3- and 6′-amine groups and their 2″-hydroxyl groups, with a single exception of the lack of AAC(6′) interaction with the amine at the 1-position. The residues involved in these interactions are predominately aspartates and glutamates, and form strong bonds with the positively charged amine groups of the antibiotics.

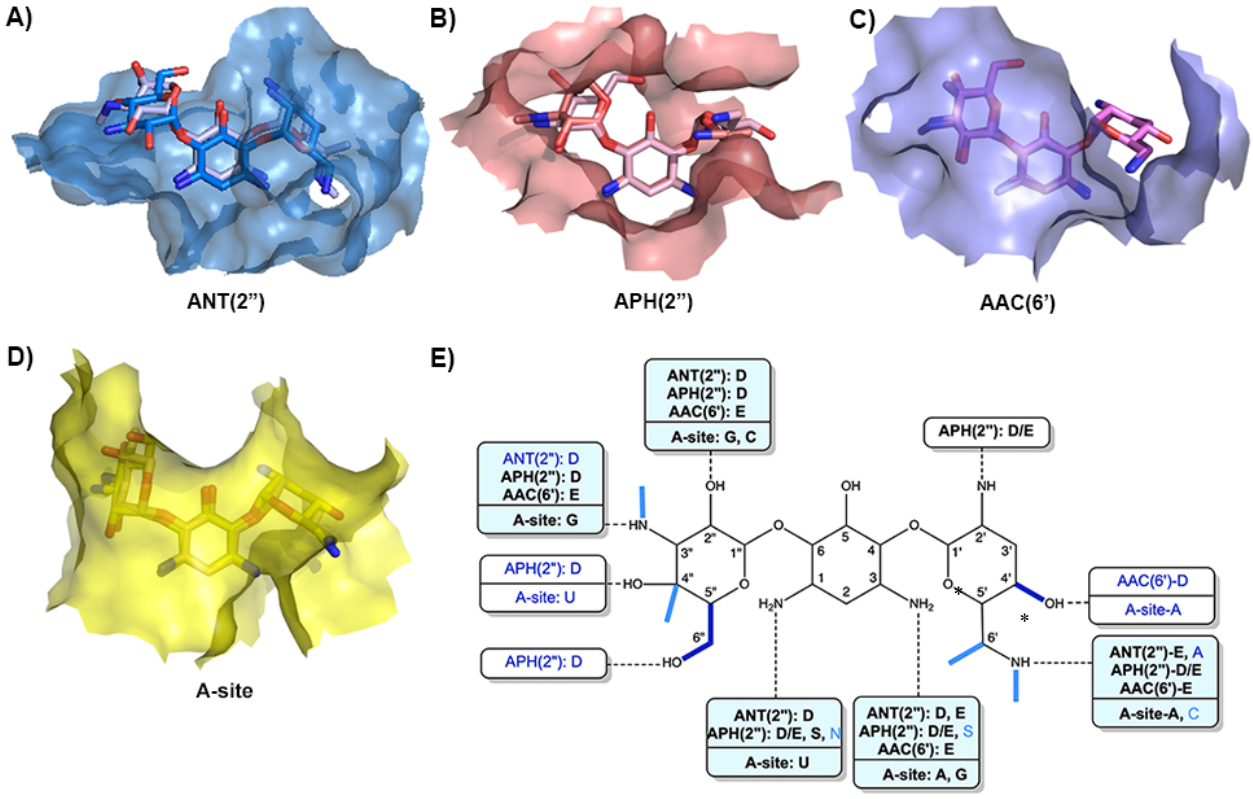

Figure 3 – 4. Comparison of tobramycin and gentamicin interactions with resistome enzymes and the bacterial ribosome. (A) van der Waals surface of tobramycin and gentamicin binding site for ANT(2″), (B) APH(2″), (C) AAC(6′), and (D) ribosomal A-site. Note that in each of these four panels tobramycin is shown in a darker color shade than gentamicin. (E) A combined chemical structure for tobramycin and gentamicin is shown with the backbone numbered. Features unique to tobramycin are highlighted in dark blue and features unique to gentamicin are highlighted in light blue, with those marked with a "*" being specifically unique to gentamicin C1. Hydrogen bond interactions are depicted in boxes. Blue boxes indicate the five sites involved in critical hydrogen bond interactions, and white boxes indicate interactions that occur less frequently. Dark blue labels indicate interactions that are unique to tobramycin, and light blue colored labels indicate interactions are unique to gentamicin.

While conformations of aminoglycosides and the specific hydrogen bond interactions they form with modifying enzymes are remarkably similar, their van der Waals interactions vary significantly (Figure 3 – 4). ANT(2″) and AAC(6′) interact with opposing faces of the aminoglycoside, where the concave site primarily interacts with ANT(2″) while the convex side makes most of its interactions with AAC(6′). On the other hand, the rim of aminoglycosides comprise most of the Van der Waals interactions with APH(2″), differing completely from interactions made with ANT(2″) and AAC(6′) (Figure 3 – 4C–E).

3.4.4 Tobramycin and gentamicin resistome vs. rRNA A-site binding

While AMEs have high affinity for tobramycin and gentamicin, their intended cellular target is the 16S rRNA A-site, where they would ultimately induce a bactericidal effect by causing errors in translation. The three-dimensional structures of A-site fragments bound to tobramycin and gentamicin C_{1a} have been previously determined (Vicens and Westhof 2002, Francois, Russell et al. 2005). Comparison of the tobramycin and gentamicin resistome to the A-site binding interactions brings up striking similarities and differences. First, the conformations of the aminoglycosides remain essentially identical regardless of the binding macromolecule. This "conformational mimicry" has been observed for other AMEs such as APH(3′), the likely explanation being that the enzymes evolved to bind the lowest energy conformer of aminoglycosides in order to compete with ribosomal binding (Fong and Berghuis 2002). Secondly, the analysis of tobramycin and gentamicin binding to the A-site reveals that the functional groups utilized are essentially identical to the moieties being exploited by AMEs, with the exception of two additional recognition sites for tobramycin at the 4′ and 4″ hydroxyl groups (Figure 3 – 4 A). Finally, comparison of van der Waals interactions between the A-site and their aminoglycoside substrates reveals limited similarity to what is seen for any of the enzymes. The van der Waals

interactions made by the ribosomal A-site is somewhat analogous to that of AAC(6′), as both interact with the convex side of the antibiotics, but distinct differences are noted for interactions with the prime ring of the aminoglycosides (Figure 3 – 4B–E).

3.4.5 Prospects for next-generation aminoglycoside design

The observation that van der Waals interactions between aminoglycosides and their various targets differ can be exploited for the development of next-generation antibiotics that retain their affinity for the A-site but lack, or have reduced, affinity for enzymes belonging to the relevant resistome (Kondo and Hotta 1999). Specifically, past efforts have focused on incorporating additions onto the basic 4,6-disubstituted aminoglycoside skeleton, with the aim of selectively interfering with binding of the antibiotics to AMEs. Two examples of this are amikacin and etimicin, which have a 4-amino-2(*S*)-hydroxybutyryl and an ethyl extension at the N1 position, respectively, thereby effecting reduced susceptibility to various AMEs in comparison to their parent compounds (Kawaguchi 1976, Zhao, Li et al. 2000). However, these efforts were performed in the absence of structural insights for aminoglycoside-target interactions.

Our analysis presented in figure 3 – 5A for the clinically relevant tobramycin and gentamicin interactome provides the critical data to effectively expand on their 4,6-disubstituted skeleton, to selectively interfere with van der Waals interactions made by ANT(2″), APH(2″), and/or AAC(6′), while not impacting favorable interactions made with the ribosomal A-site. In figure 3 – 5B the highlights of this analysis are illustrated. The ribosomal A-site exploits ~70% of the available aminoglycoside van der Waals surface for forming interactions, leaving only ~30% suitable for expansion. Additionally, because of the diversity in how different resistance enzyme form van der Waals contacts with tobramycin and gentamicin, there are very limited options to obstruct interactions simultaneously for all three enzymes, i.e. only 1/6 of the suitable expansion

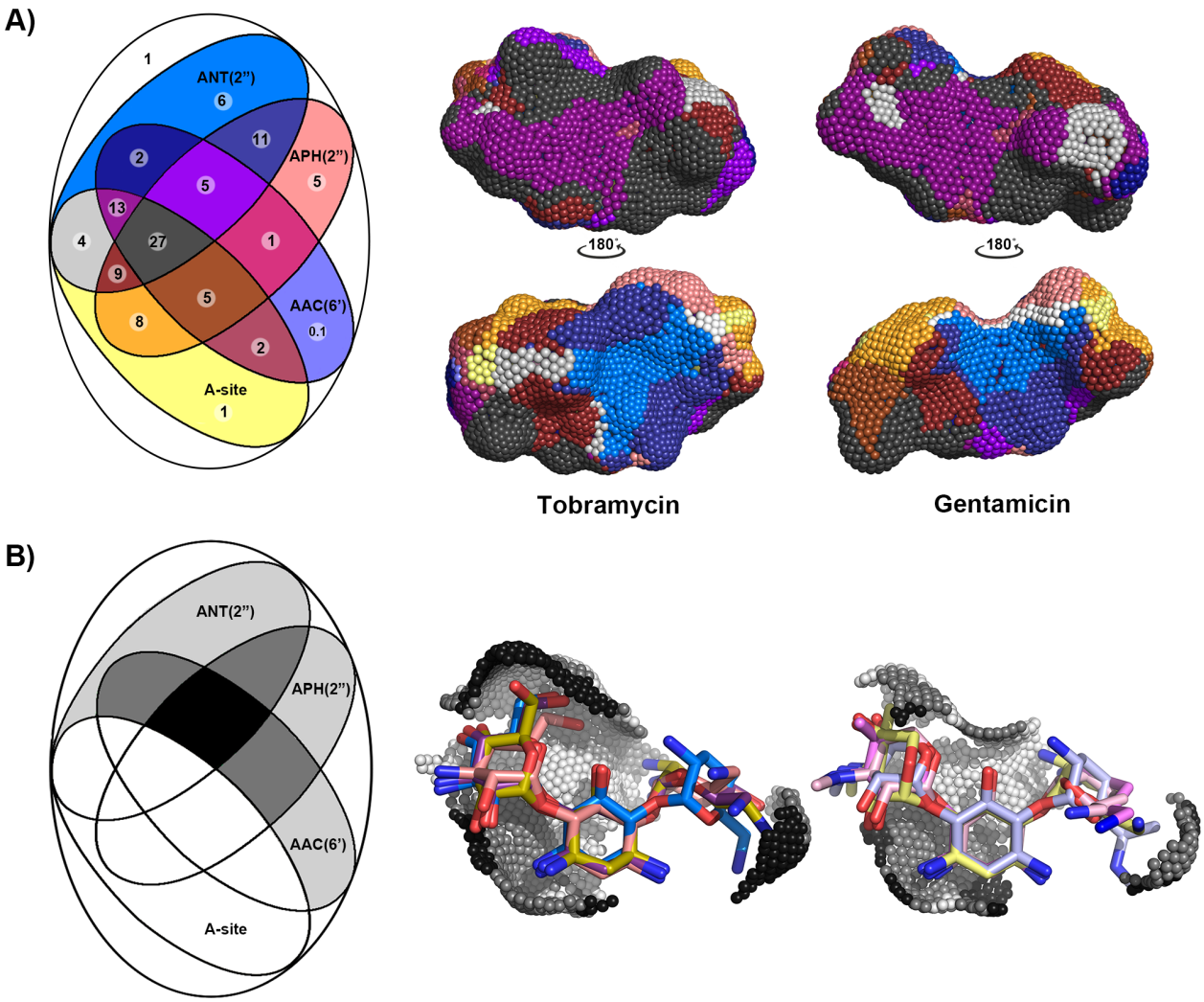

Figure 3 – 5. Aminoglycoside van der Waals interaction analyses. Shown are the van der Waals surfaces for both tobramycin and gentamicin. In panel A, the surfaces are color coded to reflect which patches participate in van der Waals interactions with ANT(2″), APH(2″), AAC(6′), and/or the ribosomal A-site. The accompanying Venn diagram provides a color legend for these patches. The percent value of the van der Waals surfaces involved in specific interactions is also shown on the Venn diagram. Note that while the details on what segment of the van der Waals surfaces contributes to which specific interactions slightly differs between tobramycin and gentamicin, the percentage values were not substantially impacted by those differences, and hence the numbers presented are applicable to both tobramycin and gentamicin. In panel B, those patches of the van der Waals surfaces for tobramycin and gentamicin are shown that are uniquely involved in interactions with resistome enzymes (i.e., no interactions with the ribosomal A-site). The corresponding Venn diagram again provides a color legend, highlighting which segment of the aminoglycoside van der Waals surface interacts with one, two, or all three clinically relevant resistance enzymes.

area is shared by ANT(2″), APH(2″), and AAC(6′). It should also be noted that this analysis does not take into consideration if the identified expansion areas can be practically exploited, that is if they are synthetically accessible. The culmination of these observations is that next-generation aminoglycoside development will have to incorporate more than one addition onto the 4,6-disubstituted skeleton in order to circumvent the clinical resistome.

The newest semi-synthetic aminoglycoside that is currently in clinical trials, plazomicin, indeed has incorporated two additions onto its gentamicin related skeleton at the N-1 and N-6′ positions (Aggen, Armstrong et al. 2010, Armstrong and Miller 2010). Purportedly, this antibiotic is not impacted by the most common clinically encountered resistance enzymes as our analysis would also predict. However, susceptibility to AAC(2′) has been reported (Armstrong and Miller 2010). This is disconcerting for two reasons: First, aminoglycoside usage impacts the prevalence of associated resistance mechanisms, and thus the clinical relevance of AAC(2′) mediated resistance will undoubtedly increase with plazomicin usage. Secondly, plazomicin susceptibility to AAC(2′) implies that this enzyme forms different van der Waals interactions than ANT(2″), APH(2″), and AAC(6′) with gentamicin related antibiotics. The consequence of this is that the expansion of the clinical resistome will further complicate next-generation aminoglycoside development.

Chapter 4 – The Future of Next-Generation Aminoglycoside Resistance: A Structural Comparison on Binding of Naturally Occurring and Semi-Synthetic Aminoglycosides, Including Next-Generation Aminoglycoside Plazomicin to AAC(2′)-Ia

4.1 Preface

The understanding of how ANT(2″) and other clinically prevalent resistance enzymes bind aminoglycoside substrates, as discussed in the preceding chapter, has shown the limited potential of next-generation drug design. To date, plazomicin is the only next-generation aminoglycoside approved for clinical use that has the potential of evading the effects of widespread resistance factors. However, plazomicin is still susceptible to the action of the resistance enzyme AAC(2′)-Ia. Moreover, the clinical use of plazomicin will undoubtedly accelerate the evolution of resistance factors, rendering this aminoglycoside increasingly obsolete. Understanding resistance to plazomicin is an important step to ensure this aminoglycoside remains a viable treatment option for the foreseeable future.

In this chapter, we describe four crystal structures of AAC(2′)-Ia, three in complex with acetylated aminoglycosides tobramycin, netilmicin, and plazomicin, and one in complex with an aminoglycoside inhibitor, amikacin. Together, these structures outline AAC(2′)-Ia's specificity for a wide range of aminoglycosides. Moreover, our survey of AAC(2′)-I homologues highlights the conservation of residues predicted to be involved in aminoglycoside and plazomicin binding. These results forecast the impending spread of plazomicin resistance and highlight the urgency for advancements in next-generation aminoglycoside design.

Adapted from Bassenden, A.V., Dumalo, L., Park, J. and Berghuis, A.M. (2020). "The Future of Next-Generation Aminoglycoside Resistance: A Structural Comparison on Binding of Naturally Occurring and Semi-Synthetic Aminoglycosides, Including Next-Generation Aminoglycoside Plazomicin to AAC(2′)-Ia" *Manuscript to be submitted.*

Individual Author Contributions are as follows, with percent of overall contribution in parentheses:

Bassenden, A.V. (70 %): Experimental design; protein expression, purification, and crystallization; data collection and analysis; preparation of manuscript.

Dumalo, L. (15%). Experimental aid; Protein expression, purification, and crystallization.

Berghuis, A.M. (15%): Supervisory guidance of experimental design; editing of manuscript.

4.2 Introduction

The discovery of the first aminoglycoside, streptomycin, revolutionized antibiotic usage, being the first useful bacterial-sourced antibiotic to offer effective treatment for tuberculosis (Schatz, Bugie et al. 2005, Arya 2007). This lead to the rapid succession of novel aminoglycoside antibiotic discovery over a 30 year period, which largely masked the emergence of aminoglycoside resistance (Becker and Cooper 2013). Their range of biological activity and medical applications, despite their toxicity, made them an essential tool in the fight against serious bacterial infections (Rougier, Claude et al. 2003, Arya 2007, Becker and Cooper 2013). Today, aminoglycoside resistance is widespread due to rampant use in clinical practice and husbandry, where aminoglycoside modifying enzymes (AMEs) are the most significant factors attributed to antibiotic inactivation (Shaw, Rather et al. 1993, Ramirez and Tolmasky 2010).

Attempts to circumvent the effects of these enzymes have been numerous, including the development of semi-synthetic derivatives of naturally occurring aminoglycosides (Kondo and Hotta 1999). Some of the first iterations of semisynthetic aminoglycosides, including amikacin, netilmicin, and isepamicin, introduced bulky sidechains to the N1-position of kanamycin, sisomicin, and gentamicin B, respectively (Kondo and Hotta 1999, Mingeot-Leclercq, Glupczynski et al. 1999). These antibiotics would prove to be more therapeutically viable than their precursor by eluding the effects of AMEs by blocking binding to their potential targets (Kondo and Hotta 1999). For example, the addition of an (S)-4-amino-2-hydroxybutyrate (HABA) group to kanamycin, reduced its susceptibility to AMEs by 40% (Bacot-Davis, Bassenden et al. 2016). Current discovery and development of next-generation aminoglycosides continue to incorporate this strategy, in combination with analyzing structural basis for antibiotic binding (Gupta 2017). Notably, these types of analyses have revealed that aminoglycosides bind to AMEs

and the ribosome in their lowest energy conformation with little changes to the antibiotic, utilizing similar motifs for hydrogen bonding, while significantly varying in their van der Waals surface interactions (Fong and Berghuis 2002, Bacot-Davis, Bassenden et al. 2016, Bassenden, Rodionov et al. 2016). Together, these techniques can pinpoint key features of aminoglycoside design that can allow them to evade the action of AME's that their parent compounds were previously susceptible to.

Plazomicin, a next-generation aminoglycoside, was introduced on the market in 2018 and is the second semisynthetic derivative of sisomicin (Noone 1984, Gupta 2017). The first, netilmicin, incorporated an ethyl group at the N1 position. This modification reduced its sensitivity to nucleotidyltransferases, specifically, ANT(2″); however, netilmicin remained ineffective against 87% of AMEs affecting sisomicin (Bacot-Davis, Bassenden et al. 2016). Contrarily, plazomicin was designed to target specific pathogens which are resistant to older aminoglycosides by introducing key structural features to sisomicin (Gupta 2017). As with amikacin, the addition of an (S)-HABA group at the N1 position shields plazomicin from action by phosphotransferases [APH(2″)], nucleotidyltransferases [ANT(2″)], and acetyltransferases [AAC(3)](Bacot-Davis, Bassenden et al. 2016, Krause, Serio et al. 2016, Gupta 2017). The second substitution, a hydroxyethyl group at the 6′ position, blocks plazomicin from the activity of the most clinically prevalent and widespread enzyme group, AAC(6′) (Krause, Serio et al. 2016). These additions to the sisomicin aminoglycoside skeleton have reduced the number of enzymes able to selectively bind and modify plazomicin to just one, AAC(2′)-Ia (Aggen, Armstrong et al. 2010, Krause, Serio et al. 2016).

AAC(2′)-Ia is universally chromosomally restricted in *Providencia stuartii,* an opportunistic pathogen responsible for catheter-associated urinary tract infections with a high

mortality rate (Macinga and Rather 1999, Aggen, Armstrong et al. 2010, Wie 2015). AAC(2′)-Ia's substrate specificity includes naturally occurring aminoglycosides such as kanamycin, tobramycin, sisomicin, and gentamicin, as well as semisynthetic aminoglycosides such as dibekacin, netilmicin, and plazomicin (Bacot-Davis, Bassenden et al. 2016). Although AAC(2′)-Ia has not been a predominant factor in antimicrobial resistance in the past, the increased use of plazomicin may increase its clinical prevalence. Understanding the structural basis for this enzyme's antibiotic selectivity is a key component in keeping plazomicin a viable treatment option for the foreseeable future. Currently, structural data for AAC(2′)-Ia is limited to a gentamicin-bound structure, which presents a model of a possible plazomicin mode; however, concrete structural data is absent (Cox, Ejim et al. 2018).

In this chapter, we present four structures of AAC(2′)-Ia in ternary complex with various naturally occurring and semisynthetic aminoglycosides including, tobramycin, amikacin, netilmicin, as well as the next-generation aminoglycoside, plazomicin. These structures have allowed us to inform the critical residues responsible for AAC(2′)-Ia′s ability to bind and modify a wide range of chemically unique 4,6-aminoglycosides. Moreover, we present a comprehensive BLAST analysis of the AAC(2′) enzymes (types Ia-Ie), outlining the conservation of residues involved in plazomicin binding across multiple bacterial species. Additionally, we explore plasmid-encoded sequences with high similarity and identity to AAC(2′)-Ia with the potential to modify plazomicin and quickly spread resistance.

4.3 Experimental Procedures

4.3.1 Cloning

The AAC(2′)-Ia gene was synthesized and subcloned into pET-15b expression vector between the NdeI and BamHI restriction sites with an N-terminal HIS-tag followed by a thrombin cleavage site; verified by DNA sequencing using the BioBasic Inc. gene synthesis service. The resulting vector was used to transform E. coli BL21(DE3) cells.

4.3.2 Expression and purification

Protein expression was carried out using the Studier method for auto-induction, as previously described (Bassenden, Rodionov et al. 2016). Cells were harvested by centrifugation at 6000g for 15 minutes at 4˚C and resuspended in 40 mL of lysis buffer containing 50 mM TRIS-HCl, pH 8.0, 200 mM NaCl, 10 mM β-mercaptoethanol, 10% (v/v) glycerol, and one EDTA-free protease inhibitor tablet (Roche). Cells were lysed by sonication, and cell debris was subsequently removed by centrifugation at 50000g for 30 minutes at 4˚C. The supernatant was further clarified by filtration through a 0.22 μm syringe-driven filter. The resulting material was applied on a 26mm i.d.x50mm Ni-IDA-Sepharose® column, equilibrated in 50 mM TRIS-HCl, pH 8.0, 200 mM NaCl, 10 mM β-mercaptoethanol, and 10% (v/v) glycerol; then eluted stepwise with starting buffer supplemented with 150 mM imidazole. AAC(2′)-Ia containing fractions were identified by SDS-PAGE and pooled. 50 μL of 1 unit μL^{-1} Thrombin was added to the pool and incubated overnight at 22˚C to remove the N-terminal HIS-tag. The pool was then applied on a HiTrap™ Benzamidine FF column (GE), equilibrated in the previously mentioned buffer, to remove thrombin from the AAC(2′)-Ia sample. AAC(2′)-Ia fractions were desalted on HiPrep 26/10 Desalting column (GE), equilibrated in 25 mM BIS-TRIS propane pH 7.5, 10 mM β-mercaptoethanol, and 10% (v/v) glycerol. The desalted material was applied on DEAE Sepharose® FF 26mm i.d. x 140mm

column, equilibrated in the identical buffer, and eluted with a 0–400 mM NaCl gradient over 16 column volumes. Peak fractions from the DEAE column were pooled, and buffer exchange was performed on the same desalting column, equilibrated in the final storage buffer consisting of 10 mM HEPES, pH 6.6, and 1 mM TRIS (2-carboxyethyl) phosphine hydrochloride (TCEP). AAC(2′)-Ia was then concentrated to 10 mg mL^{-1} and stored at 4˚C. Lastly, the enzymatic activity of the purified AAC(2′)-Ia was confirmed using a previously established assay (Serpersu, Ozen et al. 2008).

4.3.3 Crystallization

All crystal of AAC(2′)-Ia were grown at 4˚C using the sitting-drop vapour diffusion method. Drops contained a 1:1 ratio of 10 mg mL-1 of AAC(2′)-Ia in storage buffer supplemented with 10 mM acetyl-CoA and 10 mM antibiotic. Plazomicin was synthesized and generously provided by D. P. Arya. Crystals of AAC(2′)-Ia in complex with CoA and acetylated tobramycin grew when reservoir solution consisted of 35% (v/v) 2-methyl-2,4-pentanediol (MPD) and 0.1 M sodium acetate, pH 4.5. Crystals of AAC(2′)-Ia in complex with CoA and acetylated netilmicin grew when reservoir solution consisted of 0.2 M sodium thiocyanate and 40% MPD. Crystals of AAC(2′)-Ia in complex with CoA and acetylated plazomicin grew when reservoir solution consisted of 0.2 M LiCl and 40% MPD. Finally, crystals of AAC(2′)-Ia in complex with acetyl CoA and amikacin grew when reservoir solution consisted of 1 M sodium citrate, 0,2 M NaCl, and 0.1 M TRIS, pH 7.0.

4.3.4 Data collection

Diffraction data for optimized crystals of the AAC(2′)-Ia-acetylated plazomicin-CoA complex were collected at CMCF beamline 08ID-1 at the Canadian Light Source. Diffraction data for optimized crystals of the three other complexes were collected on a Bruker D8 Discovery

consisting of a METALJET source (liquid gallium) coupled with a PHOTON II CPAD detector mounted on a KAPPA goniometer. A 10-fold redundant data collection strategy was calculated for all home-source data sets using the PROTEUM3 software suite (Bruker).

4.3.5 Structure solution and refinement

Datasets for all structures were processed using the *xia2* pipeline (Winter 2010), [*CCP4*(Collaborative Computational Project 1994)*, POINTLESS* (Evans 2006)*, XDS* (Kabsch 2010)]. The structure of AAC(2′)-Ia in complex with acetylated tobramycin and CoA was solved by molecular replacement using *Phaser* (McCoy, Grosse-Kunstleve et al. 2007), exploiting previously reported structural data (PDB ID: 5US1) (Cox, Ejim et al. 2018). The structure of AAC(2′)-Ia in complex with amikacin and acetyl-CoA was solved using molecular replacement with the acetylated tobramycin-CoA complex as the search model using *Phaser.* Finally, the structures of AAC(2′)-Ia in complex with acetylated plazomicin and CoA, and in complex with acetylated netilmicin and CoA were determined using Fourier synthesis performed by *phenix.refine* (Adams, Afonine et al. 2010) using the acetylated tobramycin-CoA complex stripped of all non-protein atoms. All structures were refined by iterative cycles of reciprocal-space refinement with *phenix.refine* and real-space refinement and model building in *Coot* (Emsley, Lohkamp et al. 2010). The ligand restraints for CoA, acetyl-CoA, acetylated antibiotics, and amikacin were generated using *eLBOW* (Moriarty, Grosse-Kunstleve et al. 2009). The data collection and final refinement statistics of the four models are listed in Table 4 – 1.

Table 4 – 1: Data Collection and Refinement Statistics of Aminoglycoside-AAC(2′)-Ia Complexes

	AAC(2′)-Ia • Acetyl-CoA • Amikacin	**AAC(2′)-Ia • CoA • Acetylated-Tobramycin**	**AAC(2′)-Ia • CoA • Acetylated-Netilmicin**	**AAC(2′)-Ia • CoA • Acetylated Plazomicin**
Data Collection Statistics				
Resolution range (Å)	27.47-1.42 (1.47-1.42)	26.47-1.77 (1.833-1.77)	26.44-2.0 (2.071-2.0)	58.43-1.95 (2.02-1.95)
Space group	C 1 2 1	P 32 2 1	P 32 2 1	P 32 2 1
Unit cell (Å, °)	93.3 58.9 83.2, β=116.0	72.7 72.7 146.3	73.0 73.0 145.6	73.5 73.5 147.1
Total reflections	153279 (15254)	88897 (8600)	62260 (6120)	273474 (23178)
Unique reflections	76642 (7629)	44518 (4369)	31130 (3059)	33925 (3293)
Multiplicity	10.3 (7.1)	7.7 (5.4)	10 (6.3)	8.1 (7.0)
Completeness (%)	99.4 (98.2)	99.9 (99.4)	99.9 (99.9)	98.8 (97.5)
Mean I/sigma(I)	21.9 (2.4)	22.7 (2.5)	20.8 (2.3)	18.9 (2.1)
Wilson B-factor	10.1	17.7	24.1	39.6
R-merge	0.045 (0.58)	0.025 (0.35)	0.035 (0.37)	0.052 (0.96)
R-meas	0.063 (0.82)	0.035 (0.50)	0.049 (0.52)	0.055 (1.03)
$CC_{1/2}$	1.00 (0.48)	1.00 (0.65)	1.00 (0.72)	1.00 (0.72)
CC*	1.00 (0.81)	1.00 (0.89)	1.00 (0.91)	1.00 (0.91)
Refinement Statistics				
R_{work}	0.140 (0.284)	0.167 (0.305)	0.182 (0.301)	0.188 (0.278)
R_{free}[a]	0.182 (0.324)	0.193 (0.290)	0.226 (0.339)	0.223 (0.336)
Number of non-hydrogen atoms	3809	3427	3147	3114
macromolecules	3147	2909	2809	2774
ligands	182	194	168	224
water	480	324	170	116
Protein residues	361	353	352	350
RMS (bonds, Å)	0.005	0.006	0.006	0.006
RMS (angles, °)	0.78	0.72	0.79	0.82
Ramachandran favored (%)	98.0	97.7	96.5	97.4
Ramachandran outliers (%)	0	0	0	0
Clashscore	2.61	1.67	5.09	3.99
Average B-factor ($Å^2$)	15.9	24.7	31.5	48.6
macromolecules	13.5	23.4	31.0	47.4
ligands	17.0	30.4	36.2	62.8
solvent	31.1	33.4	35.2	49.7

Statistics for the highest-resolution shell are shown in parentheses.

[a] R_{free} was calculated by randomly omitting 10% of observed reflections from refinement.

4.3.6 Phylogenetic Analysis of Aminoglycoside 2′-Acetyltransferases

AAC(2′) sequences were identified using PSI-BLAST (Position-Specific Iterated BLAST) (Altschul, Madden et al. 1997), with five separate searches using AAC(2′)-Ia, b, c, d, and e as the respective query sequences (Rather, Orosz et al. 1993, Ainsa, Perez et al. 1997). The search was run using the reference proteins database (RefSeq), excluding models and uncultured sequences (O'Leary, Wright et al. 2016). Search parameters included 1000 maximum target sequences with an expect threshold of 10. BLOSUM62 was used as the scoring matrix. The PSI-BLAST threshold was set at 0.005 and was run for five iterations for each query sequence. Final sequences for the phylogenetic tree were chosen from each search list based on sequence identity (>23%), clinical prevalence, and lowest E-value. The alignment of the final 61 sequences was generated in NGPhylogeny.fr using the Mafft L-INS-I method (Katoh and Standley 2013, Lemoine, Correia et al. 2019). NGPhylogeny was subsequently used to generate a maximum-likelihood phylogenetic tree using the PhyML algorithm (Guindon, Dufayard et al. 2010, Lemoine, Correia et al. 2019). The final phylogenetic tree was designed using iTOL (Interactive Tree of Life) (Letunic and Bork 2019). Plasmid-encoded sequences were modelled using the SWISS-MODEL server (Benkert, Biasini et al. 2011, Bertoni, Kiefer et al. 2017, Waterhouse, Bertoni et al. 2018, Studer, Rempfer et al. 2020), with the AAC(2′)-Ia structure stripped of its ligands and water molecules used as the template.

4.4 Results

4.4.1 Structure Characteristics

Four high-resolution crystal structures of AAC(2′)-Ia were solved, three structures containing coenzyme A (CoA) and N2′-acetylated aminoglycosides tobramycin, netilmicin, and plazomicin; and one containing acetyl-CoA and aminoglycoside inhibitor amikacin, which lacks an N2′ moiety. Data collection and final refinement statistics for each of these crystal structures are listed in Table 4 – 1. The overall fold of AAC(2′)-Ia, as with all other reported structures of aminoglycoside N-acetyltransferases (Wybenga-Groot, Draker et al. 1999, Vetting, Hegde et al. 2002, Vetting, Magnet et al. 2004, Magalhaes, Vetting et al. 2008, Maurice, Broutin et al. 2008, Vetting, Park et al. 2008, Smith, Toth et al. 2014, Stogios, Kuhn et al. 2017, Kumar, Selvaraj et al. 2018, Kumar, Serpersu et al. 2018, Kumar, Agarwal et al. 2019), belongs to the GCN5 related N-acetyltransferase (GNAT) superfamily. It is dimer with in the asymmetric unit has an identical fold to another enzyme in this subclass, AAC(2′)-Ic, and shares a 55% sequence similarity and 32% sequence identity to AAC(2′)-Ia (Vetting, Hegde et al. 2002) (Figure 4 – 1).

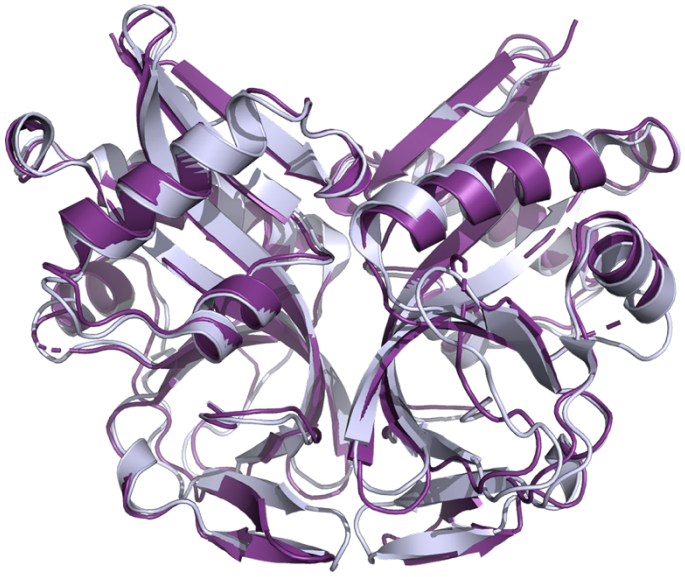

Figure 4 – 1. Structural Overlay of AAC(2′)-I enzymes. AAC(2′)-Ia is colored in purple and AAC(2′)-Ic (PDB ID: 1M41) is colored in pale purple.

4.4.2 Acetyl Coenzyme A and Coenzyme A binding

The CoA binding pocket of AAC(2′)-Ia has not previously been described. The discovery maps for each of the AAC(2′)-Ia crystal structures allow us to unambiguously place acetyl-CoA

and CoA within the enzyme's active site (Figure 4 – 2A,B). The crystal structure of AAC(2′)-Ia in complex with acetyl-CoA and amikacin, an aminoglycoside inhibitor, captures the enzyme in a pre-catalysis state. Meanwhile, the crystal structures of AAC(2′)-Ia in complex with CoA and acetylated aminoglycosides describes the enzyme in three product-bound states. While there are a large number of flexible basic residues in the CoA and acetyl-CoA binding regions, most of the interactions within the binding sites observed in each monomer are maintained. In the pre-catalyzed state, the adenine ring of acetyl-CoA is sandwiched in between two flexible loops, with residue Arg-89 on one side and Lys-121 on the other; however, this portion does not form any inter- or intramolecular hydrogen bonds. The phosphoryl-group of the 3′-phosphorylated adenine diphosphate (ADP) moiety forms hydrogen bond interactions with Arg-89, while the ribose ring is void of interactions with the enzyme (Figure 4 – 2D). The α- and β-phosphates of this same moiety form backbone hydrogen bond interactions with Gln-90, Gly-91 and Arg-94, as well as Arg-89 and Gly-93, respectively (Figure 4 – 2D). In the pantothenic acid moiety, the hydroxyl group of the carboxylic acid hydrogen bonds with Asp-118, while the oxygen can interact with Arg-88 or Val-83. The second oxygen of this moiety two interacts with Ser-116 (Figure 4 – 2D). The amide groups of acetyl-CoA form hydrogen bond with Asp-118 and the backbone oxygen of Met-81, respectively (Figure 4 – 2D). Finally, the oxygen group of the acetyl portion forms a hydrogen bond with the backbone amide of Met-81 (Figure 4 – 2D).

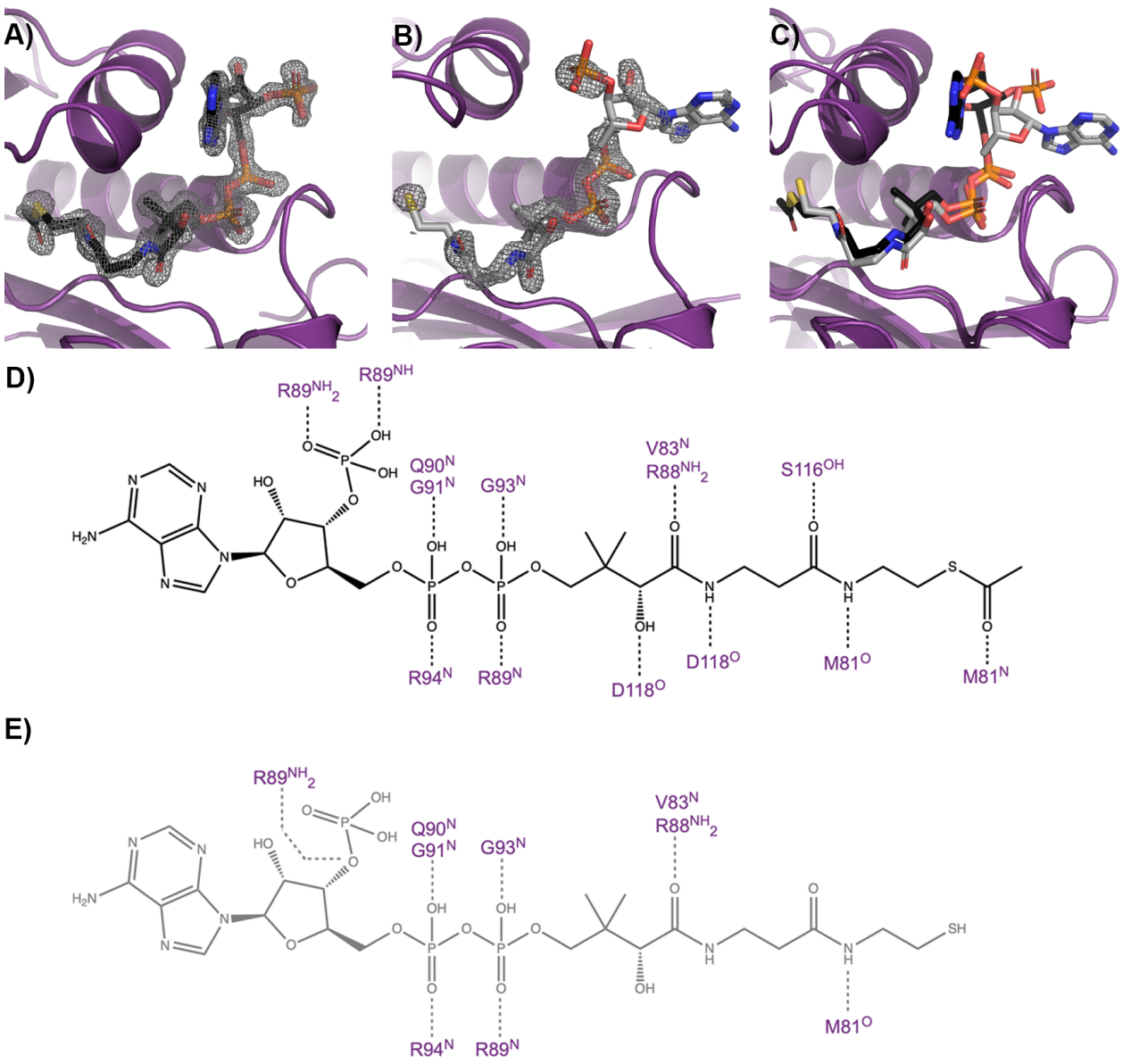

Figure 4 – 2. Interactions of Acetyl-CoA and CoA to AAC(2′)-Ia. Panels (A) and (B) depict the Fo−Fc discovery maps for ligands acetyl-CoA and CoA, respectively, at a contour level of 3σ. (C) Overlay of AAC(2′)-Ia bound to acetyl-CoA and CoA, same color scheme as panels (A) and (B). Hydrogen bond interactions between AAC(2′)-Ia and (D) acetyl-CoA (black), (E) CoA (grey).

In the three product-bound states of AAC(2′)-Ia, the pantothenic acid moiety and the α- and β-phosphates of the 3′-phosphorylated ADP moiety of CoA remain in a similar conformation to that of acetyl-CoA (Figure 4 – 2C). The hydrogen bond interactions remain similar, except towards the tail end of the CoA molecule, where the pantothenic acid moiety forms fewer

interactions with the enzyme. (Figure 4 – 2E). The most apparent difference between acetyl-CoA and CoA binding to the pre-catalyzed-state and the product-bound state is the positioning of the 3′-adenosine moiety. In the product-bound state, this portion of CoA flips roughly 270˚ towards a solvent-exposed portion of the enzyme (Figure 4 – 2C). Again, the ribose and adenine rings do not interact with the enzyme. Instead, the adenine rings are now adjacent to a loop containing residues Arg89-Gly91.

4.4.3 Structural Basis for Aminoglycoside Binding to AAC(2′)-Ia

The discovery maps for each of the AAC(2′)-Ia crystal structures allow us to unambiguously place its substrates and inhibitors within the enzyme's active site (Figure 4 – 3A-D). The structural basis for acetylated-tobramycin is similar to that of a previously reported acetylated-gentamicin-bound structure of AAC(2′)-Ia (Cox, Ejim et al. 2018). While the aminoglycoside portion of acetylated-gentamicin only hydrogen bonds with AAC(2′)-Ia via three residues, the tobramycin moiety can interact with up to 7 residues. In identical fashion to gentamicin, the central ring of tobramycin is anchored by two hydrogen bond interactions, N-1 with Glu-149 and N-3 with the C-terminal carboxylate of Trp-178 (Figure 4 – 4A) (Cox, Ejim et al. 2018). Additionally, both aminoglycosides interact with the backbone carbonyl of Ser-114 at their site of modification, N-2′ (Figure 4 – 4A) (Cox, Ejim et al. 2018). Aside from these interactions, the prime-ring of tobramycin also interacts with the backbone carbonyl of Asp-32 and the side chain of Asp-37 at the N-6′ position (Figure 4 – 4A). At the double-prime ring, tobramycin interacts with the enzyme at its N-4″ and O-5″ via hydrogen bond with Asp-117 (Figure 4 – 4A). The tobramycin molecule in chain B also forms an additional hydrogen bond interaction between its O-2″ and Glu-148 of AAC(2′)-Ia. The acetyl group modification of the molecule interacts with the enzyme by way of the backbone amine of Met-81 (Figure 4 – 4A). The

acetylated tobramycin in chain A also interacts with the backbone amine of the adjacent residue, Ala-80 (Figure 4 – 4A).

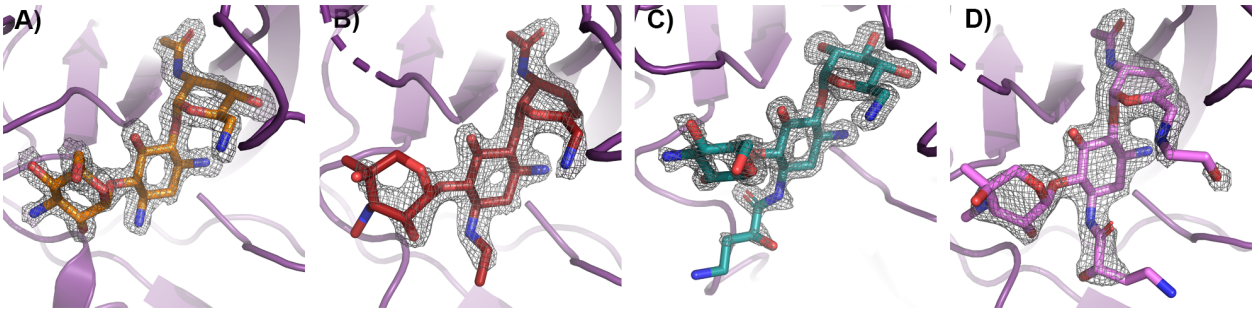

Figure 4 – 3. Binding of naturally occurring, semi-synthetic and next-generation aminoglycosides to AAC(2′)-Ia. Depicted in panels (A), (B), (C), and (D) are the Fo−Fc discovery maps for ligands tobramycin, netilmicin, amikacin, and plazomicin, respectively, at a contour level of 3σ. The enzyme is colored purple and the aminoglycosides tobramycin, netilmicin, amikacin, and plazomicin are colored in orange, red, teal, and violet, respectively.

AAC(2′)-Ia is capable of modifying three semi-synthetic aminoglycosides i.e., dibekacin, netilmicin, and plazomicin. We report here the structural basis for AAC(2′)-Ia's ability to modify netilmicin and plazomicin. Netilmicin is a semi-synthetic derivative of sisomicin, an aminoglycoside that is structurally similar and has similar bacterial targets to gentamicin. Just as for gentamicin, AAC(2′)-Ia utilizes the same three residues, Ser-114, Glu-149, and Trp-178. However, unlike gentamicin, netilmicin's N-6′ can form hydrogen bonds with both Asp-32 and -37. This is due to a slight shift in the N-6′ group's positioning. Additionally, Glu-148 in chain A flips in towards the active site to interact with the 2′′-OH and 3′′-NH segments of netilmicin. Finally, the presence of a bulky ethyl substituent at N-1 does not cause any structural rearrangements of the enzyme, since this portion of the active site is readily solvent accessible.

Plazomicin, like netilmicin, is a semi-synthetic derivative of sisomicin. As such, its binding is similar, except at its N-1 and N-6′ substituents. In addition to solving the structure of AAC(2′)-Ia in complex with acetylated-gentamicin, Cox and colleagues also attempted to model the possible binding mode of plazomicin however, the rationale for binding was inaccurate (Cox, Ejim et al.

2018). They postulated that the (S)-HABA group binds by forming an interaction with its hydroxyl-group and Asp-176. We can confirm that Asp-176 does interact with plazomicin however, this residue instead hydrogen bonds with the terminal amine of this moiety. In addition to this interaction, AAC(2′)-Ia the N-1 substituent also forms interactions with Glu-149 at the hydroxyl-group and maintains the N-1 interaction, common with all other aminoglycosides. While the (S)-HABA incorporation at N-1 is a common semi-synthetic aminoglycoside feature, the addition of the hydro-ethyl group at N-6′ is the first of its kind for this class of antibiotics. Cox et al. also hypothesized the binding mode of this moiety of plazomicin to AAC(2′)-Ia. They theorized that an interaction would occur between the hydroxyl group of the hydroxyethyl substituent and Asp-37 (Cox, Ejim et al. 2018). While this interaction does occur, there is also an additional interaction between the backbone of Asp-32 and the amide group located at N-6′.

Amikacin, a structural derivative of kanamycin, incorporates an (S)-HABA group at its N-1 position, but lacks an amine group at its N-2′ position, making it an inhibitor of AAC(2′)-Ia. Although plazomicin is the only aminoglycoside substrate of AAC(2′)-Ia with an N-1 (S)-HABA group, understanding how another N-1 substituted aminoglycoside binds to this enzyme can provide additional reasoning behind this enzyme's specificity. Amikacin's interactions are similar to those between the enzyme and its natural substrates (Figure 4 – 4C). Although interactions are maintained, especially at the prime ring, the slight movement of residues around the active site in the amikacin-bound structure causes deviations in the positioning of the central and double-prime rings of the aminoglycoside. However, unlike as discussed for plazomicin, the N-1 substitution does not form any hydrogen bond interactions with the enzyme (Figure 4 – 4C). Instead, the shift of residues Glu-148 and Glu-149 makes it so the enzyme can accommodate the (S)-HABA group in an alternative conformation, away from the active site. This also shifts the binding of the double-

prime ring to interact similarly to that of the acetylated-tobramycin-bound structure, as they both have similar chemical groups for this ring.

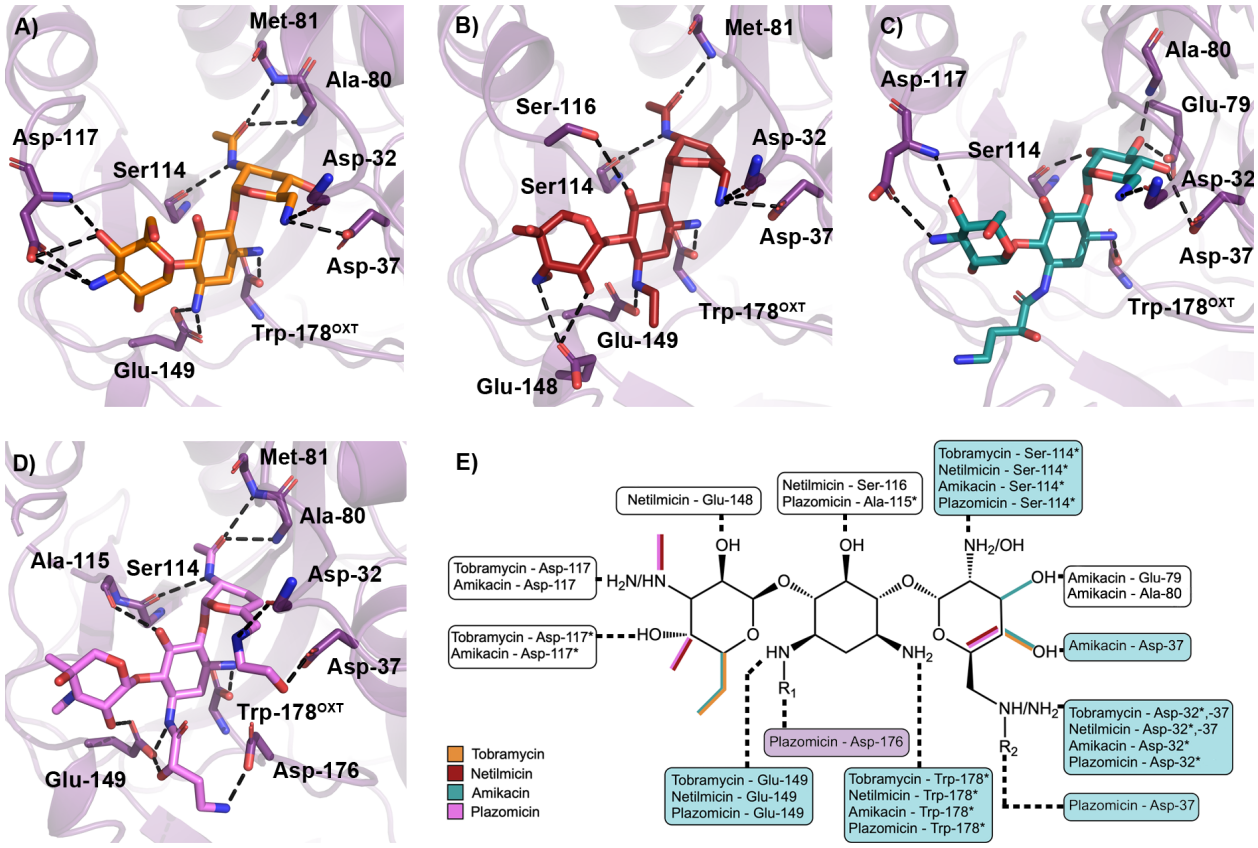

Figure 4 – 4. Interactions of naturally occurring, semi-synthetic aminoglycosides, and plazomicin to AAC(2′)-Ia. Depicted in panels (A), (B), (C), and (D) are the hydrogen bond interactions for acetylated ligands tobramycin, netilmicin, amikacin, and plazomicin, respectively. The color scheme is as in Figure 4 – 3.(E) A combined chemical structure for all four aminoglycosides is shown Features unique to each aminoglycoside are highlighted based on the previous panel's color scheme. Hydrogen bond interactions are depicted in boxes. Blue boxes indicate the four conserved sites involved in critical hydrogen bond interactions, and white boxes indicate interactions that occur less frequently. The box for the residue critical for plazomicin hydrogen bonding is colored in purple.

4.4.4 Substrate Specificity of the AAC(2′) Enzyme Class

Applying a phylogenetic analysis can provide an understanding of other potential AAC(2′) enzymes that can bind and modify plazomicin, and ultimately spread resistance. Our BLAST sequence analysis of the five members of the AAC(2′) enzyme class identified 55 additional homologues from unique bacterial species filtered from 5000 psi-BLAST result sequences (1000

sequences from each psi-BLAST search). The identified sequences had at least a 23% sequence identity to the original query sequences (AAC(2′)-Ia-Ie). Based on the substrate-binding analysis, we identified three key residues involved in AAC(2′)-Ia's aminoglycoside specificity; Asp-37, Glu-149, and Trp-178, and one additional residue, Asp-176, required for plazomicin specificity (Figure 4 – 4E). Asp-32 and Ser-114 are also important for substrate binding in all four structures; however, they were excluded from the conservation analysis since they interact with aminoglycosides using their backbone atoms (Figure 4 – 4E). Sequence alignment of all 61 unique sequences shows that these four residues are highly conserved throughout (Figure 4 – 5A). Asp-37, Glu-149, Trp-178, and Asp-176 are conserved 74, 88, 95, and 92% percent of the time, respectively, where conservation percentages for Glu-149 and Asp-176 include instances of both aspartic and glutamic acid (Figure 4 – 5A). Interestingly, although Asp-32 utilizes its backbone oxygen for binding, it is still conserved 75% of the time.

The predicted ability of the 61 enzymes to bind to either aminoglycosides or next-generation aminoglycoside plazomicin was assessed based on the number of conserved binding residues (Figure 4 – 5B,C). Note, the prediction of aminoglycoside binding is based on enzymes whose substrate specificity has been described [AAC(2′)-Ia-e], however, the prediction of plazomicin binding is based solely on data from AAC(2′)-Ia. The assembly of enzymes were classified as either non-binders, unlikely binders, likely binders, or binders of aminoglycosides if 0, 1, 2, or 3 of the binding residues were observed in a sequence, respectively. The same classification was made for plazomicin if 0-1, 2, 3, or 4 of the binding residues were observed in a sequence, respectively (Figure 4 – 5B). For aminoglycosides, it was assessed that 2%, 3%, 29%, and 66% of enzymes would be non-binders, unlikely binders, likely binders, and binders, respectively, reflective of the extensive conservation observed in the substrate binding site (Figure

4 – 5A,B). Similarly, for plazomicin, it was predicted that 3%, 3%, 30%, and 64% of enzymes would be non-binders, unlikely binders, likely binders, and binders, respectively (Figure 4 – 5B). It is meaningful to note that only three enzymes change their classification on their ability to bind either aminoglycosides or next-generation aminoglycoside plazomicin (Figure 4 – 5C).

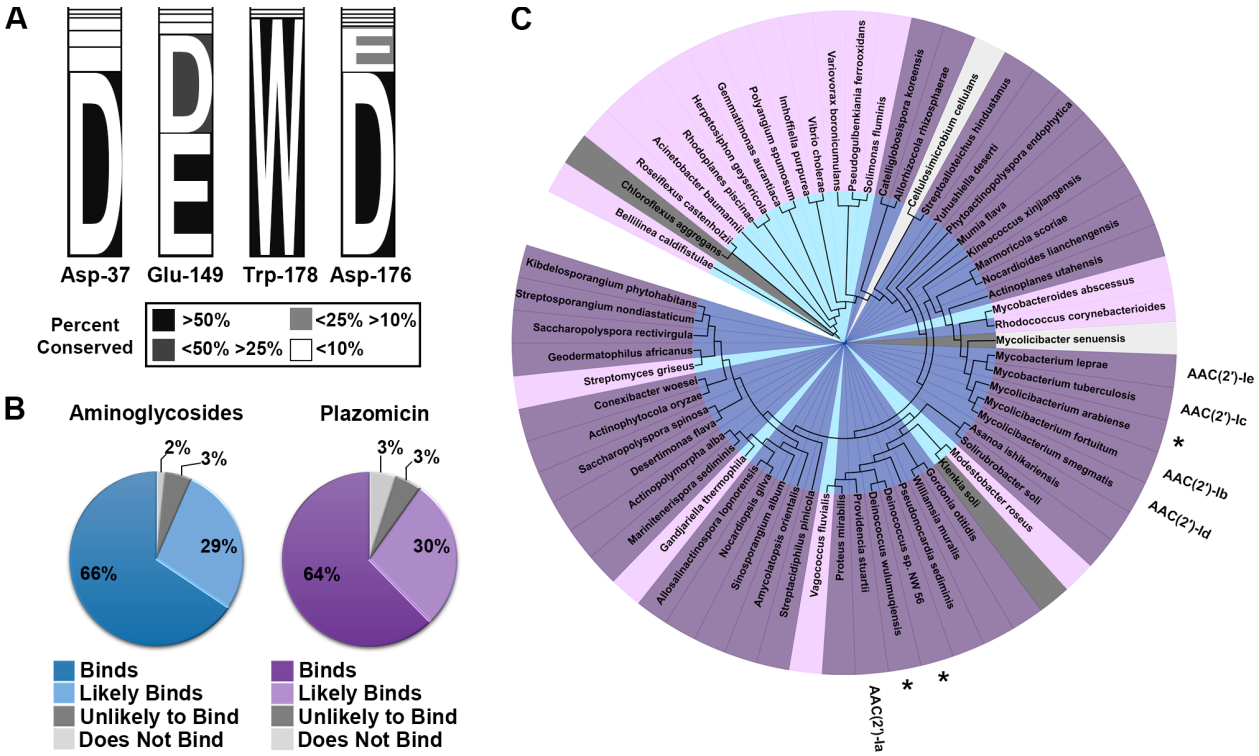

Figure 4 – 5. Phylogenetic analysis of aminoglycoside (2′)-N-acetyltransferase substrate specificity. (A) Percent conservation of key residues involved in aminoglycoside and plazomicin binding, where conservation is colored according to the legend. (B) Predicted classification of 61 identified sequences as binders, likely binders, unlikely binders, and non-binders for aminoglycosides or plazomicin, colored according to the legend. (C) Phylogenetic tree of identified sequences colored as in panel (B), with aminoglycosides' coloring in the center, and plazomicin coloring in the outer circle. The original five query sequences are labelled, and plasmid-encoded sequences are highlighted with an asterisks (*).

The majority of the sequences found are chromosomally encoded; however, three sequences are plasmid-encoded. These three sequences are found in the following bacterial species: *Mycolicibacterium arabiense, Deinococcus wulumuqiensis,* and *Deinococcus sp. NW-56* (Accession numbers: WP_163924889.1, WP_114673790.1, WP_104992197.1) (Fomenkov,

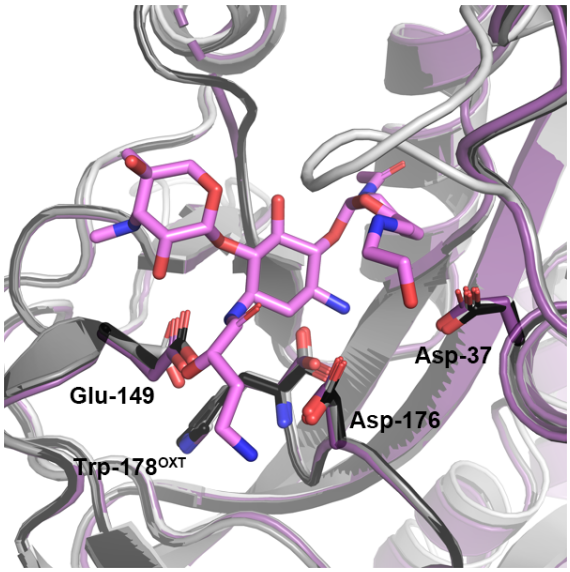

Figure 4 – 6. Active site overlay and conserved residues of AAC(2′)-Ia and modeled enzymes. AAC(2′)-Ia from *P. stuartii* is colored in purple, while the models are colored black (*D. sp. NW-56*), grey (*D. wulumuqiensis*) and light grey (*M. arabiense)*. Plazomicin is depicted in stick representation and colored in violet.

Luyten et al. 2019, Matsumoto, Kinjo et al. 2019) (Figure 4 – 5C). Each of these sequences shares a 33.5, 42.0, and 43.5% sequence identity and an 84, 98, and 99% sequence coverage with AAC(2′)-Ia from *P. stuartii*, respectively, where all four binding residues are conserved. Models of these three sequences show their aminoglycoside binding pocket can readily bind plazomicin (Figure 4 – 6).

4.5 Discussion

4.5.1 AAC(2′)-Ia can accommodate N-1 and N6′ aminoglycoside skeletal additions

Plazomicin has shown activity against methicillin-resistant *S. aureus* and multi-drug resistant *E. coli*, *K. pneumonia*, and *Enterobacter* spp, and is currently approved for the treatment of complicated urinary tract infections and pyelonephritis (Tenover, Tickler et al. 2011, Galani, Souli et al. 2012). Plazomicin's effectiveness stems from the incorporation of two chemical groups at the N-1 and N-6′ positions of its aminoglycoside precursor, sisomicin (Armstrong and Miller 2010). It is understood that elevated activity against plazomicin is exclusive to AAC(2′)-Ia, whereas van der Waals strain prevents clinically widespread resistance factors such as ANT(2″), APH(2″), and AAC(6′) from binding this antibiotic (Armstrong and Miller 2010, Bassenden, Rodionov et al. 2016). We provide here the first detailed structural analysis of an aminoglycoside modifying enzyme that can alter an aminoglycoside with two semi-synthetic additions. Our investigation presents an understanding of why AAC(2′)-Ia has the ability to accommodate the N-1 (S)-HABA group and the N-6′ hydroxy-ethyl group. Comparison of all four of our crystal structures, allows us to inspect structural differences in active site binding at both these positions.

First, at the N-1 binding site, the accommodation of the (S)-HABA group is due to the flexibility of either residue Glu-148 or Glu-149. Our structures show that Glu-148 can adopt two conformations (Figure 4 – 7). The difference in the positioning of this residue is dependent on how the enzyme harbours the N-1 expansion. In the tobramycin-bound structure, there is no chemical addition at the N-1 amine, and therefore Glu-148 can adopt either conformation (Figure 4 – 7A). In the netilmicin bound structure, the ethyl addition at N-1 sits perpendicular to the aminoglycoside

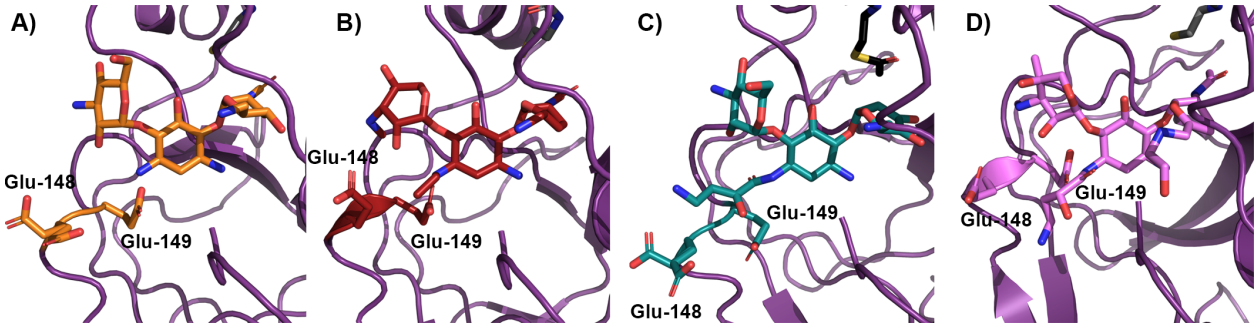

Figure 4 – 7. AAC(2′)-Ia residues responsible for aminoglycoside N-1 (S)-HABA group accommodation. Residues are colored according to the corresponding aminoglycoside; (A) tobramycin, (B) netilmicin, (C) amikacin, and (D) plazomicin. Colors are in accordance with the schemes presented in figures 4 – 3 and 4 – 4.

plane, requiring Glu-148 to flip away from the active site (Figure 4 – 7B). The plazomicin-bound structure sees the N-1 (S)-HABA adopting a similar conformation to the ethyl addition of netilmicin, where the (S)-HABA group first protrudes perpendicularly to the aminoglycoside plane, and then proceeds in a downward fashion (Figure 4 – 7 B, D). The amikacin-bound structure shows that the enzyme is also capable of adapting the (S)-HABA moiety in a second conformation. This second conformation, as displayed by amikacin, exhibits that the N-1 tail can also sit parallel to the aminoglycoside plane (Figure 4 – 7C). The adoption of this conformation is based on the movement of residue Glu-149 (Figure 4 – 7C). As opposed to the other three structures, this residue flips away from the aminoglycoside-binding site to accommodate this bulky substituent.

Second, the N-6′ binding site consists of two residues, Asp-32 and -37. With respect to aminoglycoside binding, accommodation of this chemical extension requires no conformational change when comparing binding to aminoglycosides void of this moiety. Moreover, interaction with these two residues is important for prime-ring binding in all four aminoglycoside-bound structures. Due to the structural rigidity at this site, next-generation drug design strategies should focus on disrupting the aminoglycoside-enzyme interactions in this region. AAC(2′)-Ia's flexibility at the N-1 binding-site makes it unlikely that further chemical modification of an

aminoglycoside at this location would perturb resistance by this enzyme. Additionally, chemically reinforcing the prime-ring of plazomicin could potentially produce an antibiotic capable of evading the effects of all AMEs. However, a viable next-generation aminoglycoside design strategy would have to ensure such an antibiotic could retain its affinity for the ribosomal A-site.

4.5.2 Residue conservation and aminoglycoside binding and the future of plazomicin resistance

Our analysis in figure 4 – 5 outlines the conservation of residues in the aminoglycoside/ plazomicin binding pocket across AAC(2′) enzymes. These residues are highly conserved, and our analysis suggests that 95% of the homologues that have been identified would be likely or capable of binding aminoglycosides (Figure 4 – 5B, C). From these identified homologues, 98% of them are predicted to retain their ability to bind plazomicin (Figure 4 – 5B, C). This result is troublesome as it reveals that plazomicin resistance is likely not isolated to a single bacterial species. Moreover, based on binding residue conservation, it is likely that the ability to chemically detoxify plazomicin is an innate feature of AAC(2′)-I enzymes.

Our analysis also provides an understanding of the evolutionary pathway for the AAC(2′)-I enzyme subtypes. Our survey of public sequence databases queried against five chromosomally encoded sequences from *P. stuartii*, *M. fortuitum*, *M. tuberculosis*, *M. smegmatis*, and *M. leprae* have allowed us to identify homologues from other species that are aminoglycoside and plazomicin binders (Rather, Orosz et al. 1993, Ainsa, Perez et al. 1997). While the results from this investigation show that the majority of homologues remain chromosomally encoded, three homologues were found to be plasmid-encoded (Figure 4 – 5C). Additionally, these sequences have high similarity and identity to AAC(2′)-Ia, with all binding residues being conserved (Figure 4 – 6). This finding is cause for alarm as the ability of transposable elements to disseminate quickly allows resistance to spread in pathogens of medical interest (Ramirez and Tolmasky 2010).

Moreover, this reinforces the urgency of preserving plazomicin as a viable treatment option. Currently, plazomicin is on the WHO's list of essential medicine, and is part of the reserve group of antibiotics, for use only against infections that are suspected to be caused by multidrug-resistance organisms. However, although resistance is not yet widespread, the identification of sequences which are likely capable of binding plazomicin on mobile elements indicates that the spread of resistance is no longer theoretical, it is inevitable. This result, combined with the ability of AAC(2′)-Ia to bind N-1-substituted aminoglycosides in different conformations, enforces the need for next-generation aminoglycosides with a novel or additional chemical substituent in order to curb resistance to antibiotics of last resort.

Chapter 5 – Conclusions

5.1 Aminoglycoside Resistance from a Drug-Target Perspective

Bacterial pathogens employ several mechanisms to evade the bactericidal effect of aminoglycosides, where enzymatic modification of these antibiotics is the main mode linked to clinical resistance. Although many efforts have been pursued to try and counteract the actions of these aminoglycoside modifying enzymes, nearly one hundred different bacterial enzymes capable of conferring resistance via either acetylation, phosphorylation, or nucleotidylation have been described and identified in clinical isolates. Adding to this complexity, each of these resistance enzymes has its unique substrate specificity, where a single enzyme can modify many aminoglycosides, and many enzymes can alter a single aminoglycoside through a slew of different mechanisms.

Aminoglycoside resistance is a multifactorial problem that requires a plethora of strategies. As illustrated in Figure 3 of Chapter 1, solely tackling one proponent of aminoglycoside resistance, that is, via enzymatic chemical modification, still presents researchers with numerous challenges. From a drug-target perspective, the identification and prioritization of clinically persistent targets can present a hierarchy of strategies to pursue. In line with this approach, this thesis began by identifying the important research avenues that required attention. The studies presented in this thesis collectively illustrate the structural and functional aspects of important aminoglycoside resistance factors and demonstrates a rationale for their ability to modify clinically prevalent medicines (Table 5 – 1).

Table 5 – 1: Crystal Structures of Aminoglycoside Modifying Enzymes Presented in this Thesis.

Enzyme	Ligand	Res. (Å)	R_{work}	R_{free}	PDB Code
ANT(2″)-I	Tobramycin; AMP	1.9	0.167	0.188	4XJE
ANT(2″)-I	2″-adenylated-tobramycin; PP_i; Mn^{2+}	1.8	0.145	0.174	5CFU
ANT(2″)-I	Tobramycin; AMPCPP; Mn^{2+}	1.7	0.169	0.190	5CFS
ANT(2″)-I	Gentamicin; AMPCPP; Mn^{2+}	1.5	0.149	0.174	5CFT
AAC(2′)-Ia	2′-acetylated-tobramycin; CoA	1.8	0.167	0.193	6VR2
AAC(2′)-Ia	2′-acetylated-netilmicin; CoA	2.0	0.182	0.226	6VR3
AAC(2′)-Ia	2′-acetylated-plazomicin; CoA	1.9	0.188	0.223	6VOU
AAC(2′)-Ia	Amikacin; Acetyl-CoA	1.4	0.140	0.182	6VTA

5.2 Understanding Aminoglycoside Resistance from a Target's Perspective

We first recognized a void in the knowledge framework surrounding the nucleotidyltransferase class of aminoglycoside modifying enzymes. Importantly, the details surrounding the structure and function of the most clinically prevalent resistance factor of this enzyme class, ANT(2″), were absent. In Chapter 2, we presented the structural details of this enzyme in three states along its reaction coordinate. We reveal critical details on the enzyme's kinetic mechanism, allowing us to outline the ordered sequence by which its substrates associate and its products dissociate. Moreover, we present the framework for how enzymatic modification occurs in near-atomic detail by showcasing its catalytic mechanism. Having a complete understanding of aminoglycoside resistance from the perspective of the most clinically relevant targets provides a knowledge base for the mechanism of action of a previously overlooked class

of enzymes. Additionally, this information can provide key insights into developing strategies to evade resistance by ANT(2″) and other similar resistance factors.

5.3 Understanding Aminoglycoside Resistance from a Drug's Perspective

ANT(2″) represents one of many enzymes that is capable of detoxifying two aminoglycosides that are widely used in clinical applications, tobramycin and gentamicin. In Chapter 3, we examine the aminoglycoside binding pocket of prevalent targets in each aminoglycoside modifying enzyme class as well as the ribosomal A-site, and compare the critical interactions involved in tobramycin- and gentamicin-binding. Identifying these interactions has allowed us to speculate on the development of next-generation aminoglycosides capable of evading the action of resistance enzymes, while retaining their affinity for the A-site. Although we can attempt to exploit some of these interactions, our analysis reveals that there are limited opportunities for developing aminoglycoside analogues capable of evading resistance. This result reiterates the importance of valuing the aminoglycoside library that we currently have at our disposal, and reinforces the need for developing alternative strategies to combat resistance.

5.4 Understanding Next-generation Aminoglycoside Resistance and the Inevitable Surge of Existing Targets

Recognizing the urgency in maintaining the viability of aminoglycosides, we identified a knowledge gap surrounding resistance of the newest semi-synthetic aminoglycoside derivative, plazomicin. AAC(2′)-Ia is currently the only known proponent of plazomicin resistance. Interestingly, this enzyme's substrate specificity includes tobramycin and gentamicin, as well as many semi-synthetic aminoglycosides. In Chapter 4, we reveal the structural details behind AAC(2′)-Ia's ability to bind a chemically diverse set of antibiotics, including the next-generation drug, plazomicin. The characterization of AAC(2′)-Ia's aminoglycoside binding pocket has allowed us to identify other acetyltransferase homologues from different bacterial species that

likely have the same substrate specificity. Additionally, some of these homologues have been identified as plasmid-encoded. The results from this analysis are worrisome; although plazomicin is not currently impacted by widespread resistance factors, as its usage undoubtedly increases, so too will the prevalence of enzymes within its resistome. As opportunities for next-generation aminoglycoside development are dwindling, it is imperative to establish a comprehensive understanding of underlying resistance mechanisms to ensure that we can remain one step ahead of resistance.

5.5 Aminoglycoside Resistance: Next Steps

This thesis provides a cautionary tale on the revival of a once-thriving antibiotic class. The approval of plazomicin in 2018 represents the first new antibiotic introduced into this class in nearly thirty years, and protecting its clinical value should be the main priority moving forward. Antibiotics are no longer hailed as silver bullets, nor should they be. Inevitably the introduction of new antibiotics will always be met with some form of resistance, and overcoming resistance is no small challenge. So, what are the next steps when it comes to aminoglycoside resistance?

We've outlined that prioritization is key when it comes to bridging our understanding of enzymes that cause aminoglycoside resistance. Outlining the structure and function of ANT(2″) is only one small yet important step in this process. There are still many enzymes that require this same consideration. Completing the structural and functional characterization of known enzymatic resistance factors will provide a complete framework of how three distinct classes of enzymes can detoxify the complete set of three chemically unique aminoglycoside sub-groups – i.e. 4,5-, 4,6-disubstituted, and non-deoxystreptamine aminoglycosides. This profound understanding, especially from a structural context, can allow us to pinpoint potential drug-design avenues that would form the basis for conceptualizing aminoglycosides with the ability to evade specific

resistance factors (Chapter 3). However, turning concepts into viable antibiotics requires more perspective than those offered from a structural biology standpoint. The success of future antibiotic development is contingent on scientific collaboration. A collective effort between chemists, biologists, biochemists, and bioinformaticians is crucial when considering a well-rounded approach to drug design. The intentions put forth in this thesis are just the beginning of this conversation.

Perhaps the most concerning caveat with respect to this thesis comes with the reminder that no antibiotic is safe from resistance. Although the discovery and approval of plazomicin is a monumental victory in the fight against resistance, vigilance and innovation are still important factors to consider moving forward. Next-generation aminoglycoside design is ultimately hindered by its limited potential, as the number of antibiotics that can be practically conceived is finite. Alternative strategies have already been considered, including the use of inhibitors in adjuvant therapies and regulating the expression of aminoglycoside modifying enzymes. Still, each new action plan considered in aminoglycoside therapy will likely be met with some form of resistance, and the long-term effectiveness of novel methods is dependent on having many viable options. Broadening this approach beyond aminoglycosides is also critical when considering the future of antibiotic resistance. The introduction of new techniques, including phage therapies and rapid pathogen detection, are just a few examples of technologies that can be used in combination with traditional methods to keep resistance at bay. In the end, avoiding a post-antibiotic era still requires a more thorough understanding of resistance mechanisms and the discovery of new therapies through a multidisciplinary and collaborative scientific approach.

References

Abbassi, M. S., W. Achour and A. B. Hassen (2007). "High-level gentamicin-resistant Enterococcus faecium strains isolated from bone marrow transplant patients: accumulation of antibiotic resistance genes, large plasmids and clonal strain dissemination." Int J Antimicrob Agents **29**(6): 658-664.

Abrahams, J. P. and A. G. Leslie (1996). "Methods used in the structure determination of bovine mitochondrial F1 ATPase." Acta Crystallogr D Biol Crystallogr **52**(Pt 1): 30-42.

Achaogen (2018). "Plazomicin (Zemdri) - a new aminoglycoside antibiotic." Med Lett Drugs Ther **60**(1559): 180-182.

Adams, P. D., P. V. Afonine, G. Bunkoczi, V. B. Chen, I. W. Davis, N. Echols, J. J. Headd, L. W. Hung, G. J. Kapral, R. W. Grosse-Kunstleve, A. J. McCoy, N. W. Moriarty, R. Oeffner, R. J. Read, D. C. Richardson, J. S. Richardson, T. C. Terwilliger and P. H. Zwart (2010). "PHENIX: a comprehensive Python-based system for macromolecular structure solution." Acta Crystallogr D Biol Crystallogr **66**(Pt 2): 213-221.

Agence française de sécurité sanitaire des produits de, s. (2012). "Update on good use of injectable aminoglycosides, gentamycin, tobramycin, netilmycin, amikacin. Pharmacological properties, indications, dosage, and mode of administration, treatment monitoring." Medecine et maladies infectieuses **42**(7): 301-308.

Aggen, J. B., E. S. Armstrong, A. A. Goldblum, P. Dozzo, M. S. Linsell, M. J. Gliedt, D. J. Hildebrandt, L. A. Feeney, A. Kubo, R. D. Matias, S. Lopez, M. Gomez, K. B. Wlasichuk, R. Diokno, G. H. Miller and H. E. Moser (2010). "Synthesis and spectrum of the neoglycoside ACHN-490." Antimicrob Agents Chemother **54**(11): 4636-4642.

Ainsa, J. A., E. Perez, V. Pelicic, F. X. Berthet, B. Gicquel and C. Martin (1997). "Aminoglycoside 2'-N-acetyltransferase genes are universally present in mycobacteria: characterization of the aac(2')-Ic gene from Mycobacterium tuberculosis and the aac(2')-Id gene from Mycobacterium smegmatis." Mol Microbiol **24**(2): 431-441.

Altschul, S. F., T. L. Madden, A. A. Schaffer, J. Zhang, Z. Zhang, W. Miller and D. J. Lipman (1997). "Gapped BLAST and PSI-BLAST: a new generation of protein database search programs." Nucleic Acids Res **25**(17): 3389-3402.

Aminov, R. I. (2010). "A brief history of the antibiotic era: lessons learned and challenges for the future." Front Microbiol **1**: 134.

Aonuma, S., F. Ariji, K. Oizumi and K. Konno (1987). "Electron microscopy of Pseudomonas aeruginosa treated with sulbenicillin and dibekacin." Tohoku J Exp Med **152**(2): 119-128.

Appelbaum, P. C. (2012). "2012 and beyond: potential for the start of a second pre-antibiotic era?" J Antimicrob Chemother **67**(9): 2062-2068.

Aravind, L. and E. V. Koonin (1999). "DNA polymerase beta-like nucleotidyltransferase superfamily: identification of three new families, classification and evolutionary history." Nucleic Acids Res **27**(7): 1609-1618.

Armstrong, E. S. and G. H. Miller (2010). "Combating evolution with intelligent design: the neoglycoside ACHN-490." Curr Opin Microbiol **13**(5): 565-573.

Arya, D. P. (2007). Aminoglycoside antibiotics : from chemical biology to drug discovery. Hoboken, N.J., Wiley-Interscience.

Assembly of Life Sciences (U.S.). Committee to Study the Human Health Effects of Subtherapeutic Antibiotic Use in Animal Feeds. (1980). The effects on human health of subtherapeutic use of antimicrobials in animal feeds. Washington, D.C., National Academy of Sciences.

Bacot-Davis, V. R., A. V. Bassenden and A. M. Berghuis (2016). "Drug-target networks in aminoglycoside resistance: hierarchy of priority in structural drug design." MedChemComm **7**(1): 103-113.

Baer, G. M. (1994). "Rabies--an historical perspective." Infect Agents Dis **3**(4): 168-180.

Bassenden, A. V., J. Park, D. Rodionov and A. M. Berghuis (2020). "Revisiting the Catalytic Cycle and Kinetic Mechanism of Aminoglycoside O-Nucleotidyltransferase(2"): A Structural and Kinetic Study." ACS Chem Biol **15**(3): 686-694.

Bassenden, A. V., D. Rodionov, K. Shi and A. M. Berghuis (2016). "Structural Analysis of the Tobramycin and Gentamicin Clinical Resistome Reveals Limitations for Next-generation Aminoglycoside Design." ACS Chem Biol **11**(5): 1339-1346.

Bassetti, M. and E. Righi (2014). "Eravacycline for the treatment of intra-abdominal infections." Expert Opin Investig Drugs **23**(11): 1575-1584.

Bassetti, M. and E. Righi (2015). "Development of novel antibacterial drugs to combat multiple resistant organisms." Langenbecks Arch Surg **400**(2): 153-165.

Becker, B. and M. A. Cooper (2013). "Aminoglycoside antibiotics in the 21st century." ACS Chem Biol **8**(1): 105-115.

Benkert, P., M. Biasini and T. Schwede (2011). "Toward the estimation of the absolute quality of individual protein structure models." Bioinformatics **27**(3): 343-350.

Benveniste, R. and J. Davies (1971). "R-factor mediated gentamicin resistance: A new enzyme which modifies aminoglycoside antibiotics." FEBS Lett **14**(5): 293-296.

Benveniste, R. and J. Davies (1973). "Mechanisms of antibiotic resistance in bacteria." Annu Rev Biochem **42**: 471-506.

Bertoni, M., F. Kiefer, M. Biasini, L. Bordoli and T. Schwede (2017). "Modeling protein quaternary structure of homo- and hetero-oligomers beyond binary interactions by homology." Sci Rep **7**(1): 10480.

Bode, C., C. Schafer, H. Fukui and J. C. Bode (1997). "Effect of treatment with paromomycin on endotoxemia in patients with alcoholic liver disease--a double-blind, placebo-controlled trial." Alcohol Clin Exp Res **21**(8): 1367-1373.

Bonafede, M. and L. B. Rice (1997). "Emerging antibiotic resistance." J Lab Clin Med **130**(6): 558-566.

Borovinskaya, M. A., R. D. Pai, W. Zhang, B. S. Schuwirth, J. M. Holton, G. Hirokawa, H. Kaji, A. Kaji and J. H. Cate (2007). "Structural basis for aminoglycoside inhibition of bacterial ribosome recycling." Nat Struct Mol Biol **14**(8): 727-732.

Bottger, E. C., B. Springer, T. Prammananan, Y. Kidan and P. Sander (2001). "Structural basis for selectivity and toxicity of ribosomal antibiotics." EMBO Rep **2**(4): 318-323.

Boucher, H. W., G. H. Talbot, D. K. Benjamin, Jr., J. Bradley, R. J. Guidos, R. N. Jones, B. E. Murray, R. A. Bonomo, D. Gilbert and A. Infectious Diseases Society of (2013). "10 x '20 Progress--development of new drugs active against gram-negative bacilli: an update from the Infectious Diseases Society of America." Clin Infect Dis **56**(12): 1685-1694.

Bryan, L. E. and S. Kwan (1981). "Mechanisms of aminoglycoside resistance of anaerobic bacteria and facultative bacteria grown anaerobically." J Antimicrob Chemother **8 Suppl D**: 1-8.

Burk, D. L. and A. M. Berghuis (2002). "Protein kinase inhibitors and antibiotic resistance." Pharmacol Ther **93**(2-3): 283-292.

Cameron, F. H., D. J. Groot Obbink, V. P. Ackerman and R. M. Hall (1986). "Nucleotide sequence of the AAD(2") aminoglycoside adenylyltransferase determinant aadB. Evolutionary relationship of this region with those surrounding aadA in R538-1 and dhfrII in R388." Nucleic Acids Res **14**(21): 8625-8635.

Carter, A. P., W. M. Clemons, D. E. Brodersen, R. J. Morgan-Warren, B. T. Wimberly and V. Ramakrishnan (2000). "Functional insights from the structure of the 30S ribosomal subunit and its interactions with antibiotics." Nature **407**(6802): 340-348.

Castro, C., E. Smidansky, K. R. Maksimchuk, J. J. Arnold, V. S. Korneeva, M. Gotte, W. Konigsberg and C. E. Cameron (2007). "Two proton transfers in the transition state for nucleotidyl transfer catalyzed by RNA- and DNA-dependent RNA and DNA polymerases." Proc Natl Acad Sci U S A **104**(11): 4267-4272.

Chittapragada, M., S. Roberts and Y. W. Ham (2009). "Aminoglycosides: molecular insights on the recognition of RNA and aminoglycoside mimics." Perspect Medicin Chem **3**: 21-37.

Chow, J. W. (2000). "Aminoglycoside resistance in enterococci." Clin Infect Dis **31**(2): 586-589.

Coates, A. R., G. Halls and Y. Hu (2011). "Novel classes of antibiotics or more of the same?" Br J Pharmacol **163**(1): 184-194.

Collaborative Computational Project, N. (1994). "The CCP4 suite: programs for protein crystallography." Acta Crystallogr D Biol Crystallogr **50**(Pt 5): 760-763.

Costello, S. E., L. M. Deshpande, A. P. Davis, R. E. Mendes and M. Castanheira (2019). "Aminoglycoside-modifying enzyme and 16S ribosomal RNA methyltransferase genes among a global collection of Gram-negative isolates." J Glob Antimicrob Resist **16**: 278-285.

Cowtan, K. (2000). "General quadratic functions in real and reciprocal space and their application to likelihood phasing." Acta Crystallogr D Biol Crystallogr **56**(Pt 12): 1612-1621.

Cowtan, K. (2006). "The Buccaneer software for automated model building. 1. Tracing protein chains." Acta Crystallogr D Biol Crystallogr **62**(Pt 9): 1002-1011.

Cox, G., L. Ejim, P. J. Stogios, K. Koteva, E. Bordeleau, E. Evdokimova, A. O. Sieron, A. Savchenko, A. W. Serio, K. M. Krause and G. D. Wright (2018). "Plazomicin Retains Antibiotic Activity against Most Aminoglycoside Modifying Enzymes." ACS Infect Dis **4**(6): 980-987.

Cox, G., P. J. Stogios, A. Savchenko and G. D. Wright (2015). "Structural and molecular basis for resistance to aminoglycoside antibiotics by the adenylyltransferase ANT(2")-Ia." MBio **6**(1).

Davies, J. (2006). "Where have All the Antibiotics Gone?" Can J Infect Dis Med Microbiol **17**(5): 287-290.

Davies, J., L. Gorini and B. D. Davis (1965). "Misreading of RNA codewords induced by aminoglycoside antibiotics." Mol Pharmacol **1**(1): 93-106.

Davies, J. C. (2002). "Pseudomonas aeruginosa in cystic fibrosis: pathogenesis and persistence." Paediatr Respir Rev **3**(2): 128-134.

Deguchi, K., M. Koguchi, Y. Suzuki, S. Tanaka, S. Fukayama, R. Ishihara and S. Oda (1996). "[Antibacterial activities of combination uses of isepamicin and beta-lactams in vitro against clinically isolated strains. Part 3. The results against Pseudomonas aeruginosa]." Jpn J Antibiot **49**(5): 509-516.

Demirjian, A., G. V. Sanchez, J. A. Finkelstein, S. M. Ling, A. Srinivasan, L. A. Pollack, L. A. Hicks and J. K. Iskander (2015). "CDC Grand Rounds: Getting Smart About Antibiotics." MMWR Morb Mortal Wkly Rep **64**(32): 871-873.

Denisuik, A. J., J. A. Karlowsky, T. Denisuik, W. W. Nichols, T. A. Keating, H. J. Adam, M. Baxter, A. Walkty and G. G. Zhanel (2015). "In vitro activity of ceftazidime-avibactam against 338 molecularly characterized gentamicin-nonsusceptible Gram-negative clinical isolates obtained from patients in Canadian hospitals." Antimicrob Agents Chemother **59**(6): 3623-3626.

Disney, M. D. (2012). "Studying modification of aminoglycoside antibiotics by resistance-causing enzymes via microarray." Methods Mol Biol **808**: 303-320.

Drusano, G. L. and A. Louie (2011). "Optimization of aminoglycoside therapy." Antimicrob Agents Chemother **55**(6): 2528-2531.

Dunkle, J. A., K. Vinal, P. M. Desai, N. Zelinskaya, M. Savic, D. M. West, G. L. Conn and C. M. Dunham (2014). "Molecular recognition and modification of the 30S ribosome by the aminoglycoside-resistance methyltransferase NpmA." Proc Natl Acad Sci U S A **111**(17): 6275-6280.

Ekman, D. R., E. L. DiGiammarino, E. Wright, E. D. Witter and E. H. Serpersu (2001). "Cloning, overexpression, and purification of aminoglycoside antibiotic nucleotidyltransferase (2")-Ia: conformational studies with bound substrates." Biochemistry **40**(24): 7017-7024.

Emsley, P., B. Lohkamp, W. G. Scott and K. Cowtan (2010). "Features and development of Coot." Acta Crystallogr D Biol Crystallogr **66**(Pt 4): 486-501.

Evans, P. (2006). "Scaling and assessment of data quality." Acta Crystallogr D Biol Crystallogr **62**(Pt 1): 72-82.

Fair, R. J. and Y. Tor (2014). "Antibiotics and bacterial resistance in the 21st century." Perspect Medicin Chem **6**: 25-64.

Ferretti, J. J., K. S. Gilmore and P. Courvalin (1986). "Nucleotide sequence analysis of the gene specifying the bifunctional 6'-aminoglycoside acetyltransferase 2"-aminoglycoside phosphotransferase enzyme in Streptococcus faecalis and identification and cloning of gene regions specifying the two activities." J Bacteriol **167**(2): 631-638.

Finberg, R. W., R. C. Moellering, F. P. Tally, W. A. Craig, G. A. Pankey, E. P. Dellinger, M. A. West, M. Joshi, P. K. Linden, K. V. Rolston, J. C. Rotschafer and M. J. Rybak (2004). "The importance of bactericidal drugs: future directions in infectious disease." Clin Infect Dis **39**(9): 1314-1320.

Fischbach, M. A. and C. T. Walsh (2009). "Antibiotics for emerging pathogens." Science **325**(5944): 1089-1093.

Fomenkov, A., Y. Luyten, T. Vincze, B. P. Anton, R. J. Roberts and R. D. Morgan (2019). "Complete Genome Sequence and Methylome Analysis of Deinococcus wulumuqiensis 479." Microbiol Resour Announc **8**(12).

Fong, D. H. and A. M. Berghuis (2002). "Substrate promiscuity of an aminoglycoside antibiotic resistance enzyme via target mimicry." EMBO J **21**(10): 2323-2331.

Fong, D. H., D. L. Burk and A. M. Berghuis (2005). Aminoglycoside Kinases and Antibiotic Resistance. Handbook of Experimental Pharmacology. Berlin, Heidelberg, Springer. **167**.

Forge, A. and J. Schacht (2000). "Aminoglycoside antibiotics." Audiol Neurootol **5**(1): 3-22.

Foster, T. J. (1983). "Plasmid-determined resistance to antimicrobial drugs and toxic metal ions in bacteria." Microbiol Rev **47**(3): 361-409.

Fourmy, D., S. Yoshizawa and J. D. Puglisi (1998). "Paromomycin binding induces a local conformational change in the A-site of 16 S rRNA." J Mol Biol **277**(2): 333-345.

Francois, B., R. J. Russell, J. B. Murray, F. Aboul-ela, B. Masquida, Q. Vicens and E. Westhof (2005). "Crystal structures of complexes between aminoglycosides and decoding A site oligonucleotides: role of the number of rings and positive charges in the specific binding leading to miscoding." Nucleic Acids Res **33**(17): 5677-5690.

Galani, I., M. Souli, G. L. Daikos, Z. Chrysouli, G. Poulakou, M. Psichogiou, T. Panagea, A. Argyropoulou, I. Stefanou, G. Plakias, H. Giamarellou and G. Petrikkos (2012). "Activity of plazomicin (ACHN-490) against MDR clinical isolates of Klebsiella pneumoniae, Escherichia coli, and Enterobacter spp. from Athens, Greece." J Chemother **24**(4): 191-194.

Galimand, M., P. Courvalin and T. Lambert (2012). "RmtF, a new member of the aminoglycoside resistance 16S rRNA N7 G1405 methyltransferase family." Antimicrob Agents Chemother **56**(7): 3960-3962.

Gates, C. A. and D. B. Northrop (1988a). "Substrate specificities and structure-activity relationships for the nucleotidylation of antibiotics catalyzed by aminoglycoside nucleotidyltransferase 2"-I." Biochemistry **27**(10): 3820-3825.

Gates, C. A. and D. B. Northrop (1988b). "Alternative substrate and inhibition kinetics of aminoglycoside nucleotidyltransferase 2"-I in support of a Theorell-Chance kinetic mechanism." Biochemistry **27**(10): 3826-3833.

Gates, C. A. and D. B. Northrop (1988c). "Determination of the rate-limiting segment of aminoglycoside nucleotidyltransferase 2"-I by pH and viscosity-dependent kinetics." Biochemistry **27**(10): 3834-3842.

Gonzalez-Bello, C. (2017). "Antibiotic adjuvants - A strategy to unlock bacterial resistance to antibiotics." Bioorg Med Chem Lett **27**(18): 4221-4228.

Gould, K. (2016). "Antibiotics: from prehistory to the present day." J Antimicrob Chemother **71**(3): 572-575.

Gray, G. S. and W. M. Fitch (1983). "Evolution of antibiotic resistance genes: the DNA sequence of a kanamycin resistance gene from Staphylococcus aureus." Mol Biol Evol **1**(1): 57-66.

Guindon, S., J. F. Dufayard, V. Lefort, M. Anisimova, W. Hordijk and O. Gascuel (2010). "New algorithms and methods to estimate maximum-likelihood phylogenies: assessing the performance of PhyML 3.0." Syst Biol **59**(3): 307-321.

Gupta, A. (2017). "Plazomicin: A step toward next generation aminoglycosides. Review." Asian J. Res. Pharm. Sci. **7**(3): 173-180.

Hidalgo, L., K. L. Hopkins, B. Gutierrez, C. M. Ovejero, S. Shukla, S. Douthwaite, K. N. Prasad, N. Woodford and B. Gonzalez-Zorn (2013). "Association of the novel aminoglycoside resistance

determinant RmtF with NDM carbapenemase in Enterobacteriaceae isolated in India and the UK." J Antimicrob Chemother **68**(7): 1543-1550.

Holm, L. and C. Sander (1995). "DNA polymerase beta belongs to an ancient nucleotidyltransferase superfamily." Trends Biochem Sci **20**(9): 345-347.

Hulse, E. V. (1972). "Leprosy and ancient Egypt." Lancet **2**(7788): 1203-1204.

Hutchings, M. I., A. W. Truman and B. Wilkinson (2019). "Antibiotics: past, present and future." Curr Opin Microbiol **51**: 72-80.

Jana, S. and J. K. Deb (2006). "Molecular understanding of aminoglycoside action and resistance." Appl Microbiol Biotechnol **70**(2): 140-150.

Johnson, S. J., J. S. Taylor and L. S. Beese (2003). "Processive DNA synthesis observed in a polymerase crystal suggests a mechanism for the prevention of frameshift mutations." Proc Natl Acad Sci U S A **100**(7): 3895-3900.

Kabsch, W. (2010). "Xds." Acta Crystallogr D Biol Crystallogr **66**(Pt 2): 125-132.

Kalan, L. and G. D. Wright (2011). "Antibiotic adjuvants: multicomponent anti-infective strategies." Expert Rev Mol Med **13**: e5.

Katoh, K. and D. M. Standley (2013). "MAFFT multiple sequence alignment software version 7: improvements in performance and usability." Mol Biol Evol **30**(4): 772-780.

Kawaguchi, H. (1976). "Discovery, chemistry, and activity of amikacin." J Infect Dis **134 SUPPL**: S242-248.

Kealey, C., C. A. Creaven, C. D. Murphy and C. B. Brady (2017). "New approaches to antibiotic discovery." Biotechnol Lett **39**(6): 805-817.

Kobayashi, F., M. Yamaguchi and S. Mitsuhashi (1972). "Activity of lividomycin against Pseudomonas aeruginosa: its inactivation by phosphorylation induced by resistant strains." Antimicrob Agents Chemother **1**(1): 17-21.

Kondo, S. and K. Hotta (1999). "Semisynthetic aminoglycoside antibiotics: Development and enzymatic modifications." J Infect Chemother **5**(1): 1-9.

Krause, K. M., A. W. Serio, T. R. Kane and L. E. Connolly (2016). "Aminoglycosides: An Overview." Cold Spring Harb Perspect Med **6**(6).

Kumar, P., P. K. Agarwal, M. B. Waddell, T. Mittag, E. H. Serpersu and M. J. Cuneo (2019). "Low-Barrier and Canonical Hydrogen Bonds Modulate Activity and Specificity of a Catalytic Triad." Angew Chem Int Ed Engl **58**(45): 16260-16266.

Kumar, P., B. Selvaraj, E. H. Serpersu and M. J. Cuneo (2018). "Encoding of Promiscuity in an Aminoglycoside Acetyltransferase." J Med Chem **61**(22): 10218-10227.

Kumar, P., E. H. Serpersu and M. J. Cuneo (2018). "A low-barrier hydrogen bond mediates antibiotic resistance in a noncanonical catalytic triad." Sci Adv **4**(4): eaas8667.

Kurumbang, N. P., K. Liou and J. K. Sohng (2011). "Biosynthesis of ribostamycin derivatives by reconstitution and heterologous expression of required gene sets." Appl Biochem Biotechnol **163**(3): 373-382.

Laxminarayan, R., A. Duse, C. Wattal, A. K. Zaidi, H. F. Wertheim, N. Sumpradit, E. Vlieghe, G. L. Hara, I. M. Gould, H. Goossens, C. Greko, A. D. So, M. Bigdeli, G. Tomson, W. Woodhouse, E. Ombaka, A. Q. Peralta, F. N. Qamar, F. Mir, S. Kariuki, Z. A. Bhutta, A. Coates, R. Bergstrom, G. D. Wright, E. D. Brown and O. Cars (2013). "Antibiotic resistance-the need for global solutions." Lancet Infect Dis **13**(12): 1057-1098.

Laxminarayan, R., P. Matsoso, S. Pant, C. Brower, J. A. Rottingen, K. Klugman and S. Davies (2016). "Access to effective antimicrobials: a worldwide challenge." Lancet **387**(10014): 168-175.

Lee, C. S., S. Vasoo, F. Hu, R. Patel and Y. Doi (2014). "Klebsiella pneumoniae ST147 coproducing NDM-7 carbapenemase and RmtF 16S rRNA methyltransferase in Minnesota." J Clin Microbiol **52**(11): 4109-4110.

Lemoine, F., D. Correia, V. Lefort, O. Doppelt-Azeroual, F. Mareuil, S. Cohen-Boulakia and O. Gascuel (2019). "NGPhylogeny.fr: new generation phylogenetic services for non-specialists." Nucleic Acids Res **47**(W1): W260-W265.

Leroy, A., G. Humbert, G. Oksenhendler and J. P. Fillastre (1976). "Comparative pharmacokinetics of lividomycin, amikacin and sisomicin in normal subjects and in uraemic patients." The Journal of antimicrobial chemotherapy **2**(4): 373-381.

Letunic, I. and P. Bork (2019). "Interactive Tree Of Life (iTOL) v4: recent updates and new developments." Nucleic Acids Res **47**(W1): W256-W259.

Levy, S. B. and B. Marshall (2004). "Antibacterial resistance worldwide: causes, challenges and responses." Nat Med **10**(12 Suppl): S122-129.

Liou, G. F., S. Yoshizawa, P. Courvalin and M. Galimand (2006). "Aminoglycoside resistance by ArmA-mediated ribosomal 16S methylation in human bacterial pathogens." J Mol Biol **359**(2): 358-364.

Lombardini, J. B. (1980). "Effects of isoproterenol and methoxamine on the contents of taurine in rat tissues." J Pharmacol Exp Ther **213**(2): 399-405.

Lombardini, J. B. and M. Cheng-Chu (1980). "Properties of gentamicin adenylyl transferase obtained from R-factor-resistant Escherichia coli." Int J Biochem **12**(3): 427-431.

Lopez-Novoa, J. M., Y. Quiros, L. Vicente, A. I. Morales and F. J. Lopez-Hernandez (2011). "New insights into the mechanism of aminoglycoside nephrotoxicity: an integrative point of view." Kidney International **79**(1): 33-45.

Lovering, A. M., L. O. White and D. S. Reeves (1987). "AAC(1): a new aminoglycoside-acetylating enzyme modifying the Cl aminogroup of apramycin." J Antimicrob Chemother **20**(6): 803-813.

Lumen. (2015). "Boundless Biology: History of Bacterial Diseases." Retrieved August 30, 2015, from https://courses.lumenlearning.com/boundless-biology/chapter/bacterial-diseases-in-humans/.

Macinga, D. R. and P. N. Rather (1999). "The chromosomal 2'-N-acetyltransferase of Providencia stuartii: physiological functions and genetic regulation." Front Biosci **4**: D132-140.

Magalhaes, M. L., M. W. Vetting, F. Gao, L. Freiburger, K. Auclair and J. S. Blanchard (2008). "Kinetic and structural analysis of bisubstrate inhibition of the Salmonella enterica aminoglycoside 6'-N-acetyltransferase." Biochemistry **47**(2): 579-584.

Magnet, S., P. Courvalin and T. Lambert (2001). "Resistance-nodulation-cell division-type efflux pump involved in aminoglycoside resistance in Acinetobacter baumannii strain BM4454." Antimicrob Agents Chemother **45**(12): 3375-3380.

Martens, E. and A. L. Demain (2017). "The antibiotic resistance crisis, with a focus on the United States." J Antibiot (Tokyo) **70**(5): 520-526.

Matsumoto, Y., T. Kinjo, D. Motooka, D. Nabeya, N. Jung, K. Uechi, T. Horii, T. Iida, J. Fujita and S. Nakamura (2019). "Comprehensive subspecies identification of 175 nontuberculous mycobacteria species based on 7547 genomic profiles." Emerg Microbes Infect **8**(1): 1043-1053.

Matt, T., C. L. Ng, K. Lang, S.-H. Sha, R. Akbergenov, D. Shcherbakov, M. Meyer, S. Duscha, J. Xie, S. R. Dubbaka, D. Perez-Fernandez, A. Vasella, V. Ramakrishnan, J. Schacht and E. C. Böttger (2012). "Dissociation of antibacterial activity and aminoglycoside ototoxicity in the 4-monosubstituted 2-deoxystreptamine apramycin." Proceedings of the National Academy of Sciences **109**(27): 10984.

Maurice, F., I. Broutin, I. Podglajen, P. Benas, E. Collatz and F. Dardel (2008). "Enzyme structural plasticity and the emergence of broad-spectrum antibiotic resistance." EMBO Rep **9**(4): 344-349.

Mayers, D. L. (2009). Antimicrobial Drug Resistance: Mechanisms of Drug Resistance. New York, NY, Humana Press.

McCoy, A. J., R. W. Grosse-Kunstleve, P. D. Adams, M. D. Winn, L. C. Storoni and R. J. Read (2007). "Phaser crystallographic software." J Appl Crystallogr **40**(Pt 4): 658-674.

McKay, G. A., P. R. Thompson and G. D. Wright (1994). "Broad spectrum aminoglycoside phosphotransferase type III from Enterococcus: overexpression, purification, and substrate specificity." Biochemistry **33**(22): 6936-6944.

Mildvan, A. S. (1997). "Mechanisms of signaling and related enzymes." Proteins **29**(4): 401-416.

Miller, G. H., F. J. Sabatelli, R. S. Hare, Y. Glupczynski, P. Mackey, D. Shlaes, K. Shimizu and K. J. Shaw (1997). "The most frequent aminoglycoside resistance mechanisms--changes with time and geographic area: a reflection of aminoglycoside usage patterns? Aminoglycoside Resistance Study Groups." Clin Infect Dis **24 Suppl 1**: S46-62.

Mingeot-Leclercq, M. P., Y. Glupczynski and P. M. Tulkens (1999). "Aminoglycosides: activity and resistance." Antimicrob Agents Chemother **43**(4): 727-737.

Moazed, D. and H. F. Noller (1987). "Interaction of antibiotics with functional sites in 16S ribosomal RNA." Nature **327**(6121): 389-394.

Moriarty, N. W., R. W. Grosse-Kunstleve and P. D. Adams (2009). "electronic Ligand Builder and Optimization Workbench (eLBOW): a tool for ligand coordinate and restraint generation." Acta Crystallogr D Biol Crystallogr **65**(Pt 10): 1074-1080.

Murshudov, G. N., P. Skubak, A. A. Lebedev, N. S. Pannu, R. A. Steiner, R. A. Nicholls, M. D. Winn, F. Long and A. A. Vagin (2011). "REFMAC5 for the refinement of macromolecular crystal structures." Acta Crystallogr D Biol Crystallogr **67**(Pt 4): 355-367.

Newman, D. J. and G. M. Cragg (2007). "Natural products as sources of new drugs over the last 25 years." J Nat Prod **70**(3): 461-477.

Noone, P. (1984). "Sisomicin, netilmicin and dibekacin. A review of their antibacterial activity and therapeutic use." Drugs **27**(6): 548-578.

O'Connell, K. M., J. T. Hodgkinson, H. F. Sore, M. Welch, G. P. Salmond and D. R. Spring (2013). "Combating multidrug-resistant bacteria: current strategies for the discovery of novel antibacterials." Angew Chem Int Ed Engl **52**(41): 10706-10733.

O'Leary, N. A., M. W. Wright, J. R. Brister, S. Ciufo, D. Haddad, R. McVeigh, B. Rajput, B. Robbertse, B. Smith-White, D. Ako-Adjei, A. Astashyn, A. Badretdin, Y. Bao, O. Blinkova, V. Brover, V. Chetvernin, J. Choi, E. Cox, O. Ermolaeva, C. M. Farrell, T. Goldfarb, T. Gupta, D. Haft, E. Hatcher, W. Hlavina, V. S. Joardar, V. K. Kodali, W. Li, D. Maglott, P. Masterson, K. M. McGarvey, M. R. Murphy, K. O'Neill, S. Pujar, S. H. Rangwala, D. Rausch, L. D. Riddick, C. Schoch, A. Shkeda, S. S. Storz, H. Sun, F. Thibaud-Nissen, I. Tolstoy, R. E. Tully, A. R. Vatsan, C. Wallin, D. Webb, W. Wu, M. J. Landrum, A. Kimchi, T. Tatusova, M. DiCuccio, P. Kitts, T. D. Murphy and K. D. Pruitt (2016). "Reference sequence (RefSeq) database at NCBI: current status, taxonomic expansion, and functional annotation." Nucleic Acids Res **44**(D1): D733-745.

Olsen, S. C. and S. A. Carlson (2015). "In vitro bactericidal activity of aminoglycosides, including the next-generation drug plazomicin, against Brucella spp." Int J Antimicrob Agents **45**(1): 76-78.

Olshansky, S. J., B. Carnes, R. G. Rogers and L. Smith (1997). "Infectious diseases -- new and ancient threats to world health." Popul Bull **52**(2): 1-52.

Pass, H. A., M. Kalil and S. Grutman (2007). "A call to arms." Am J Surg **194**(4): 423-425.

Pedersen, L. C., M. M. Benning and H. M. Holden (1995). "Structural investigation of the antibiotic and ATP-binding sites in kanamycin nucleotidyltransferase." Biochemistry **34**(41): 13305-13311.

Pflugrath, J. W. (1999). "The finer things in X-ray diffraction data collection." Acta Crystallogr D Biol Crystallogr **55**(Pt 10): 1718-1725.

Pilch, D. S., M. Kaul, C. M. Barbieri and J. E. Kerrigan (2003). "Thermodynamics of aminoglycoside-rRNA recognition." Biopolymers **70**(1): 58-79.

Poole, K. (2005). "Aminoglycoside resistance in Pseudomonas aeruginosa." Antimicrob Agents Chemother **49**(2): 479-487.

Prayle, A. and A. R. Smyth (2010). "Aminoglycoside use in cystic fibrosis: therapeutic strategies and toxicity." Curr Opin Pulm Med **16**(6): 604-610.

Price, K. E., M. D. DeFuria and T. A. Pursiano (1976). "Amikacin, an aminoglycoside with marked activity against antibiotic-resistant clinical isolates." J Infect Dis **134 SUPPL**: S249-261.

Ramirez, M. S., C. Quiroga and D. Centron (2005). "Novel rearrangement of a class 2 integron in two non-epidemiologically related isolates of Acinetobacter baumannii." Antimicrob Agents Chemother **49**(12): 5179-5181.

Ramirez, M. S. and M. E. Tolmasky (2010). "Aminoglycoside modifying enzymes." Drug Resist Updat **13**(6): 151-171.

Rather, P. N., E. Orosz, K. J. Shaw, R. Hare and G. Miller (1993). "Characterization and transcriptional regulation of the 2'-N-acetyltransferase gene from Providencia stuartii." J Bacteriol **175**(20): 6492-6498.

Recht, M. I., S. Douthwaite and J. D. Puglisi (1999). "Basis for prokaryotic specificity of action of aminoglycoside antibiotics." EMBO J **18**(11): 3133-3138.

Ribeiro da Cunha, B., L. P. Fonseca and C. R. C. Calado (2019). "Antibiotic Discovery: Where Have We Come from, Where Do We Go?" Antibiotics (Basel) **8**(2).

Riley, D. R., K. B. Sieber, K. M. Robinson, J. R. White, A. Ganesan, S. Nourbakhsh and J. C. Dunning Hotopp (2013). "Bacteria-human somatic cell lateral gene transfer is enriched in cancer samples." PLoS Comput Biol **9**(6): e1003107.

Rodriquez Torres, A. (1979). "[Sisomicin sulfate: its efficacy in the treatment of urologic infections]." Arch Esp Urol **32**(4): 387-396.

Romanowska, J., J. A. McCammon and J. Trylska (2011). "Understanding the origins of bacterial resistance to aminoglycosides through molecular dynamics mutational study of the ribosomal A-site." PLoS Comput Biol **7**(7): e1002099.

Rosenberg, E. Y., D. Ma and H. Nikaido (2000). "AcrD of Escherichia coli is an aminoglycoside efflux pump." J Bacteriol **182**(6): 1754-1756.

Rougier, F., D. Claude, M. Maurin, A. Sedoglavic, M. Ducher, S. Corvaisier, R. Jelliffe and P. Maire (2003). "Aminoglycoside nephrotoxicity: modeling, simulation, and control." Antimicrob Agents Chemother **47**(3): 1010-1016.

Salian, S., T. Matt, R. Akbergenov, S. Harish, M. Meyer, S. Duscha, D. Shcherbakov, B. B. Bernet, A. Vasella, E. Westhof and E. C. Bottger (2012). "Structure-activity relationships among the kanamycin aminoglycosides: role of ring I hydroxyl and amino groups." Antimicrob Agents Chemother **56**(12): 6104-6108.

Samadi, N., I. Pakzad, A. Monadi Sefidan, H. Hosainzadegan and A. Tanomand (2015). "Study of aminoglycoside resistance genes in enterococcus and salmonella strains isolated from ilam and milad hospitals, iran." Jundishapur J Microbiol **8**(4): e18102.

Schatz, A., E. Bugie and S. A. Waksman (2005). "Streptomycin, a substance exhibiting antibiotic activity against gram-positive and gram-negative bacteria. 1944." Clin Orthop Relat Res(437): 3-6.

Schmidt, F. (1984). "The role of insertions, deletions, and substitutions in the evolution of R6 related plasmids encoding aminoglycoside transferase ANT-(2")." Mol Gen Genet **194**(1-2): 248-259.

Schultz, M. (2001). "Paleohistopathology of bone: a new approach to the study of ancient diseases." Am J Phys Anthropol **Suppl 33**: 106-147.

Serio, A. W., T. Keepers, L. Andrews and K. M. Krause (2018). "Aminoglycoside Revival: Review of a Historically Important Class of Antimicrobials Undergoing Rejuvenation." EcoSal Plus **8**(1).

Serpersu, E. H., C. Ozen and E. Wright (2008). "Studies of enzymes that cause resistance to aminoglycosides antibiotics." Methods Mol Med **142**: 261-271.

Shaeer, K. M., M. T. Zmarlicka, E. B. Chahine, N. Piccicacco and J. C. Cho (2019). "Plazomicin: A Next-Generation Aminoglycoside." Pharmacotherapy **39**(1): 77-93.

Shakil, S., R. Khan, R. Zarrilli and A. U. Khan (2008). "Aminoglycosides versus bacteria--a description of the action, resistance mechanism, and nosocomial battleground." J Biomed Sci **15**(1): 5-14.

Shaw, K. J., P. N. Rather, R. S. Hare and G. H. Miller (1993). "Molecular genetics of aminoglycoside resistance genes and familial relationships of the aminoglycoside-modifying enzymes." Microbiol Rev **57**(1): 138-163.

Sheldrick, G. M. (2008). "A short history of SHELX." Acta Crystallogr A **64**(Pt 1): 112-122.

Shi, K. and A. M. Berghuis (2012). "Structural basis for dual nucleotide selectivity of aminoglycoside 2"-phosphotransferase IVa provides insight on determinants of nucleotide specificity of aminoglycoside kinases." J Biol Chem **287**(16): 13094-13102.

Shi, K., S. J. Caldwell, D. H. Fong and A. M. Berghuis (2013). "Prospects for circumventing aminoglycoside kinase mediated antibiotic resistance." Front Cell Infect Microbiol **3**: 22.

Shi, K., D. R. Houston and A. M. Berghuis (2011). "Crystal structures of antibiotic-bound complexes of aminoglycoside 2"-phosphotransferase IVa highlight the diversity in substrate binding modes among aminoglycoside kinases." Biochemistry **50**(28): 6237-6244.

Shimizu, K., T. Kumada, W. C. Hsieh, H. Y. Chung, Y. Chong, R. S. Hare, G. H. Miller, F. J. Sabatelli and J. Howard (1985). "Comparison of aminoglycoside resistance patterns in Japan, Formosa, and Korea, Chile, and the United States." Antimicrob Agents Chemother **28**(2): 282-288.

Silver, L. L. (2011). "Challenges of antibacterial discovery." Clin Microbiol Rev **24**(1): 71-109.

Skubak, P. and N. S. Pannu (2013). "Automatic protein structure solution from weak X-ray data." Nat Commun **4**: 2777.

Skubak, P., W. J. Waterreus and N. S. Pannu (2010). "Multivariate phase combination improves automated crystallographic model building." Acta Crystallogr D Biol Crystallogr **66**(Pt 7): 783-788.

Smith, C. A., M. Toth, T. M. Weiss, H. Frase and S. B. Vakulenko (2014). "Structure of the bifunctional aminoglycoside-resistance enzyme AAC(6')-Ie-APH(2")-Ia revealed by crystallographic and small-angle X-ray scattering analysis." Acta Crystallogr D Biol Crystallogr **70**(Pt 10): 2754-2764.

Spellberg, B., R. Guidos, D. Gilbert, J. Bradley, H. W. Boucher, W. M. Scheld, J. G. Bartlett, J. Edwards, Jr. and A. Infectious Diseases Society of (2008). "The epidemic of antibiotic-resistant infections: a call to action for the medical community from the Infectious Diseases Society of America." Clin Infect Dis **46**(2): 155-164.

Stock, J. T. (2008). "Are humans still evolving? Technological advances and unique biological characteristics allow us to adapt to environmental stress. Has this stopped genetic evolution?" EMBO Rep **9 Suppl 1**: S51-54.

Stogios, P. J., M. L. Kuhn, E. Evdokimova, M. Law, P. Courvalin and A. Savchenko (2017). "Structural and Biochemical Characterization of Acinetobacter spp. Aminoglycoside Acetyltransferases Highlights Functional and Evolutionary Variation among Antibiotic Resistance Enzymes." ACS Infect Dis **3**(2): 132-143.

Studer, G., C. Rempfer, A. M. Waterhouse, R. Gumienny, J. Haas and T. Schwede (2020). "QMEANDisCo-distance constraints applied on model quality estimation." Bioinformatics **36**(8): 2647.

Studier, F. W. (2005). "Protein production by auto-induction in high density shaking cultures." Protein Expr Purif **41**(1): 207-234.

Tenover, F. C., I. Tickler, E. S. Armstrong, A. Kubo, S. Lopez, D. H. Persing and G. H. Miller (2011). "Activity of ACHN-490 against meticillin-resistant Staphylococcus aureus (MRSA) isolates from patients in US hospitals." Int J Antimicrob Agents **38**(4): 352-354.

Thompson, P. R., D. D. Boehr, A. M. Berghuis and G. D. Wright (2002). "Mechanism of aminoglycoside antibiotic kinase APH(3')-IIIa: role of the nucleotide positioning loop." Biochemistry **41**(22): 7001-7007.

Thompson, P. R., D. W. Hughes and G. D. Wright (1996). "Regiospecificity of aminoglycoside phosphotransferase from Enterococci and Staphylococci (APH(3')-IIIa)." Biochemistry **35**(26): 8686-8695.

Thorn, A. and G. M. Sheldrick (2011). "ANODE: anomalous and heavy-atom density calculation." J Appl Crystallogr **44**(Pt 6): 1285-1287.

Tsai, A., S. Uemura, M. Johansson, E. V. Puglisi, R. A. Marshall, C. E. Aitken, J. Korlach, M. Ehrenberg and J. D. Puglisi (2013). "The impact of aminoglycosides on the dynamics of translation elongation." Cell Rep **3**(2): 497-508.

Tsukamura, M. (1972). "A preliminary trial of lividomycin in patients with pulmonary tuberculosis." Tubercle **53**(1): 43-46.

Vakulenko, S. B. and S. Mobashery (2003). "Versatility of aminoglycosides and prospects for their future." Clin Microbiol Rev **16**(3): 430-450.

Van Pelt, J. E., R. Iyengar and P. A. Frey (1986). "Gentamicin nucleotidyltransferase. Stereochemical inversion at phosphorus in enzymatic 2'-deoxyadenylyl transfer to tobramycin." J Biol Chem **261**(34): 15995-15999.

Van Pelt, J. E. and D. B. Northrop (1984). "Purification and properties of gentamicin nucleotidyltransferase from Escherichia coli: nucleotide specificity, pH optimum, and the separation of two electrophoretic variants." Arch Biochem Biophys **230**(1): 250-263.

Vaziri, F., S. N. Peerayeh, Q. B. Nejad and A. Farhadian (2011). "The prevalence of aminoglycoside-modifying enzyme genes (aac (6')-I, aac (6')-II, ant (2")-I, aph (3')-VI) in Pseudomonas aeruginosa." Clinics (Sao Paulo) **66**(9): 1519-1522.

Vetting, M. W., S. S. Hegde, F. Javid-Majd, J. S. Blanchard and S. L. Roderick (2002). "Aminoglycoside 2'-N-acetyltransferase from Mycobacterium tuberculosis in complex with coenzyme A and aminoglycoside substrates." Nat Struct Biol **9**(9): 653-658.

Vetting, M. W., S. Magnet, E. Nieves, S. L. Roderick and J. S. Blanchard (2004). "A bacterial acetyltransferase capable of regioselective N-acetylation of antibiotics and histones." Chem Biol **11**(4): 565-573.

Vetting, M. W., C. H. Park, S. S. Hegde, G. A. Jacoby, D. C. Hooper and J. S. Blanchard (2008). "Mechanistic and structural analysis of aminoglycoside N-acetyltransferase AAC(6')-Ib and its bifunctional, fluoroquinolone-active AAC(6')-Ib-cr variant." Biochemistry **47**(37): 9825-9835.

Vicens, Q. and E. Westhof (2002). "Crystal structure of a complex between the aminoglycoside tobramycin and an oligonucleotide containing the ribosomal decoding a site." Chem Biol **9**(6): 747-755.

von Bubnoff, A. (2006). "Seeking new antibiotics in nature's backyard." Cell **127**(5): 867-869.

Waterhouse, A., M. Bertoni, S. Bienert, G. Studer, G. Tauriello, R. Gumienny, F. T. Heer, T. A. P. de Beer, C. Rempfer, L. Bordoli, R. Lepore and T. Schwede (2018). "SWISS-MODEL: homology modelling of protein structures and complexes." Nucleic Acids Res **46**(W1): W296-W303.

Wie, S. H. (2015). "Clinical significance of Providencia bacteremia or bacteriuria." Korean J Intern Med **30**(2): 167-169.

Winter, G. (2010). "xia2: an expert system for macromolecular crystallography data reduction." Journal of Applied Crystallography **43**(1): 186-190.

Wolf, E., A. Vassilev, Y. Makino, A. Sali, Y. Nakatani and S. K. Burley (1998). "Crystal structure of a GCN5-related N-acetyltransferase: Serratia marcescens aminoglycoside 3-N-acetyltransferase." Cell **94**(4): 439-449.

World Health Organization. (2014). ", Antimicrobial Resistance: Global Report on Surveillance 2014." from https://www.who.int/drugresistance/documents/surveillancereport/en/.

Wright, E. and E. H. Serpersu (2004). "Isolation of aminoglycoside nucleotidyltransferase (2")-Ia from inclusion bodies as active, monomeric enzyme." Protein Expr Purif **35**(2): 373-380.

Wright, E. and E. H. Serpersu (2005). "Enzyme-substrate interactions with an antibiotic resistance enzyme: aminoglycoside nucleotidyltransferase(2")-Ia characterized by kinetic and thermodynamic methods." Biochemistry **44**(34): 11581-11591.

Wybenga-Groot, L. E., K. Draker, G. D. Wright and A. M. Berghuis (1999). "Crystal structure of an aminoglycoside 6'-N-acetyltransferase: defining the GCN5-related N-acetyltransferase superfamily fold." Structure **7**(5): 497-507.

Young, P. G., R. Walanj, V. Lakshmi, L. J. Byrnes, P. Metcalf, E. N. Baker, S. B. Vakulenko and C. A. Smith (2009). "The crystal structures of substrate and nucleotide complexes of Enterococcus faecium aminoglycoside-2"-phosphotransferase-IIa [APH(2")-IIa] provide insights into substrate selectivity in the APH(2") subfamily." J Bacteriol **191**(13): 4133-4143.

Zarrilli, R., M. F. Tripodi, A. Di Popolo, R. Fortunato, M. Bagattini, M. Crispino, A. Florio, M. Triassi and R. Utili (2005). "Molecular epidemiology of high-level aminoglycoside-resistant enterococci isolated from patients in a university hospital in southern Italy." J Antimicrob Chemother **56**(5): 827-835.

Zgurskaya, H. I., J. W. Weeks, A. T. Ntreh, L. M. Nickels and D. Wolloscheck (2015). "Mechanism of coupling drug transport reactions located in two different membranes." Front Microbiol **6**: 100.

Zhanel, G. G., C. D. Lawson, S. Zelenitsky, B. Findlay, F. Schweizer, H. Adam, A. Walkty, E. Rubinstein, A. S. Gin, D. J. Hoban, J. P. Lynch and J. A. Karlowsky (2012). "Comparison of the next-generation aminoglycoside plazomicin to gentamicin, tobramycin and amikacin." Expert Rev Anti Infect Ther **10**(4): 459-473.

Zhao, C., J. Li, J. Hou, M. Guo, Y. Zhang and Y. Chen (2000). "A randomized controlled clinical trial on etimicin, a new aminoglycoside antibiotic, versus netilmicin in the treatment of bacterial infections." Chin Med J (Engl) **113**(11): 1026-1030.

Zumla, A., P. Nahid and S. T. Cole (2013). "Advances in the development of new tuberculosis drugs and treatment regimens." Nat Rev Drug Discov **12**(5): 388-404.